AD-A079878

14

AFIT/GAE/AA/79D-16

12 169

6 VELOCITY PROFILES IN A LONG INLET DUCT EMPLOYING A PHOTON CORRELATING LASER VELOCIMETER WITHOUT SEEDING.

9 Master's THESIS

Presented to the Faculty of the School of Engineering
of the Air Force Institute of Technology
Air University
in Partial Fulfillment of the Requirements
for the Degree of Master of Science

by

10 Harley J. V. Rogers ~~Captain~~ B Eng. RMC CAF

Graduate Aeronautical Engineering

11 December 1979

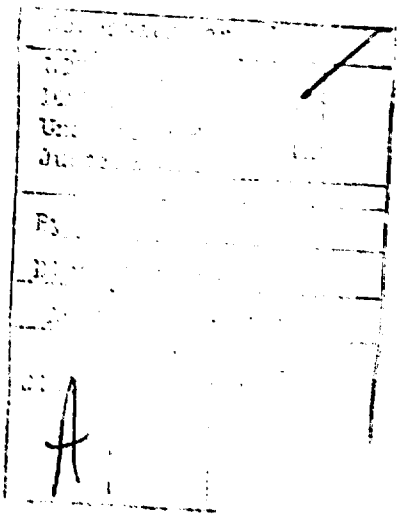

Approved for public release; distribution unlimited

012 225

Preface

This study was conceived as a follow on project from the work recently completed by Captain Nino G. Cerullo, CAF, who graduated in June of 1979. As Captain Cerullo's Thesis involved a comparison study between the Malvern Digital Correlating Laser Velocimeter (LV) and the conventional Hot Wire Anemometer System, it was decided to use this LV System in a "real world" application to obtain a further indication of its performance. This study entailed employing the LV System to determine the velocity profile across a 29.5 inch duct through which passes air on its way to the face of a J-85 jet engine compressor. By employing this system the mean velocity profile was obtained without either employing any device which would obstruct the flow in the pipe or having any requirement to "seed" the flow with particles which is an inherent problem of some LV systems. In addition to the mean velocity profiles, turbulence intensity profiles were also derived and, for comparison purposes, to evaluate the quality of the LV data, hot wire traverses and a pitot-static traverse were made to give mean velocity and turbulence intensity profiles.

Throughout the initial planning, the performance and the final completion of this study, a number of people were instrumental in providing valuable assistance and a considerable wealth of experience. To Dr. Harold Wright, my principal advisor, Capt. (Dr.) George Catalano, Dr. William Elrod and Dr. James Hitchcock, I would like to extend my sincere thanks

for the extensive assistance provided throughout my work. I would also like to thank Dr. Richard Rivir, Dr. Francis Ostdiek and Mr. Norm Poti who, in addition to scheduling the numerous engine test runs, on many occasions assisted me by helping to obtain the data I required. Finally, to Mr. Carl Short, Mr. Ron Ruley and Mr. Russell Murray of the AFIT School Shops, I would like to voice my appreciation for the excellent manner in which all the various apparatus required for this study was constructed.

Contents

Contents

List of Figures

List of Figures

List of Figures

List of Tables

Symbols

Symbol	Description	Units
LV	Laser Velocimeter	
M	Mach number	
L	The distance from the laser beam intersection point to any reference vertical surface onto which the beam shines	inches
D	The distance that the laser beams are apart at this reference vertical surface	inches
λ	Wavelength of the helium-neon gas of the laser = $.6328 \times 10^{-6}_{m}$	meters
μ	The index of refractivity of air = 1.0	
S	The number of fringes	
K	A constant whose value depends upon the lense and spacer combination used	
rms Voltage	Root mean square voltage or fluctuating component	volts
RPM	Revolutions per minute	
η	Turbulence Intensity	
PM Tube	Photo Multiplier Tube	
A	Distance from the laser beam intersection point to the lense of the Photo-Multiplier Tube	cm
θ	One-half the angle between the two laser beams	degrees
g_1	The first minimum point on the oscilloscope readout	
g_2	The first peak on the oscilloscope readout	
g_3	The second minimum point on the oscilloscope readout	

Symbols

Symbol	Description	Units
r_o	Laser beam radius	m.m.
F_d*	Doppler Shift frequency with Phase Modulator	Khz
U	Mean velocity	ft/sec
U*	Mean velocity with Phase Modulator	ft/sec
Δf	Frequency shift	Khz
P_o	Total Pressure	lb_f/in^2
T_o	Total Temperature	°.
U_{cen}	Centerline Velocity	ft/sec
U_p	Particle velocity	ft/sec
U_a	Air velocity	ft/sec
α	Slope of the divergent or convergent section	
X	The distance from the exit of the divergent or convergent section to the point of testing	inches
μ	Viscosity of air	$\frac{lb_m\text{-sec}}{ft^2}$
ρ_p	Density of particulate matter in the air	lb_m/ft^3
D	Diameter of the particles	1μm

ABSTRACT

This thesis involves a practical application of the Malvern Laser Velocimeter System (LV). In this work, the LV was used to measure mean velocity profiles across the inside diameter of a duct which supplies air to the compressor of a jet engine. The engine, which is a General Electric J-85 turbo-jet engine is located in the Propulsion Laboratories of Wright-Patterson Air Force Base in Ohio. In addition to the mean velocity profiles, the LV was used to measure turbulence intensity profiles across the inside diameter of the duct at each of the three test points. To analyse the quality of the LV data as obtained, alternate mean velocity profiles and turbulence intensity profiles were obtained with the aid of a Hot Wire Anemometer System and a Pitot-Static Tube.

During each of the traverses, or tests, with the LV System, the Hot Wire System and the Pitot-Static Tube, the engine was held at a fixed RPM, being 50% or 70% of maximum engine RPM. Good correlation was achieved between each of the three systems in respect to the mean velocity profiles obtained at each of the three test positions while the turbulence intensity profiles matched well in the regions of the flow where turbulence levels of 2% to 30% were encountered.

VELOCITY PROFILES IN A LONG INLET DUCT EMPLOYING A PHOTON CORRELATING LASER VELOCIMETER WITHOUT SEEDING

I. INTRODUCTION

To obtain an accurate measurement of flow properties in a pipe, especially in the vicinity of the walls without affecting the flow by a measuring device in the stream has been a long sought after capability in the field of experimental and related work. With the advent of Laser Velocimeter Systems and especially the current Malvern Laser Velocimeter, flow velocities can now be measured without obstructing the flow. In the case of the Malvern Laser Velocimeter System, no "seeding" or the introduction of artificial particles into the airflow is normally required which previous LV systems needed to function effectively, and it is expected that in this flow field, this "no seeding" capability will hold true. As there are many areas where such a system can be effectively used, particularly in the area of Aeronautical Research, this "real world" project was initiated to further evaluate the quality of this system's data gathering capabilities.

Previous Work. During the past year (1978-79) Capt. N. G. Cerullo completed a Masters' Thesis which involved the use of a Malvern Laser Velocimeter System (See Reference 2). In his application, the LV was used to determine air velocities along both the "x" and "y" axes of a free air jet operating

at velocities of M. = .4, .6 and .8 at standard room temperature. The data obtained was then compared both to data from a Hot Wire Anemometer system used under the same conditions as well as comparison to established theory. Comparing the two sets of data, close correlation was in evidence with respect to the mean velocity profiles but the LV system was found to be partially ineffective in turbulent flow. In addition to the work carried out by Capt. Cerullo, Capt. (Dr.) George Catalano and the author utilized the equipment at the Flight Dynamics two foot wind tunnel. In this application, the Laser Velocimeter System was used to measure air velocity and turbulence intensity around the upper fuselage surface of a model of a KC-135 aircraft with an attached fairing. In this application, the Laser Velocimeter System was operated in the back-scatter mode with both the Photo Multiplier (PM) tube and the Laser being located on the same side of the wind tunnel. Although some difficulty was encountered in focusing and aligning the set-up, mean velocity and turbulence intensity data was obtained for various points in flow around the model of the attached fairing.

Present Study. As a follow on to the previous work, and as a further test of the Laser Velocimeter's capabilities, it was decided to use the LV system to study the airflow in a duct which supplies air to the compressor of a jet engine. With the engine operating at both 50% or 70% of maximum engine RPM, the resulting air velocities through the test

section were in the order of 50 to 100 ft/sec. The objectives of this study were as follows:

1. Using the Laser Velocimeter, obtain and plot mean velocity and turbulence intensity profiles across the test section at each of the three designated points in the flow, for comparison with the Hot Wire and Pitot-static data.
2. Using the Pitot-static Tube, obtain and plot a mean velocity profile at a single location in the flow.
3. Using the Hot Wire Anemometer System, obtain and plot a mean velocity and turbulence intensity profile across the test section at each of the three designated points in the flow.

Scope. This paper will deal with the objectives as listed above and will also include an extensive operational description of the Malvern Laser Velocimeter System. In addition, any problem areas, inherent to this LV System, will be described as well as any possible solutions to these problems.

II. TEST APPARATUS

The apparatus used consisted primarily of the J-85 test cell located in the Air Force Aero-Propulsion Laboratory at Wright-Patterson Air Force Base. Other than a smaller turbine inlet area and the existence of various probes and pressure sensing devices, the GE J-85 engine is essentially a stock engine with very few modifications. The engine is located inside a pressure chamber which, if required, can simulate high altitude conditions for the engine.

Ahead of the engine is a parabolic inlet bell mouth extending from the 16.09 inch inside diameter of the compressor face out to the 29.5 inch inside diameter of the air supply duct or "White Pipe" as it is termed in this report. The White Pipe is a 33.7 ft. long duct which supplies air from a large filter box assembly to the compressor and is as illustrated in Figure 1. The White Pipe contains three special sections. The first is a section of pipe that is 65 inches in length and contains a conical venturi with no by-pass as illustrated in Figures 2 and 3. The purpose for placing this venturi in the flow is to allow metering of the flow. The second section is 17 inches long and contains several types of screens and flow conditioners to prepare the flow for the compressor by reducing the boundary layer thickness and reducing the effect of any upstream flow disturbances on the velocity profile. The third section is the test section

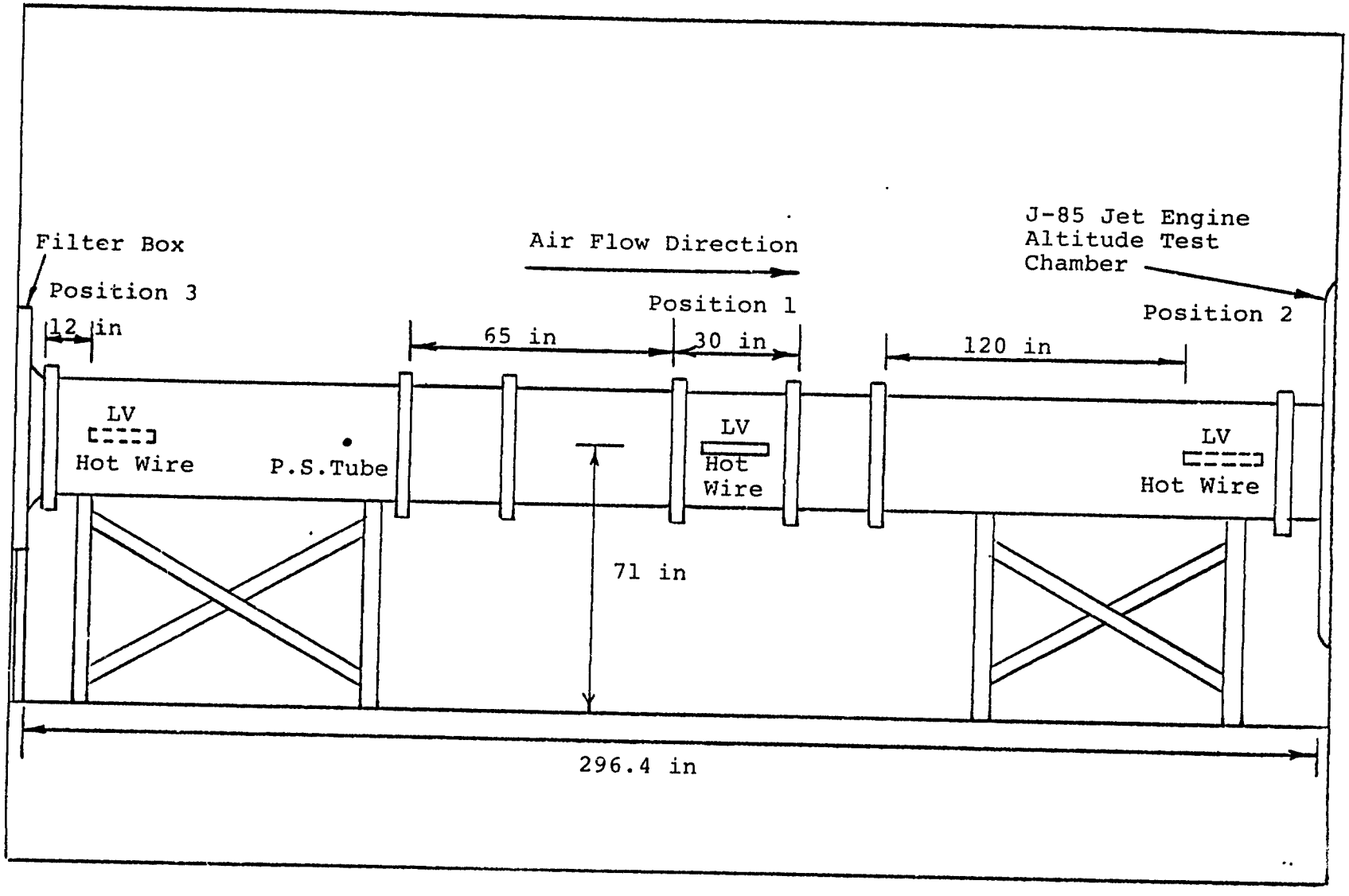

Figure 1 White Pipe Dimensions

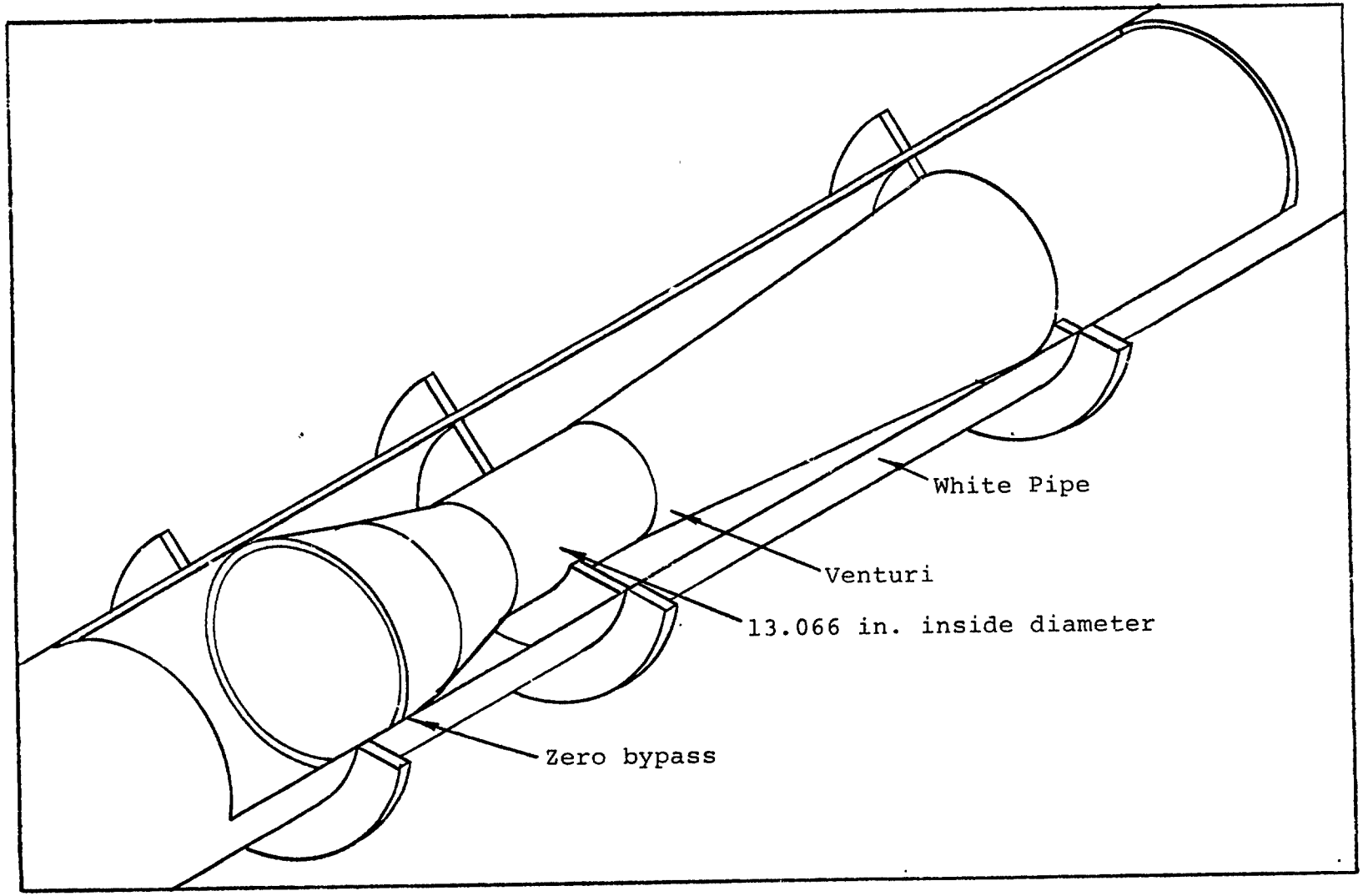

Figure 2 White Pipe Venturi

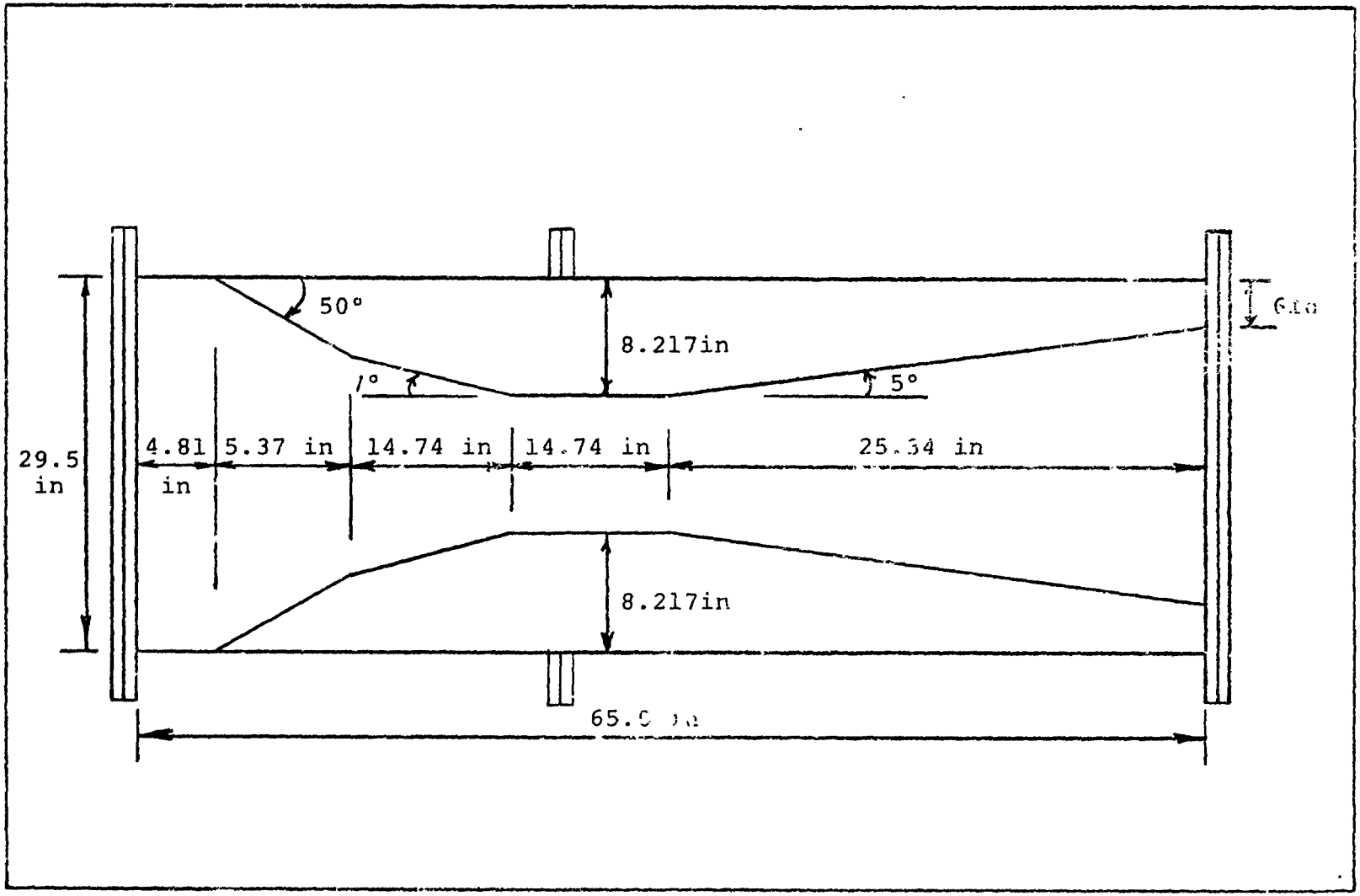

Figure 3 White Pipe Venturi Dimensions

which is 30 inches long and is capable of being moved to various other locations along the length of the White Pipe to allow flow conditions to be investigated at other stations. Thirty-three point seven feet from the compressor face there is a bell mouth inlet which expands from an inside diameter of the pipe of 29.5 inches to 59.5 inches in a circular arc. Upstream of this bell mouth is a large filter box with all but one of its six walls containing filter sections. The dimensions of the filter box are: 65 inches x 80.5 inches x 85 inches. Figure 1 pictorially illustrates the White Pipe and indicates the position of the filter box for a more complete understanding of the layout.

In order to do the traverses across the inside diameter of the White Pipe at a height of 5 feet 10 inches off the floor, a system was designed which incorporated two diametrically opposing windows in the walls of the test section as well as a traversing table. The windows, which were made of an optical grade of glass, were installed so as to allow the laser velocimeter system to "see" the air flow in the pipe. The traversing table was employed to support the laser tube, Phase Modulator and PM Tube at the same height as the windows. The final design which was built is as illustrated in Figure 4. Once secured onto the traversing mechanism, the laser and photo multiplier tube could be set to give readings at any point, along the horizontal diameter of the pipe between the two windows. Following each reading, the entire rail

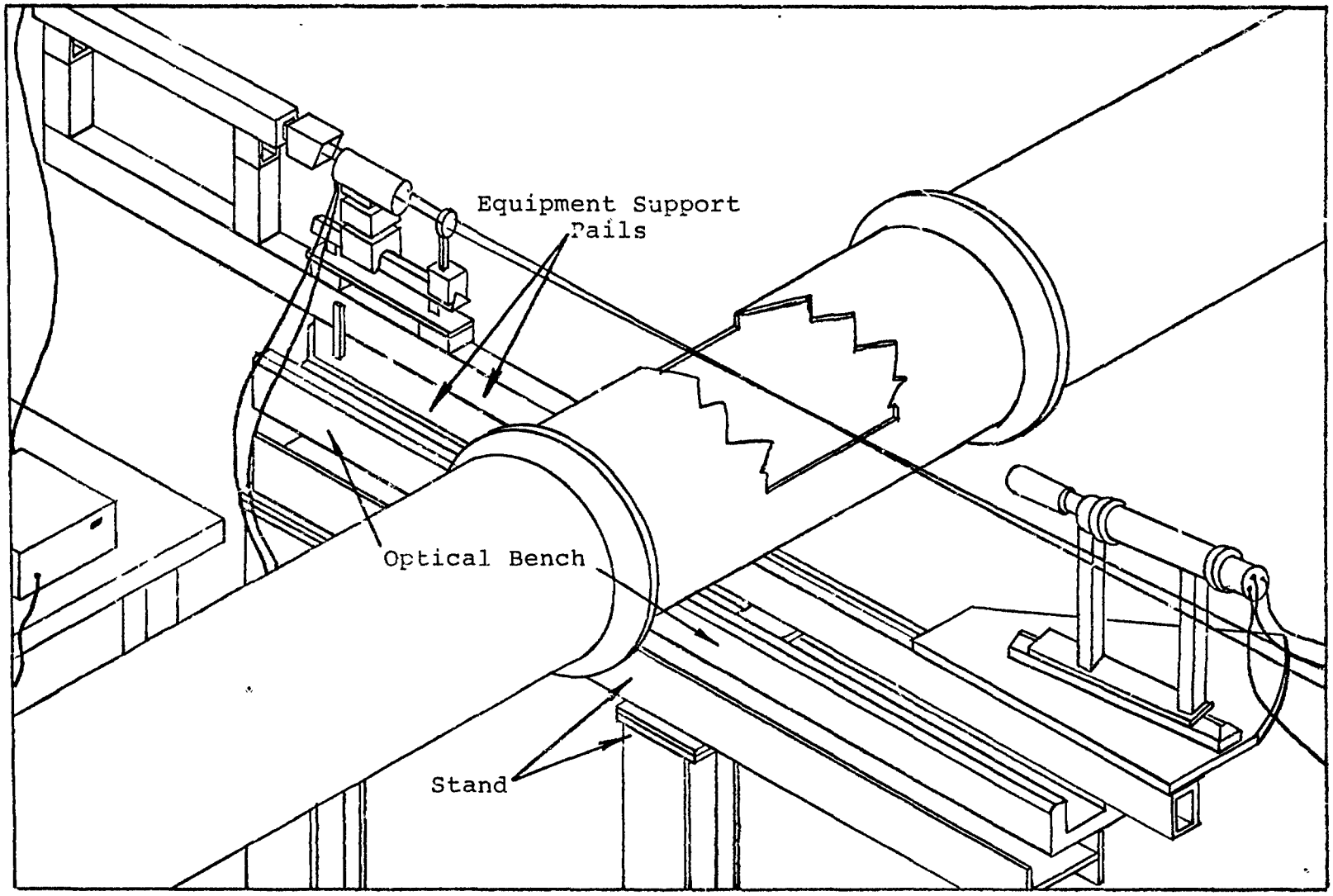

Figure 4 Cut-away view of "White Pipe" and Traversing Mechanism

holding this equipment could then be moved back and forth to allow readings to be taken at other points in the flow. This traversing capability overcame the necessity of having to re-focus the photo multiplier tube on the intersection of the two laser beams each time a movement to another point in the flow was made.

With respect to the Pitot-static system, a pitot-static probe and traversing mechanism was placed at a point 25.5 feet ahead of the compressor face. This combination probe and traversing mechanism was capable of measuring pitot and static pressures from within 2.82 inches from one wall to a point 18 inches from the same wall or a total travel of 15.18 inches.

The Hot Wire Anemometer system consisted of a hot wire probe held in the plane of the flow, pointing in an upstream direction. The probe was held in place by a traversing mechanism which was designed to allow the probe to travel from one wall to within 4.1 inches of the other wall for a total travel of 25.4 inches. The traversing mechanism itself, was held in place by blanking plates, which were designed to fit into the spaces where the windows for the LV system were placed, in the test section. By designing the Hot Wire System to be used in the test section, it had the capability of being placed at the same three locations in the flow where the LV data was taken which allowed good comparison of results.

III. INSTRUMENTATION

The three principal groups of equipment which were employed in this study were the Laser Velocimeter System, the Hot Wire Anemometer System and the Pitot-static System. Of these three groups, the most complex system to use was the LV assembly. The component parts of each of the three assemblies are as follows, with pictorial representation included:

A. Laser Velocimeter

1. Laser - the laser employed in this system is a 15 milliwatt helium-neon laser, model 124A produced by Spectra Physics. Incorporated into the laser is a Model 255 DC exciter and together they produce a single laser beam of 1.1 millimeters (.0011m) in diameter. Visually, this beam appears as a single well defined red beam of light.

2. Beamsplitter - This is the Malvern RF307 transmitter beamsplitter and polarization unit which is used to produce two beams from the single input laser beam. These beams are both 1.1 mm in diameter and can be spaced up to 20 mm apart. The beamsplitter has two controls, one of which controls the intersection point of the two beams from a point 15 cms

in front of the beam splitter to a point several meters away. The other control is used to vary the distance that the two beams are apart when they emerge from the beam splitter.

3. Phase-Modulator Unit - As the basic Laser Velocimeter System is not capable of sensing flow directions and has signal processing difficulties when trying to measure velocities in high speed flow or highly turbulent flow, the Malvern K-9023 Phase Modulator with two crystals can be incorporated into the system if required. As the laser beams must enter the unit parallel to one another, a focusing lense is also required whenever this unit is used. The focal length of the lense will be determined by the physical distance from the Phase Modulator unit to the point where the measurements are to be made. To determine the exact frequency shift produced by the Phase Modulator drive unit when in operation, a Hewlett-Packard 5325B Universal Counter is used.

4. Photo-Multiplier Tube - The Photo Multiplier (PM) Tube is an EMI 9863 model KE/100 unit supplied by Malvern Instruments. Mounted on the front of the PM tube is either a 200 mm telephoto lense or a 105 mm lense which is

used to focus the scattered light from the laser beam intersection point onto the aperture of the lense and subsequently onto the pinhole of the PM tube. Powering the PM tube is the EMI power supply unit which provides a constant 1850 volts to the cathode of the PM tube during its operation.

5. Digital Correlator - The type K7023 Unit consists of a digital correlator and a storage unit. It is capable of accepting continuous output from the PM tube, storing it, processing it and updating it while continually reproducing the information on an oscilloscope for data evaluation. At any time, the output can be halted while the correlator continues to accept information from the PM tube and update its storage unit. With the output halted, the oscilloscope provides an easy method for determining maximum and minimum values of the signal which is required for velocity and turbulence intensity determination.
6. Oscilloscope - The oscilloscope used in conjunction with the digital correlator is a Tektronics scope which gives a pictorial representation of channel content in addition to maximum and minimum values.

Figures 5, 6, 7 and 8 give both a diagramatic and pictorial view of the component parts of the Laser Velocimeter System.

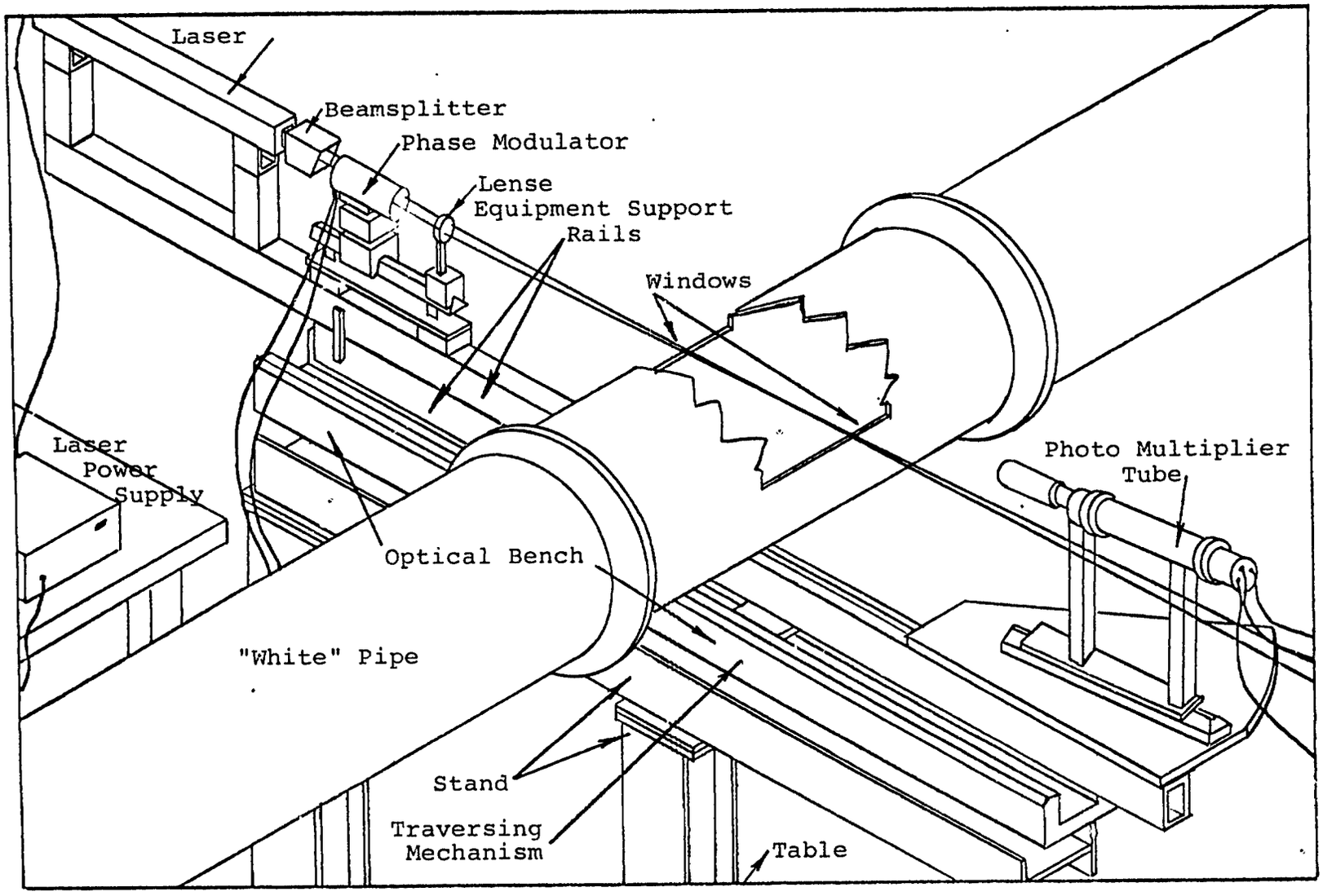

Figure 5 Laser and Photo-Multiplier Tube Traversing Mechanism

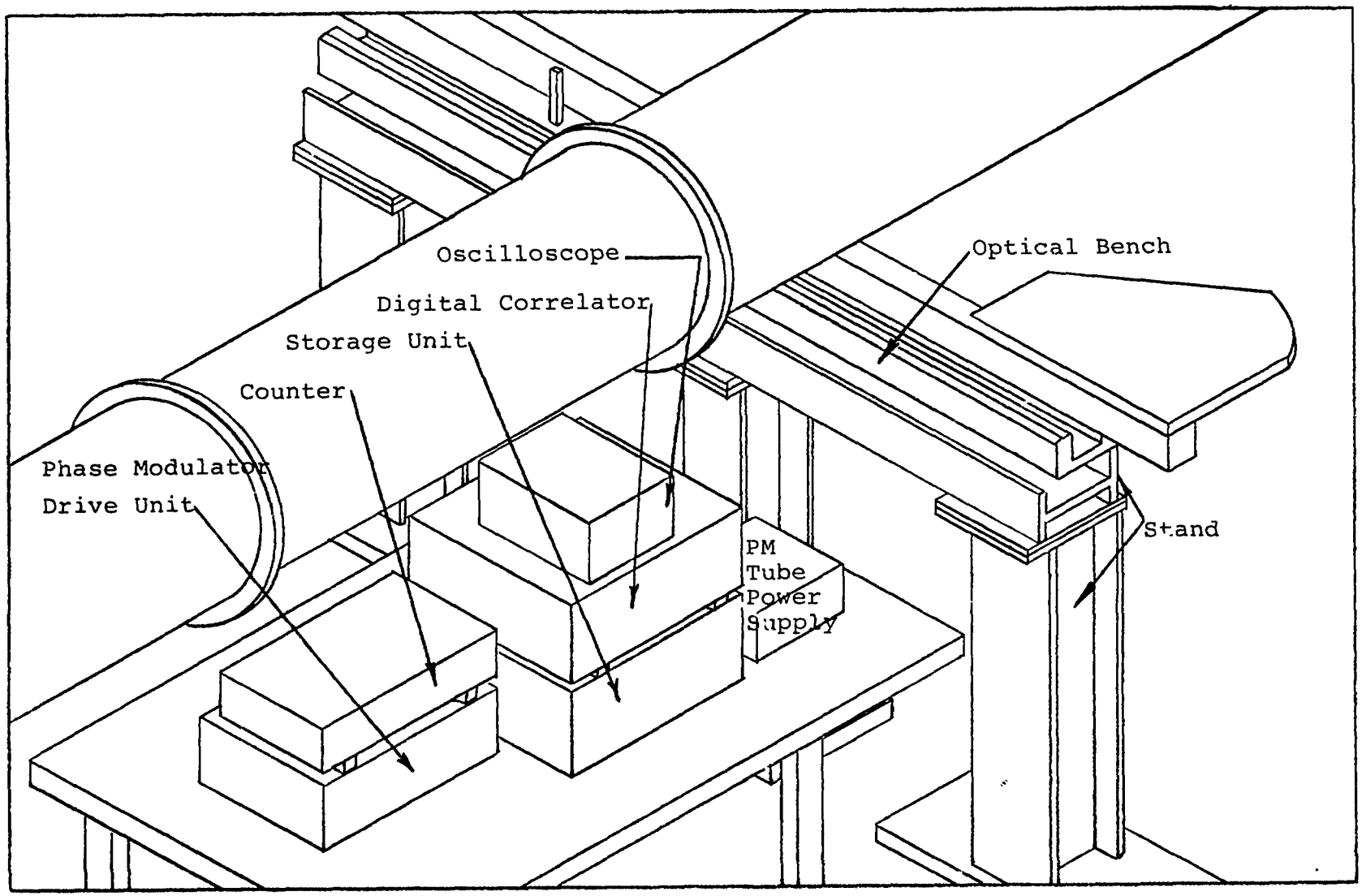

Figure 6 Laser Velocimeter Support Equipment Set-up

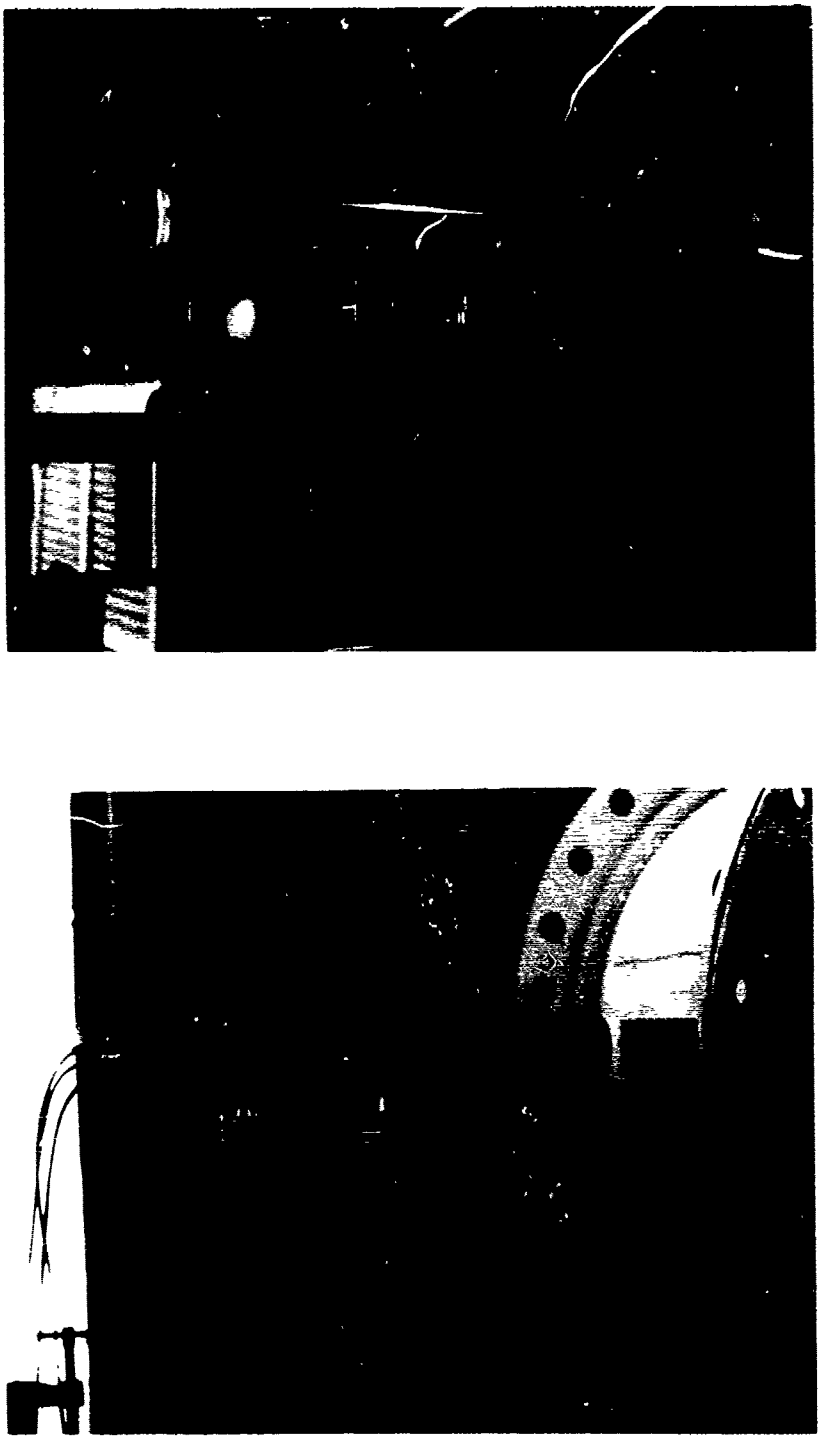

Figure 7 Pictorial Views of Laser Velocimeter (A)

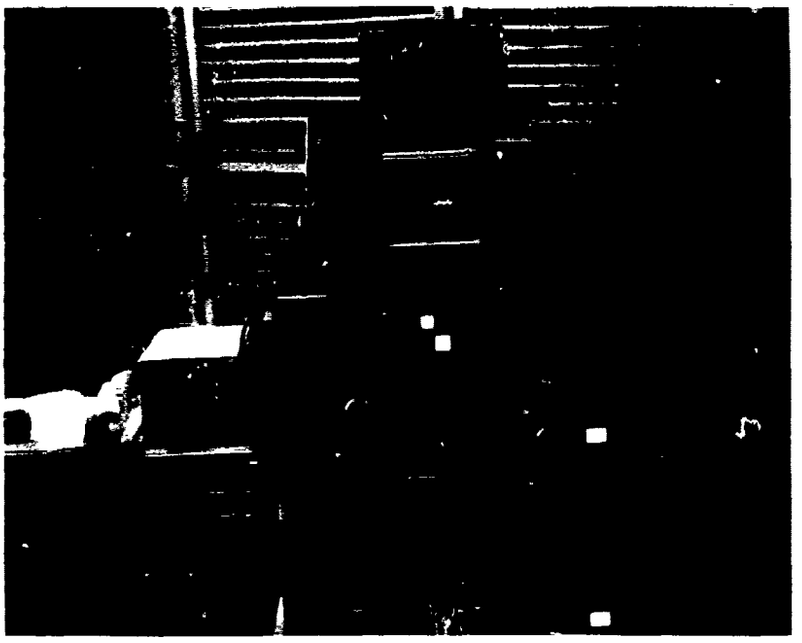

Figure 8 Pictorial Views of Laser Velocimeter (B)

B. Pitot-Static System

The Pitot-static System used in this project consisted of a pitot-static probe, a traversing mechanism and a micromanometer. The pitot-static probe had a single pitot hole on the tip of the probe with four static ports located back behind the conical head of the probe. The probe was mounted on a traversing mechanism and secured in place, in the flow, by pipe fittings on each side of the White Pipe. As previously stated, the pitot-static probe was located 25.5 feet ahead of the compressor face and had a 15.18 inch travel normal to the pipe flow. Attached to the end of the traversing mechanism were plastic tubes which connected the pitot and static ports to a micromanometer for pressure difference measurement. Figure 9 illustrates this system.

C. Hot Wire Anemometer System

The Hot Wire Anemometer System consisted of a hot wire probe, a traversing mechanism, an anemometer, a universal counter, a volt-meter, an oscilloscope and a micromanometer. The hot wire probe was a single wire probe and was orientated to point upstream into the flow, with the wire in a vertical position. From the probe, a 90 degree holder for the probe was fastened into the traversing tube which was supported on either end by the LV window blanking plates. Connected to the end of the probe holder of the traversing mechanism, by a co-axial cable, were the anemometer, which was used to set and monitor the bridge DC voltage, a Hewlett-Packard digital

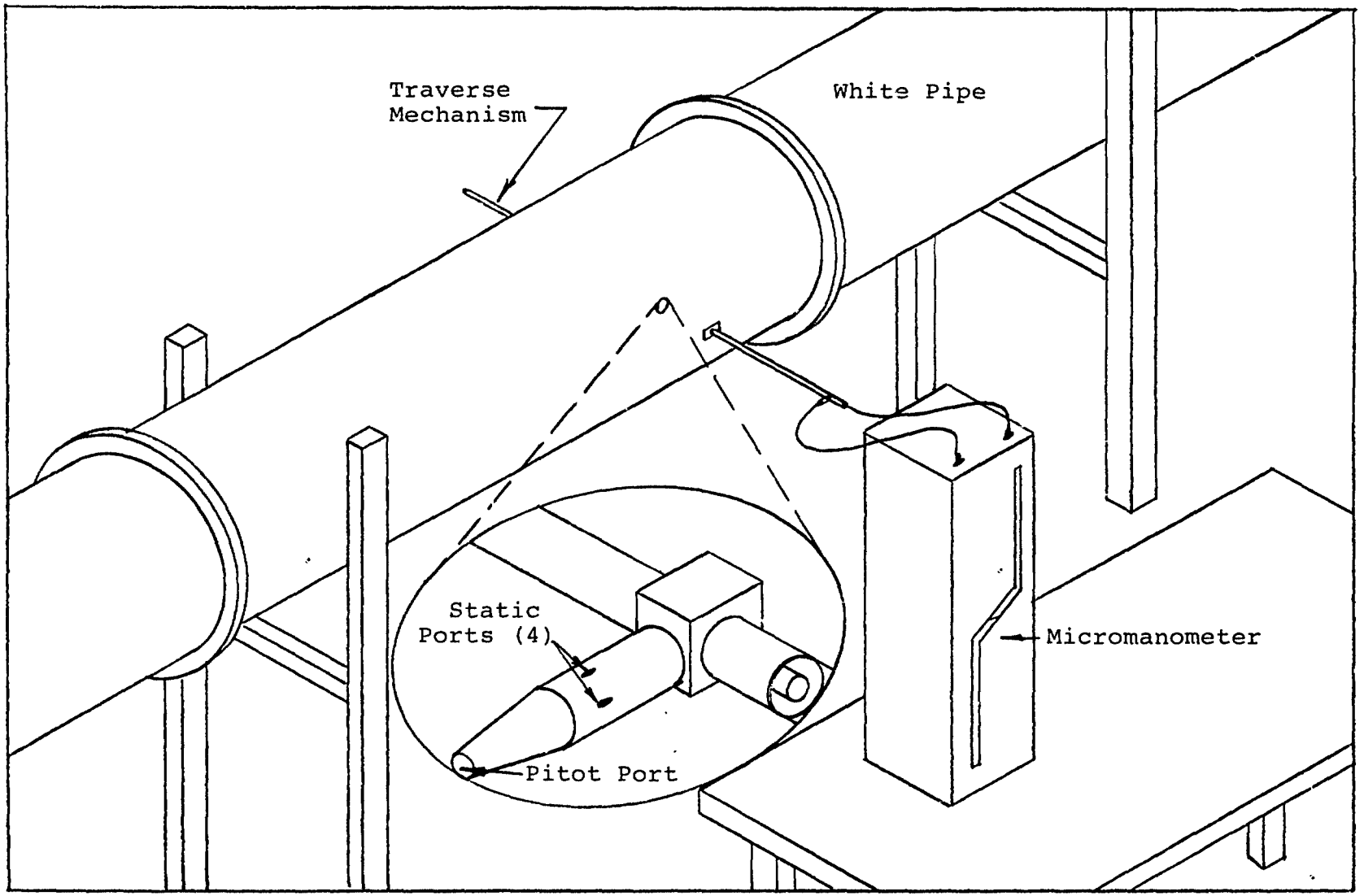

Figure 9 Pitot-Static Tube System

counter for registering this voltage, a voltmeter to observe and record the r.m.s. voltage and an oscilloscope which was used to ensure the transmission of a square wave signal for calibration. From a static port on the wall of the test section, a flexible plastic pipe was connected to a micromanometer to observe and record variations in pressure on this inner surface. Figure 10 illustrates the component parts of this system.

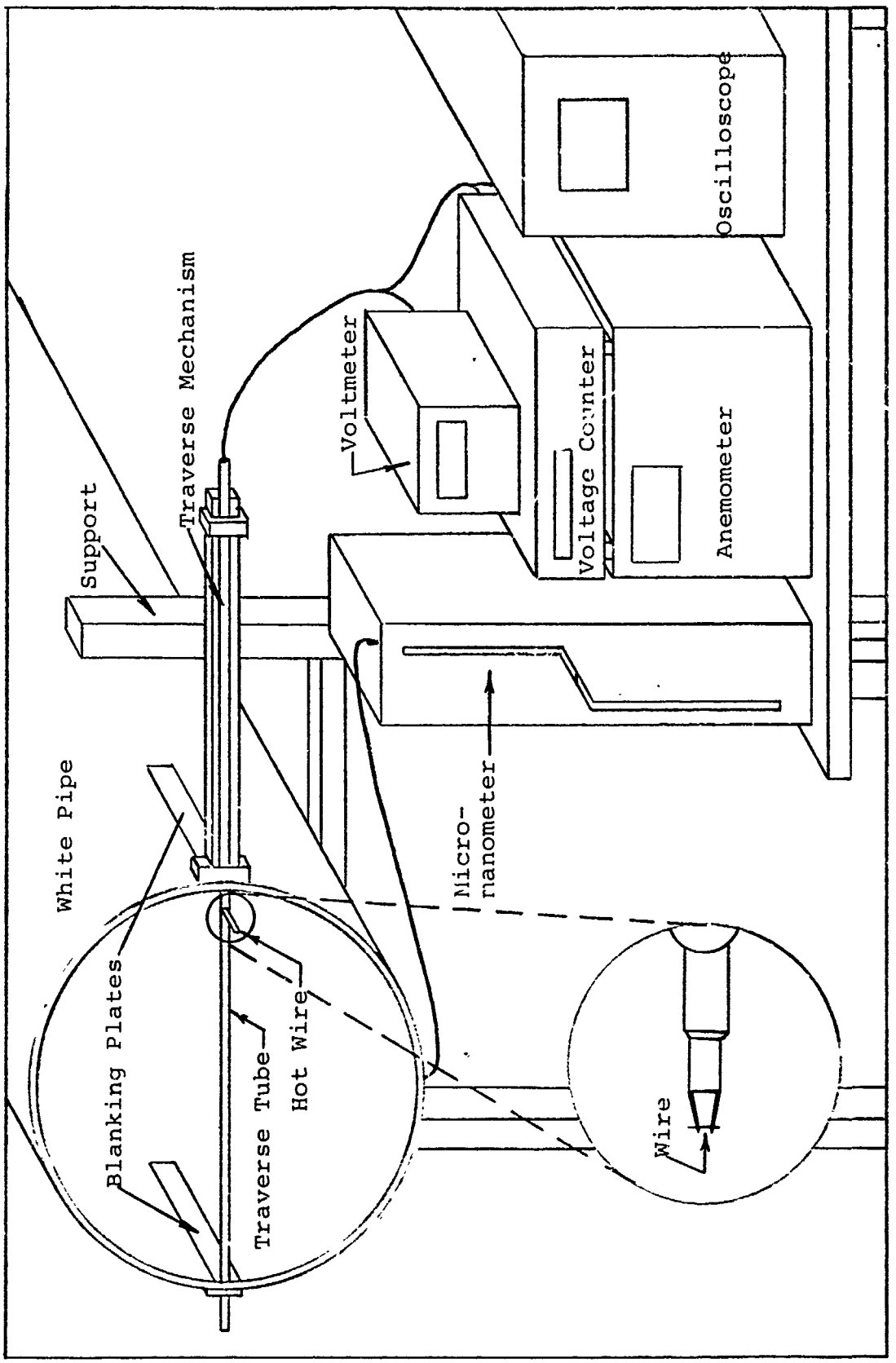

Figure 10 Hot Wire Anemometer System

IV. PRINCIPLE OF OPERATION

The Malvern Laser Anemometer System is composed of a Spectra Physics 15 mw Helium-Neon Laser, a coated Beam-splitter, a Photo Multiplier Tube, a Digital Correlator plus storage unit, an oscilloscope and a Phase Modulator plus drive unit and counter. As each system is complex in nature, each system will be dealt with individually to explain its particular principle of operation and how it fits into the overall system.

A. Spectra Physics 15 mw Laser. This particular type of laser consists of a glass tube with polished mirrors at either end and contains a mixture of 90 percent helium gas and 10 percent neon gas. The neon atoms, once excited are capable of amplifying light by stimulated emission with the end mirrors providing reflecting surfaces for bouncing the beam backwards and forwards through the gas, allowing the laser beam to build itself up. Once sufficiently built up, the beam will shine through a hole in one of the end mirrors.

B. Malvern Beamsplitter. The function of a beamsplitter is to take a single incoming beam and by some optical method split the beam into two beams which may be of equal intensity. In the case of the Malvern Beamsplitter, the single beam is brought

into an optical "diamond" shaped piece of coated glass as indicated in Figure 11

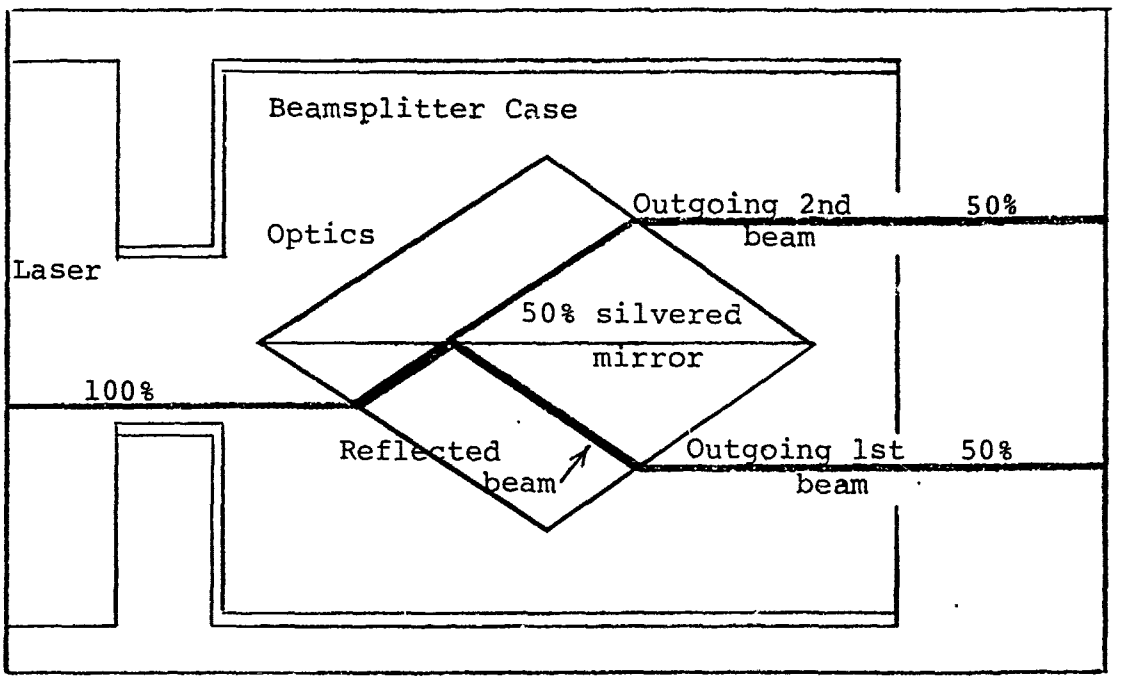

Figure 11 Malvern Beamsplitter Optics

As the initial beam enters the 6328Å coated glass ($.6328 \times 10^{-6}$m wavelength) it is deflected roughly as shown in Figure 11 and encounters a 50 percent silvered mirror. As this type of mirror suggests, 50% of the beam is allowed to pass through the mirror and onto the front edge where it is deflected out as shown, while 50% of the original beam is reflected to the other front edge and subsequently deflected out as shown. As a result of using this optical device, two beams of equal intensity have been achieved and can be made to

converge or diverge merely by changing the orientation of the optics with respect to the incoming beam.

C. Laser Beam Ellipsoidal Control Volume. At the point of intersection of the two laser beams, an ellipsoidal control volume composed of alternating vertical light and dark "slices" or fringes is set up. The number of fringes created can be determined by the following method. First, the calculation of the fringe spacing:

$$S = \text{fringe spacing} = \frac{L}{D} \frac{\lambda}{\mu}$$

where: L = the distance from the intersection point to any reference vertical surface onto which the beam shines

D = the distance the beams are apart at this reference surface

λ = wavelength of the helium-neon gas of the laser = $.6328 \times 10^{-6}$m.

μ = the index of refraction of air = 1.0

Now the number of fringes is calculated as follows:

$$\text{No. of fringes} = \frac{\text{Beam diameter}}{S}$$

where: Beam diameter = 1.1 mm

S = fringe spacing

If these fringes could be physically seen, they would appear as indicated in Figure 12:

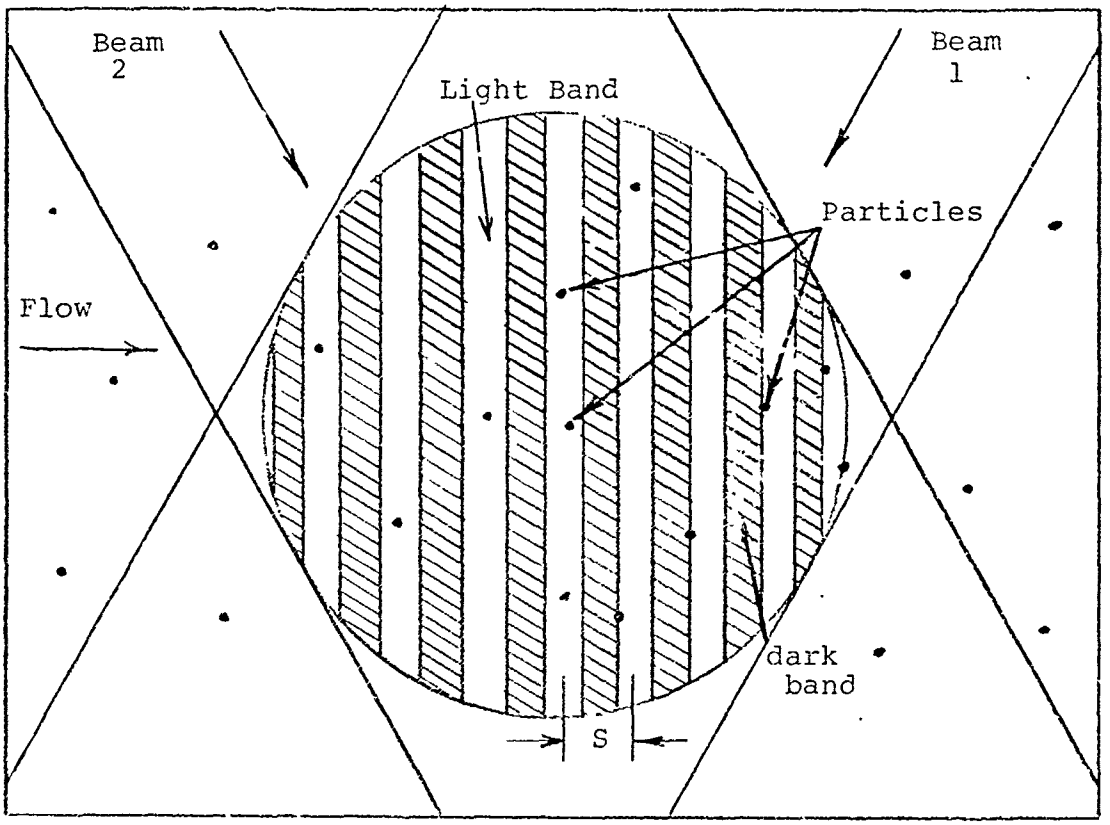

Figure 12 Laser Beam Intersection Point and Fringe Spacing

As illustrated in Figure 12, a number of particles can be seen passing through the light and dark regions. These particles, as they pass through the light bands, scatter light in all directions which the Photo Multiplier tube can "see".

D. Photo Multiplier Tube - The Photo Multiplier tube is composed of two distinct assemblies, one being the Receiver Photon Detection Unit and the other being the Photo Multiplier tube. Once aligned and focused onto the ellipsoidal control volume of the intersection point of the two laser beams,

the function of the Receiver Photon Detection Unit is to collect the light scattered when the particles cross a lighted region and focus this light back onto an aperture-pinhole combination. This combination of pinhole, which could be of the 100, 200 or 400 μm size, and aperture, in addition to the particular lense and spacer system in use, will determine the diameter of the flow control volume being observed. This diameter is calculated as follows:

Diameter = K (Diameter of pinhole)

where: K = a constant whose value depends upon the lense and spacer combination used.

The values for K are according to those specified in Table II. Once the scattered light passes through the pinhole, it then enters the Photo Multiplier Tube. This light, as it hits the cathode of the PM Tube causes a pulse train burst which is then passed onto a high gain amplifier and discriminator which eliminates the amplitude modulation and maintains only the frequency modulation. At this time, the signal or data is then passed onto the Digital Correlator for further processing.

E. Digital Correlator. The Digital Correlator in use here is the Malvern Digital Correlator type K7023 and it consists of a storage unit and a correlator as two separate pieces of equipment. This particular system has a 50 nano second (50×10^{-9} seconds) resolution time and can be operated in the single clipped autocorrelation, double clipped autocorrelation or the cross correlation modes. The correlator system operates on information received from the Photo Multiplier Tube which comes in the form of pulses, each of which is activated by the light scattered when a particle crosses a light fringe in the ellipsoidal control. By interpreting this information, which essentially involves the periodicity of the pulses, an output is achieved which could appear on the oscilloscope as in Figure 13 (ideal flow with a low turbulence level).

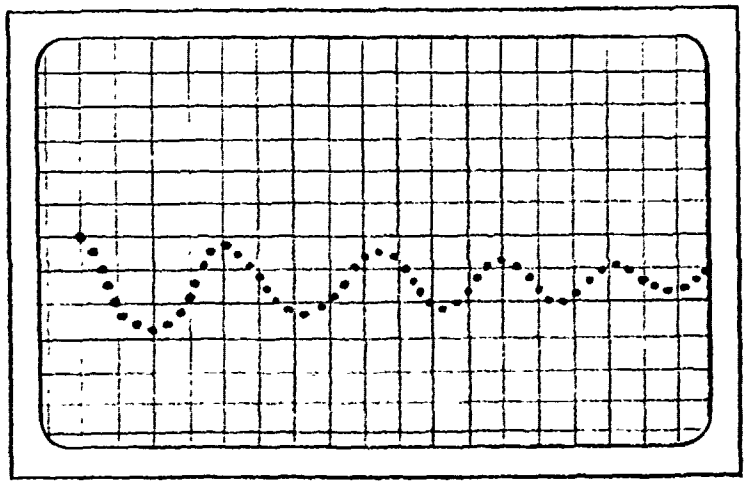

Figure 13 Digital Correlator Oscilloscope Output

From this output, mean velocity and turbulence intensity determinations can be made by employing the methods as explained in Appendix C, the Laser Velocimeter Data Reduction Method.

F. Phase Modulator. Periodically, flows will be encountered which are either of too high a velocity, too turbulent in nature or too slow moving for the standard Laser Velocimeter System, without a phase modulator, to deal with. Also, on occasion, flow direction determination may be required and the standard system without the modulator is not capable of making this evaluation. As a result, a Phase Modulator plus a drive unit and counter are put into the system to assist in overcoming or reducing the effect of these practical problems. Under normal operating conditions, the fringes set up at the intersection point of the two laser beams do not move with respect to the flow but remain stationary with the particles in the flow crossing these light and dark regions. Once the Phase Modulator is installed ahead of the beamsplitter, it takes the two parallel and nearly equal intensity beams from the beamsplitter and passes these through an electro-optic crystal onto which a suitable voltage is applied. In this way, the phase of each light beam is either advanced or retarded depending on the saw-tooth voltage which

is applied to the crystal. As a result of this, the fringes can be made to move with respect to the flow and thus, in low speed flow, by making the fringes move opposed to the direction of flow, the flow, or particles, will "appear" to be moving faster and consequently can be handled by the PM tube and Digital Correlator with much more effective results. Similarly, for high speed flow, the fringes would be made to move with the direction of the flow causing the flow to "appear" to slow down. By making the fringes move with respect to the particle flow, the particles will cross the light fringes at different rates than they would if the Phase Modulator were not in use. By allowing a slow moving particle to cross a light fringe more often and subsequently, scatter more light, the P.M. tube can operate more effectively and provide more information to the correlator thereby enhancing the auto-correlation function. By doing this, the evaluation of the output on the oscilloscope will allow easier determination of minimum and maximum values required for turbulence intensity and velocity calculations. In addition, since the movement of the fringes in the ellipsoidal control volume may be either in the same direction as the flow, or opposing it, the differential doppler frequency detected by the

signal processor will be consequently increased or decreased which will then enable the directional sense of the flow to be determined.

signal processor will be consequently increased or decreased which will then enable the directional sense of the flow to be determined.

V. EXPERIMENTAL PROCEDURE

The following is a description of the experimental procedure which was followed for each of the three systems employed in this study.

A. Laser Velocimeter

1. Traverse Locations - A total of three points along the "White Pipe" were selected at which the Laser Velocimeter traverses were made. These points were as follows:

   a. 12 inches inside the inlet Bell Mouth.

   b. White Pipe midsection - 12 inches downstream from the exit of the venturi.

   c. 10 feet downstream from the flow conditioners.

   For an explanation of the location of these traverse points, see Figure 14 which is a schematic of the system. At each of these points, a number of traverses were made. The following is a list of traverses with any changes which were introduced from one test to the next:

   a. Position: 12 inches inside inlet bell mouth (3)

      Traverse 1: 50% engine RPM
      No Phase Modulator

      Traverse 2: 70% engine RPM
      No Phase Modulator

   b. Position: White Pipe midsection (1)

      Traverse 3: 50 Engine RPM
      No Phase Modulator

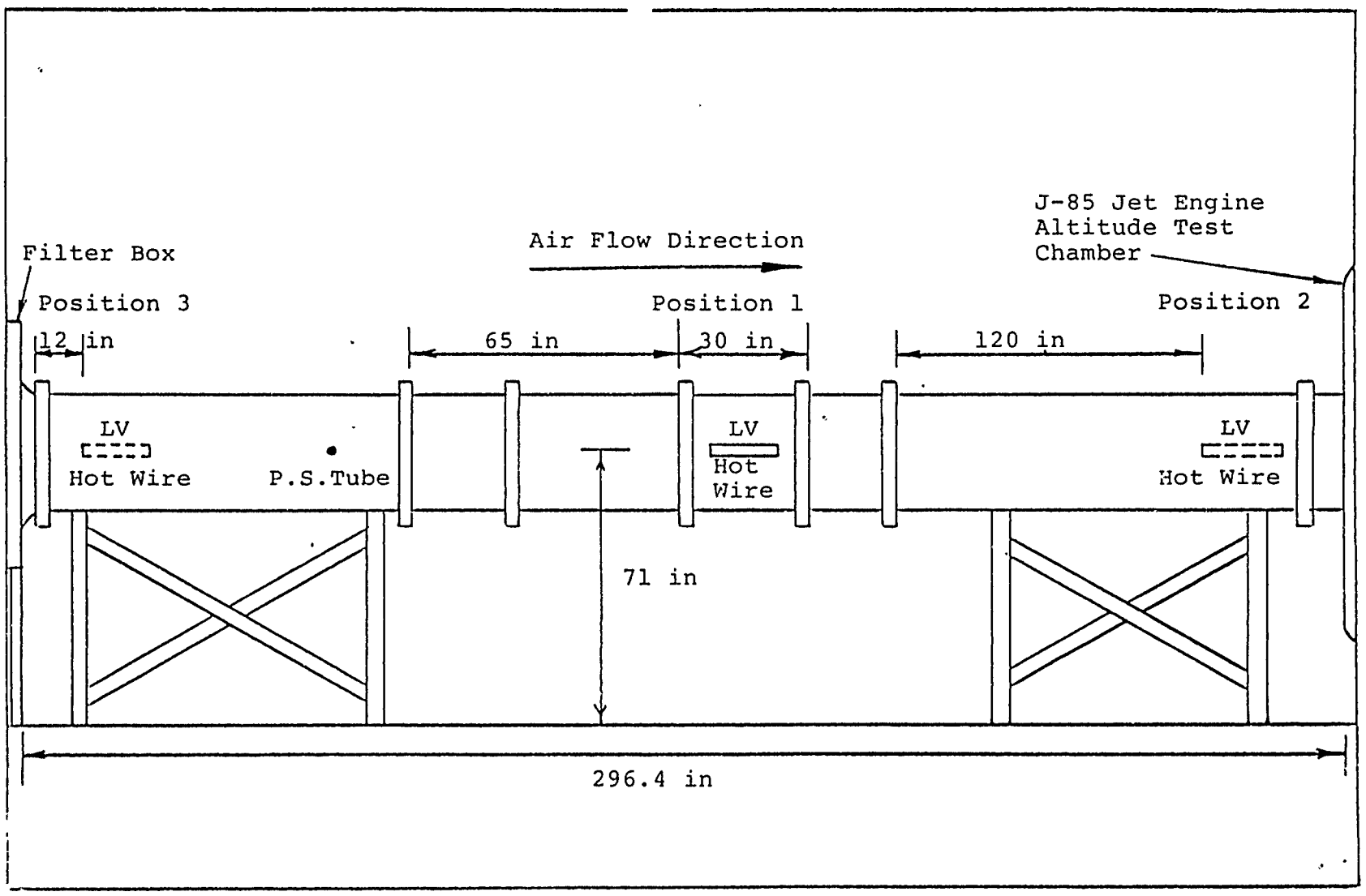

Figure 14 Locations of the LV, Hot Wire and Pitot-Static Tube Traverses

Traverse 4: 50% engine RPM

Phase Modulator included

Traverse 5: 70% engine RPM

Phase Modulator included

c. Position: 10 feet downstream of flow conditioners (2)

Traverse 6: 50% engine RPM

No Phase Modulator

Traverse 7: 70% engine RPM

No Phase Modulator

These traverses were made over a period of two weeks and under varying weather conditions. The dates of the respective tests as well as the weather conditions that existed on that day during the test, have been included with the data in Appendix B. Weather conditions were noted on each of the test days for the purpose of determining the effect, if any, that the prevailing weather would have on the particulate matter present in the White Pipe air flow and subsequently on the operation of the LV.

2. Mean Velocity and Turbulence Intensity Evaluations - As the object of this project was to obtain mean velocity and turbulence intensity profiles across the inside diameter of the White Pipe, the traversing mechanism was set up to move through one inch intervals across the majority of this diameter but to make much smaller movements as it approached either wall

of the pipe. In this way, a total of thirty-six data points were set-up across the diameter of the pipe. At each designated point in the flow, the Digital Correlator and Oscilloscope, in conjunction with the remainder of the LV equipment, gave an output on the oscilloscope from which the required data for the mean velocity and turbulence intensity calculations could be obtained. This data, for illustrative purposes using an example point, was obtained as indicated in Figure 15. Once the data was obtained for the test point, the table supporting the complete optical system was moved, by means of an electric motor, to the next test point.

B. Pitot-Static Tube

The Pitot-static tube was physically located at only one point in the flow, 25.5 feet ahead of the compressor face or about 12 inches ahead of the inlet to the venturi. This pitot-static tube and traversing mechanism was designed to move from a position 2.82 inches from one wall to 18.0 inches from the same wall or a total traversing distance of 15.18 inches. Data was taken at one inch intervals and at each point, measurements of pitot and static pressure were made which were required in the evaluation of the mean velocity at

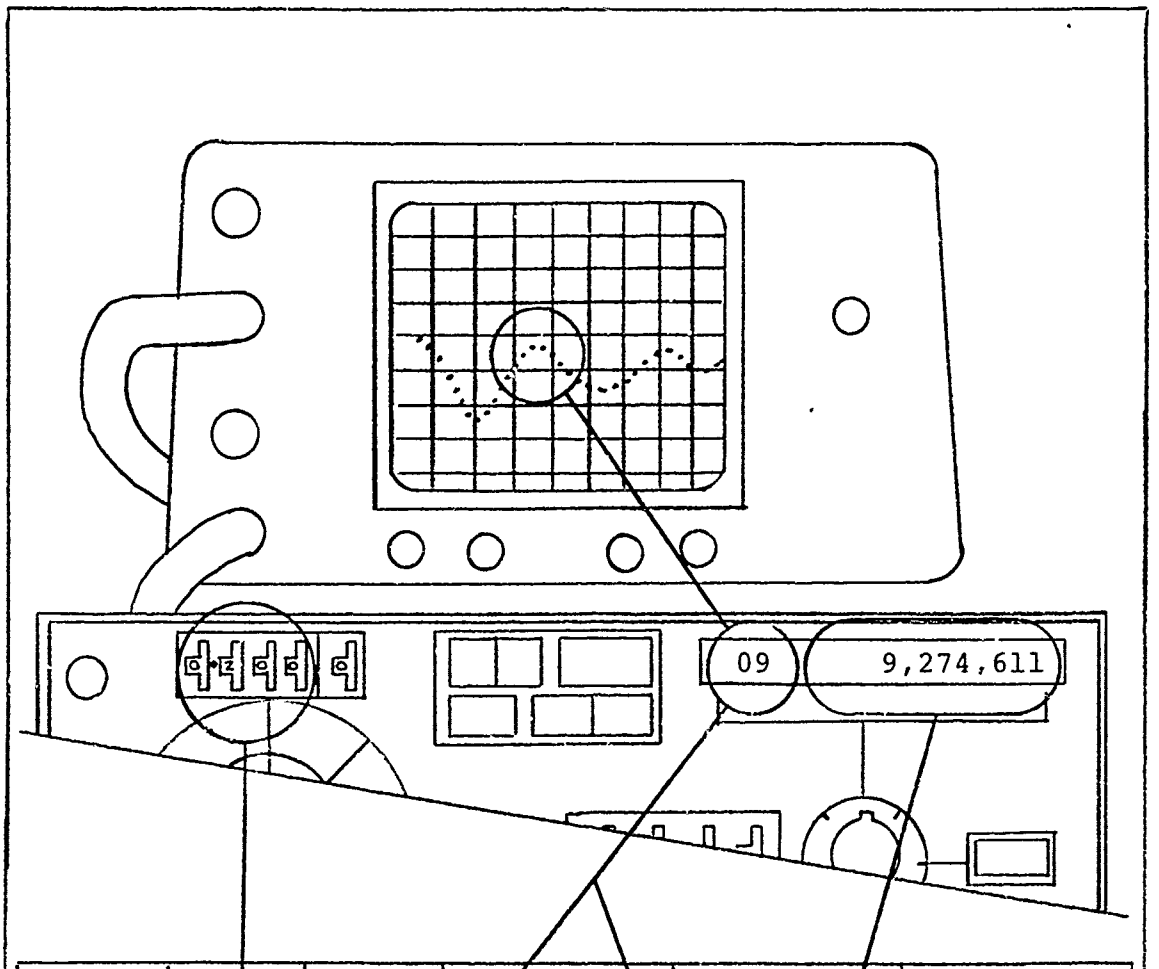

Position (inch)	Sample Time $\times 10^{-9}$ sec	Peak	g_1 chan		g_2 chan		g_3 chan	
26	200	9	6	9206946	9	9274611	13	9249040

Figure 15 Mean Velocity and Turbulence Intensity Measurements showing the measurement of g_2.

that point. The purpose for making a traverse at this point, where neither an LV or Hot Wire traverse had been made, was to provide a completely separate velocity profile with which to compare to the other results.

C. Hot Wire Anemometer

As in the case of the Laser Velocimeter, Hot Wire Anemometer measurements were made at each of the three test points as indicated in Figure 14. A total of 5 traverses were made with two traverses each at Positions 2 and 3 and one traverse at Position 1 with the only variable being the % RPM of the engine which, like the LV data, was either 50% or 70%. The traversing mechanism of the hot wire anemometer allowed movement from one wall to a point 25.4 inches away for a total movement of 25.4 inches. This traverse distance was again divided into one inch intervals except at the inlet position, where measurements every two inches were made due to repetition of the results. At each test point, measurements of bridge DC voltage, rms voltage and pressure differences were made. This data, with the previously measured total temperature and pressure in the room as well as the resistance of the probe, was required for the computer program to evaluate the mean velocity and turbulence intensity values. The computer program used was previously developed by Dr. Richard Rivir of the Propulsion Laboratory.

I. RESULTS AND DISCUSSION OF RESULTS

A. Laser Velocimeter Results

In the following pages, the mean velocity and turbulence intensity profiles are presented with the order of presentation being as follows:

1. Position #1; RPM 50%; Mean velocity profile
2. Position #1; RPM 50%; Mean velocity profile
3. Position #1; RPM 70%; Mean velocity profile
4. Position #1; RPM 50%; Turbulence intensity profile
5. Position #1; RPM 50%; Turbulence intensity profile
6. Position #1; RPM 70%; Turbulence intensity profile
7. Position #2; RPM 50%; Mean velocity profile
8. Position #2; RPM 70%; Mean velocity profile
9. Position #2; RPM 50%; Turbulence intensity profile
10. Position #2; RPM 70%; Turbulence intensity profile
11. Position #3; RPM 50%; Mean velocity profile
12. Position #3; RPM 70%; Mean velocity profile
13. Position #3; RPM 50%; Turbulence intensity profile
14. Position #3; RPM 70%; Turbulence intensity profile

Here the positions correspond to:

1. Position #1 - "White" Pipe midsection
2. Position #2 - 10 feet downstream of flow conditioners
3. Position #3 - 12 inches inside the inlet bell mouth

1. White Pipe Midsection. As the velocity profiles of Figures 16-18 at the 50% engine RPM indicate, both with and without the Phase Modulator in the circuit, as well as at the 70% engine RPM, there is a very discernible "top-hat" or constant peak velocity region of between 10 and 13 inches in width. Ahead of this particular test section is a venturi which has a throat of diameter 13.066 inches and this throat is situated 37.3 inches ahead of the LV test point. On either side of the constant velocity region, the velocities dropped off rapidly and measurements were possible only up to approximately 5 inches from either wall where, due to the flow conditions, which were assumed to be very turbulent, data for the mean velocity and turbulence intensity calculation could not be obtained at this time. In the case of the turbulence intensity profiles of Figures 19-21, each of the three resultant profiles at this position exhibited an "inverted top-hat", each going to zero turbulence for between 5 to 7 inches in the center of the flow and then growing to high turbulence levels on either side of this "ideal flow" area. As the formula as presented in the Malvern text, (Reference 6) which accompanied this equipment, for the calculation of turbulence intensity, is to be used only

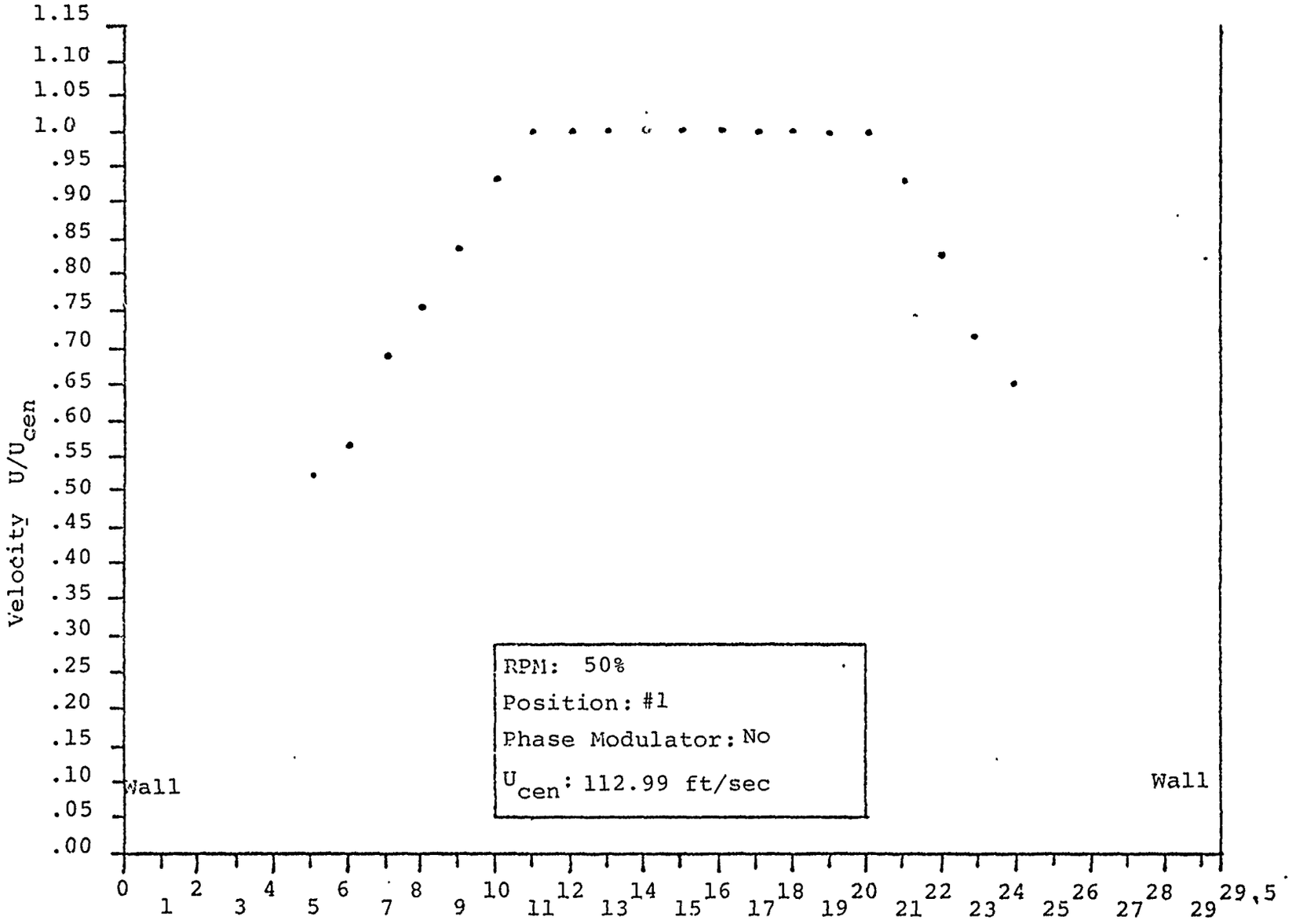

Fig 16 Velocity Profile, Laser Velocimeter

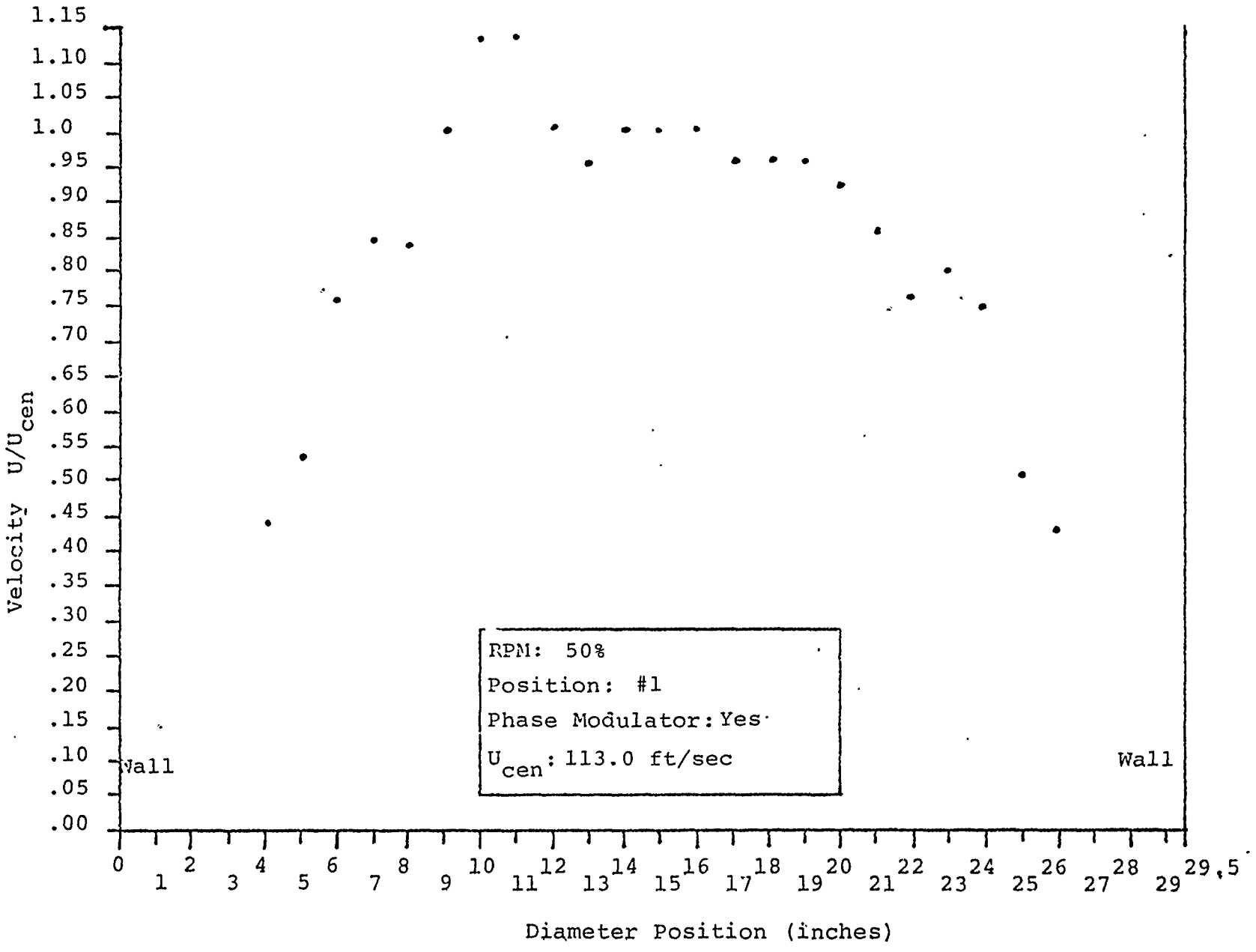

Fig 17 Velocity Profile, Laser Velocimeter

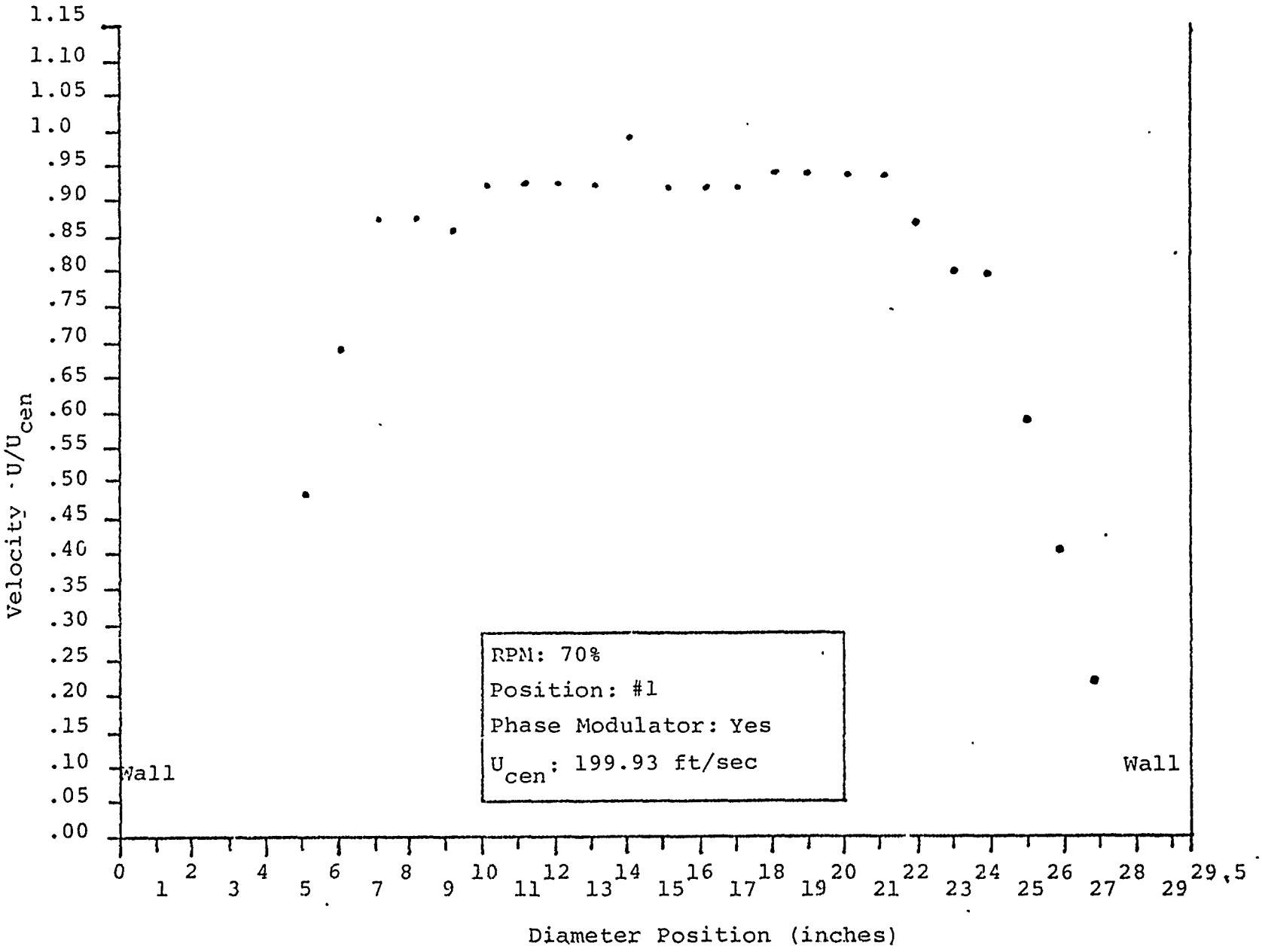

Fig 18 Velocity Profile, Laser Velocimeter

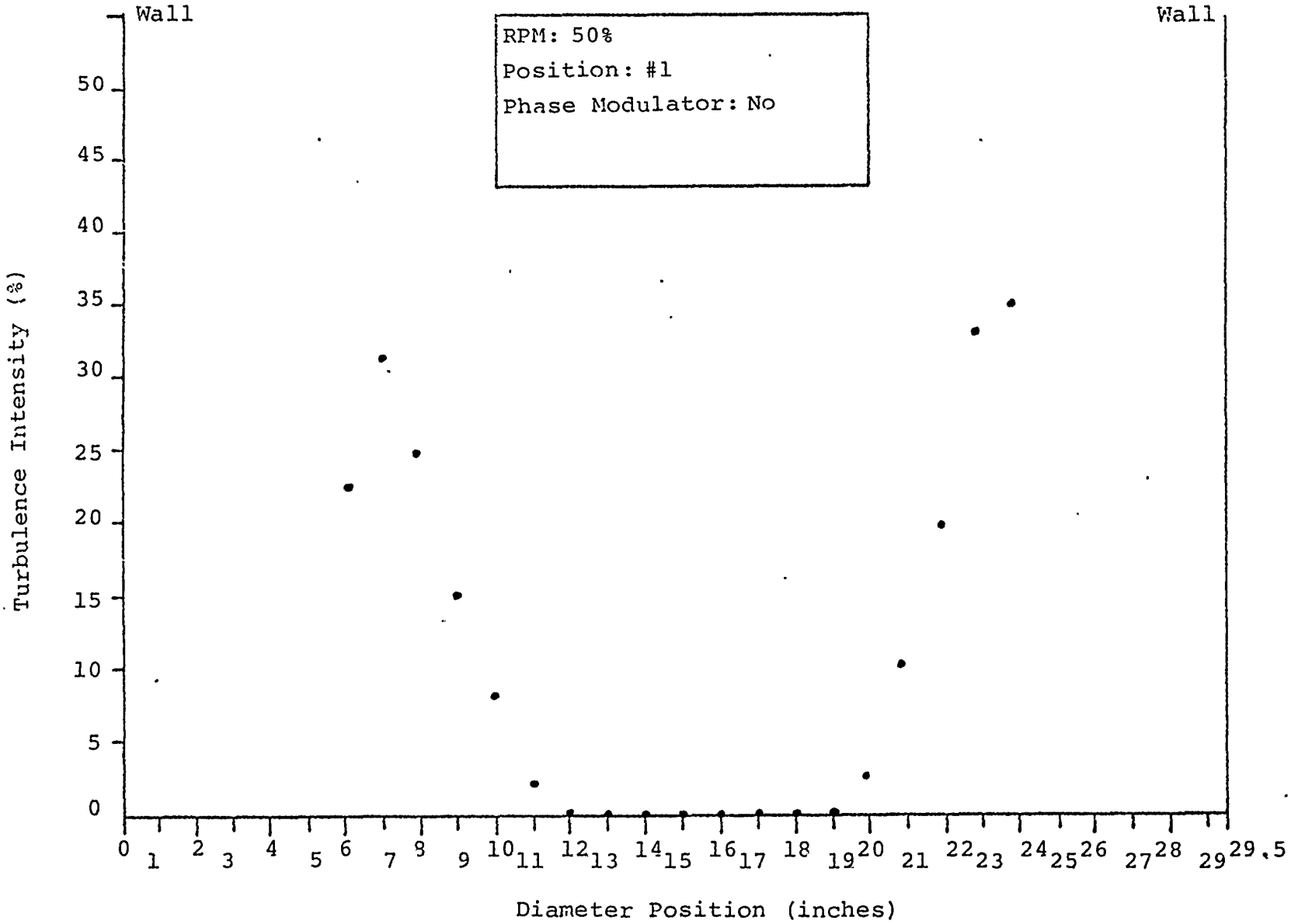

Fig 19 Turbulence Intensity Profile, Laser Velocimeter

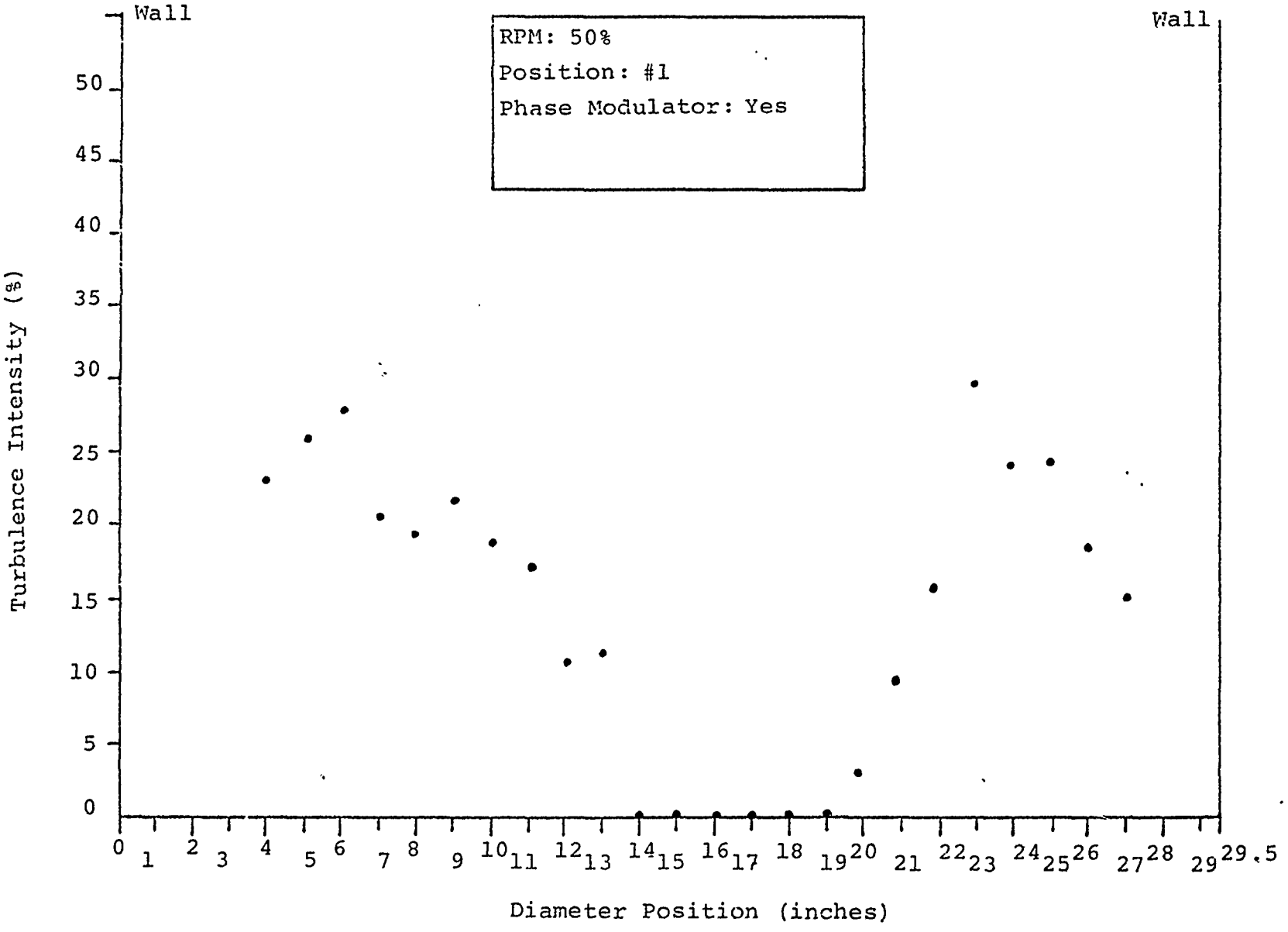

Fig 20 Turbulence Intensity Profile, Laser Velocimeter

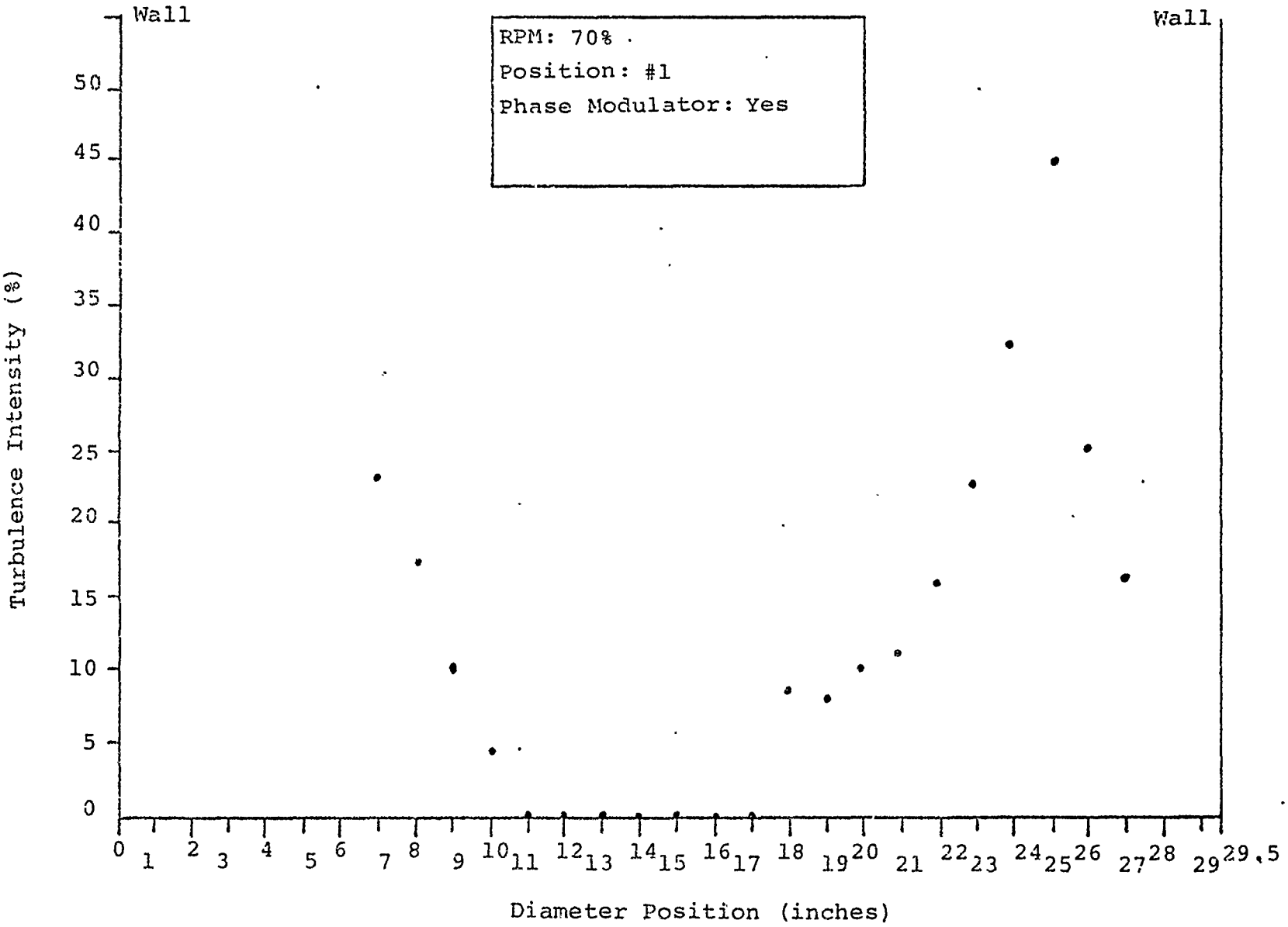

Fig 21 Turbulence Intensity Profile, Laser Velocimeter

up to turbulence (η) levels of .20 (20%), those values over this limit must be viewed accordingly. In some instances, as can be seen from the profiles, turbulence intensity points at the outer edges of the profiles, drop off to lower values. This is due in part to the limitations in discerning "peaks" and "valleys" on the oscilloscope from which the turbulence intensity values are calculated and to the fact that the flow was probably approaching a zero velocity condition and subsequently lower turbulence levels, in this area.

2. Ten Feet Downstream of the Flow Conditioners. At this point in the flow, the velocity profiles (Figures 22-23) once again exhibit the "top-hat" velocity profile only with a reduced width of the constant velocity section, being between 6 to 8 inches in width. On either side of this level section, the velocities drop off gradually, and at a much slower rate than was experienced at Position #1. Ahead of this particular position, by 10 feet, there is a section of the pipe which contains a number of different types of flow straighteners and conditioners with their primary purpose being to reduce the boundary layer thickness and produce a constant velocity profile for the compressor to "digest".

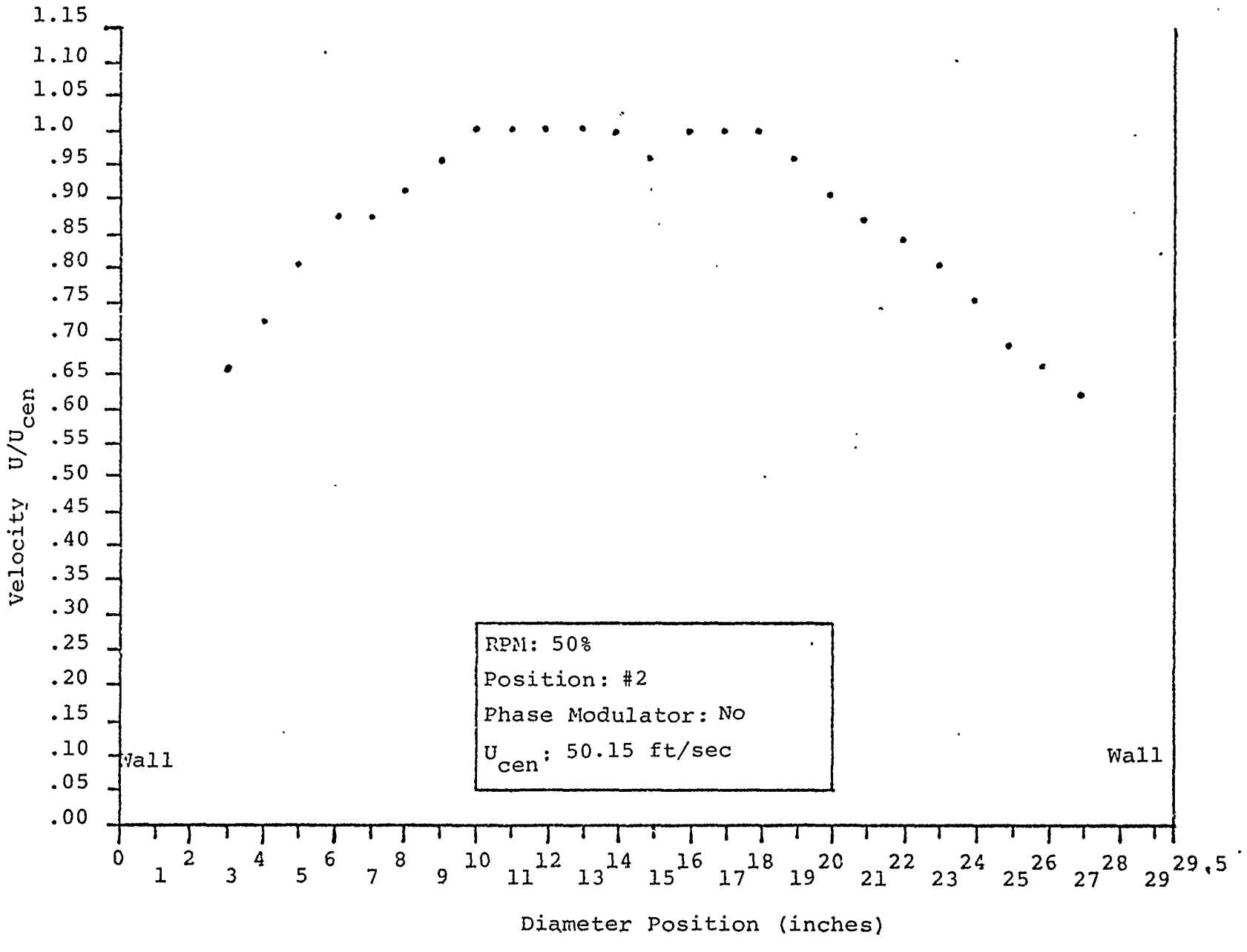

Fig 22 Velocity Profile, Laser Velocimeter

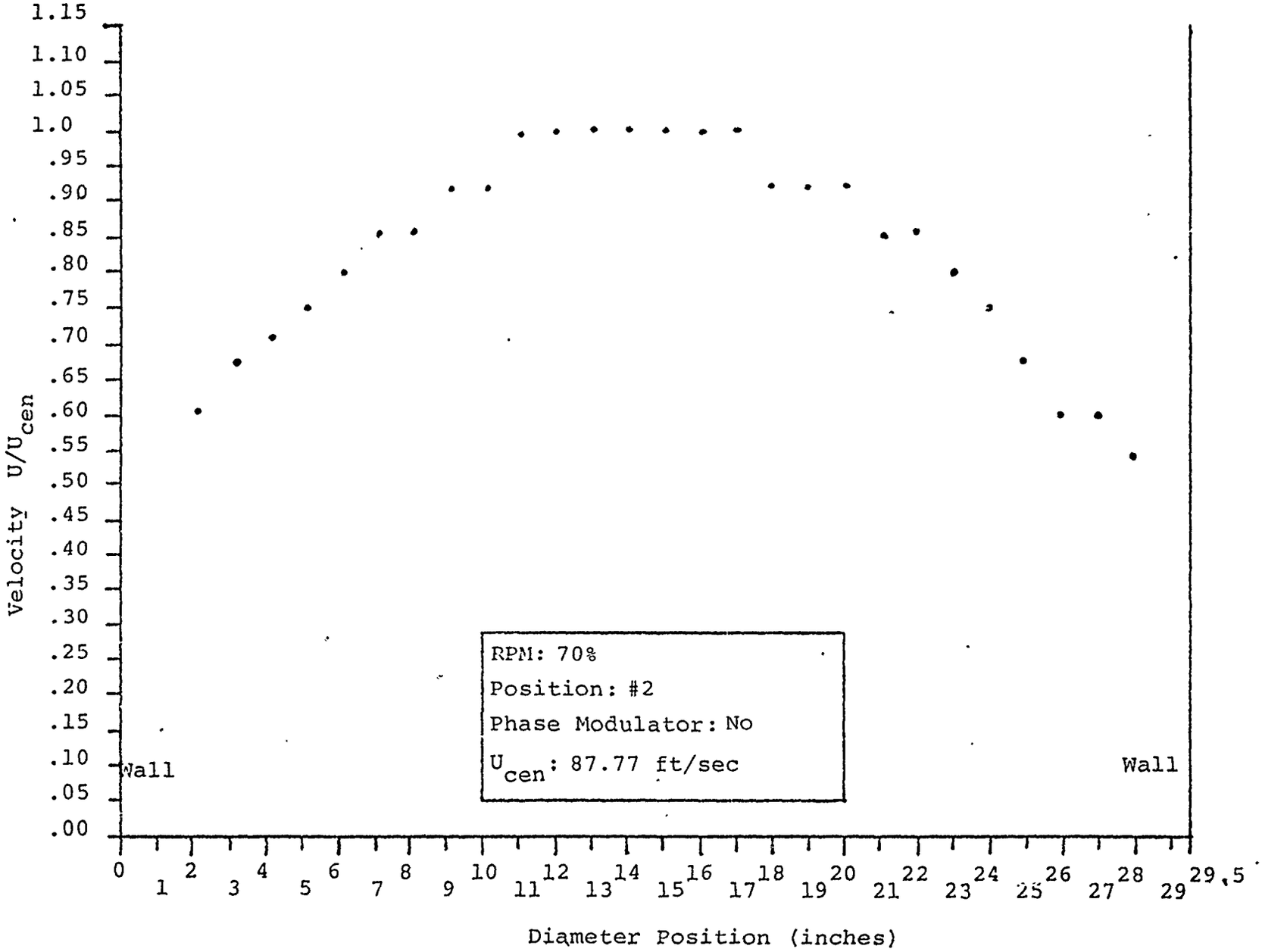

Fig 23 Velocity Profile, Laser Velocimeter

As can be seen by the velocity profiles and the turbulence intensity profiles (Figures 24-25), these conditioners are being reasonably successful at this job although the boundary layer is once again starting to form and the turbulence levels in the outer regions are beginning to increase again.

3. Twelve Inches Downstream of the Inlet Bell Mouth. As can be seen immediately from Figures 26-29 the velocity profile for the inlet is almost entirely flat or at constant velocity with only small fluctuations. Unfortunately due to the incapability of the LV system to operate in the close vicinity of either wall, a velocity drop-off cannot be seen at either RPM condition which, in essence, is due to the fact that the boundary layer has just begun to build. The turbulence intensity levels experienced, fluctuated from zero to four percent with the profile at the 70% RPM condition being almost entirely zero. Ahead of this test section, there is a circular arc bell mouth which has an outside diameter of 59.5 inches and an inside diameter of 29.5 inches. Ahead of this bell mouth is a filter box into which the air flows for the White Pipe which, in addition to filtering the air, reduces the effect of wind gusts on the air entering the pipe.

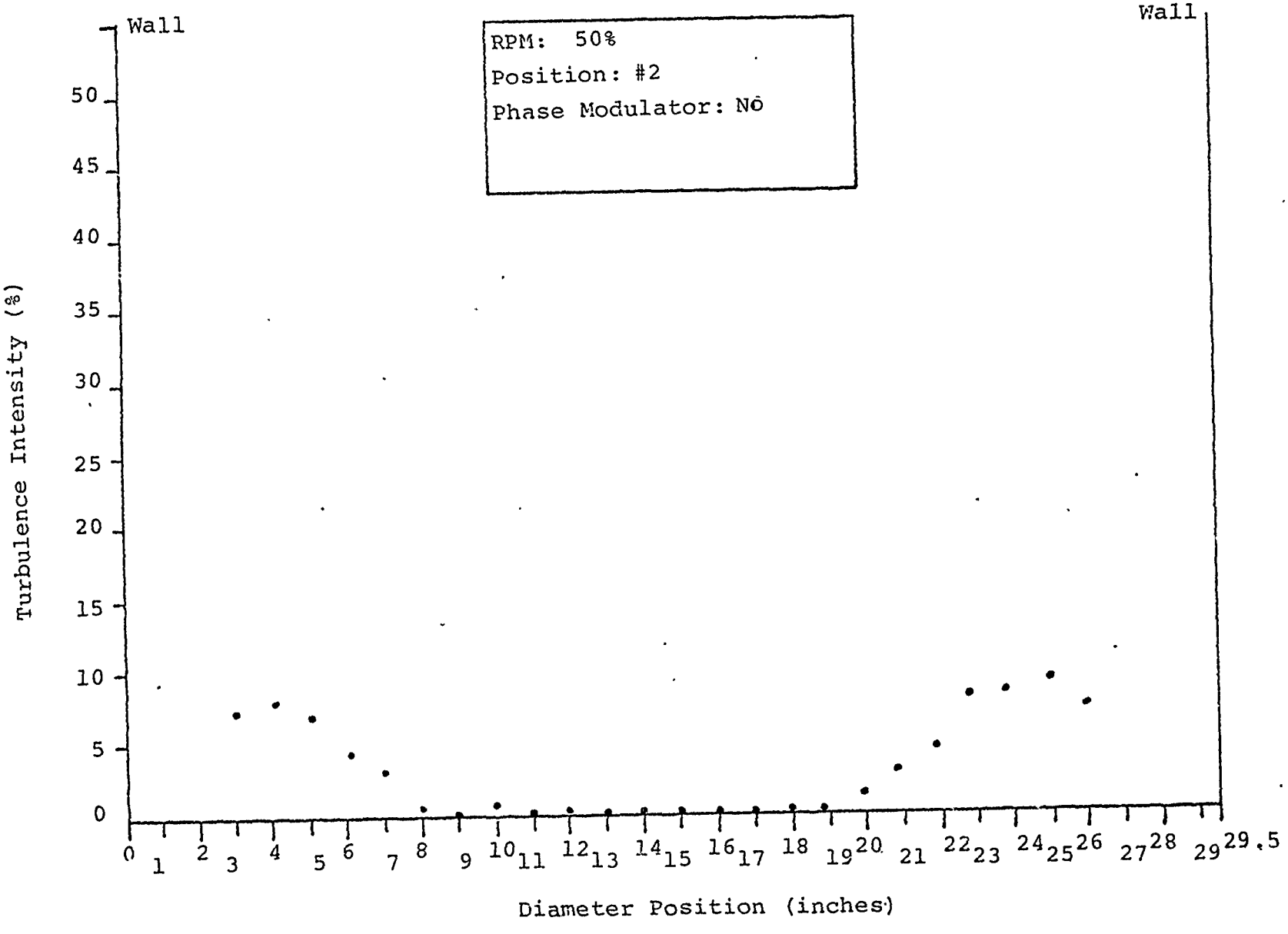

Fig 24 Turbulence Intensity Profile, Laser Velocimeter

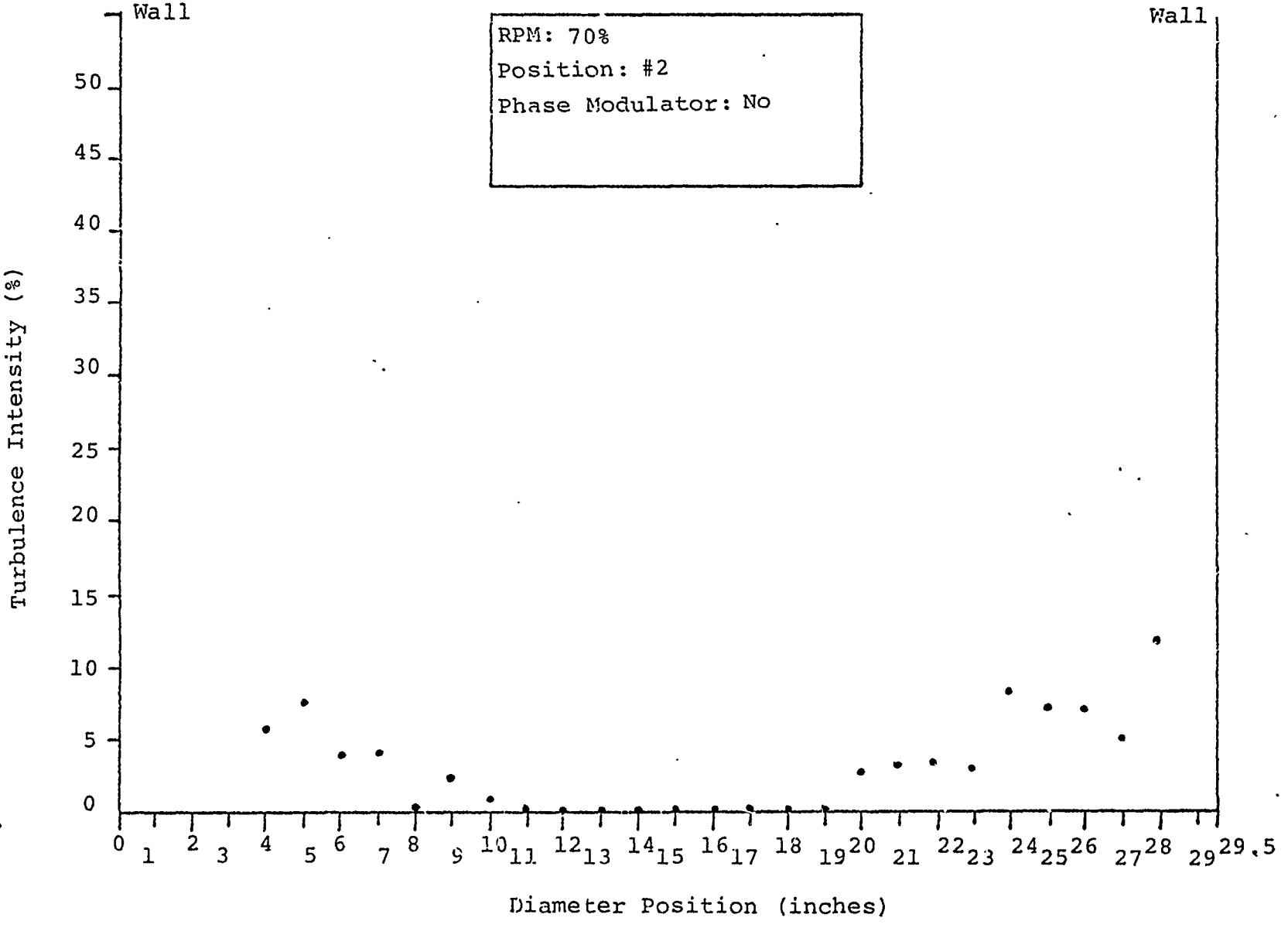

Fig 25 Turbulence Intensity Profile, Laser Velocimeter

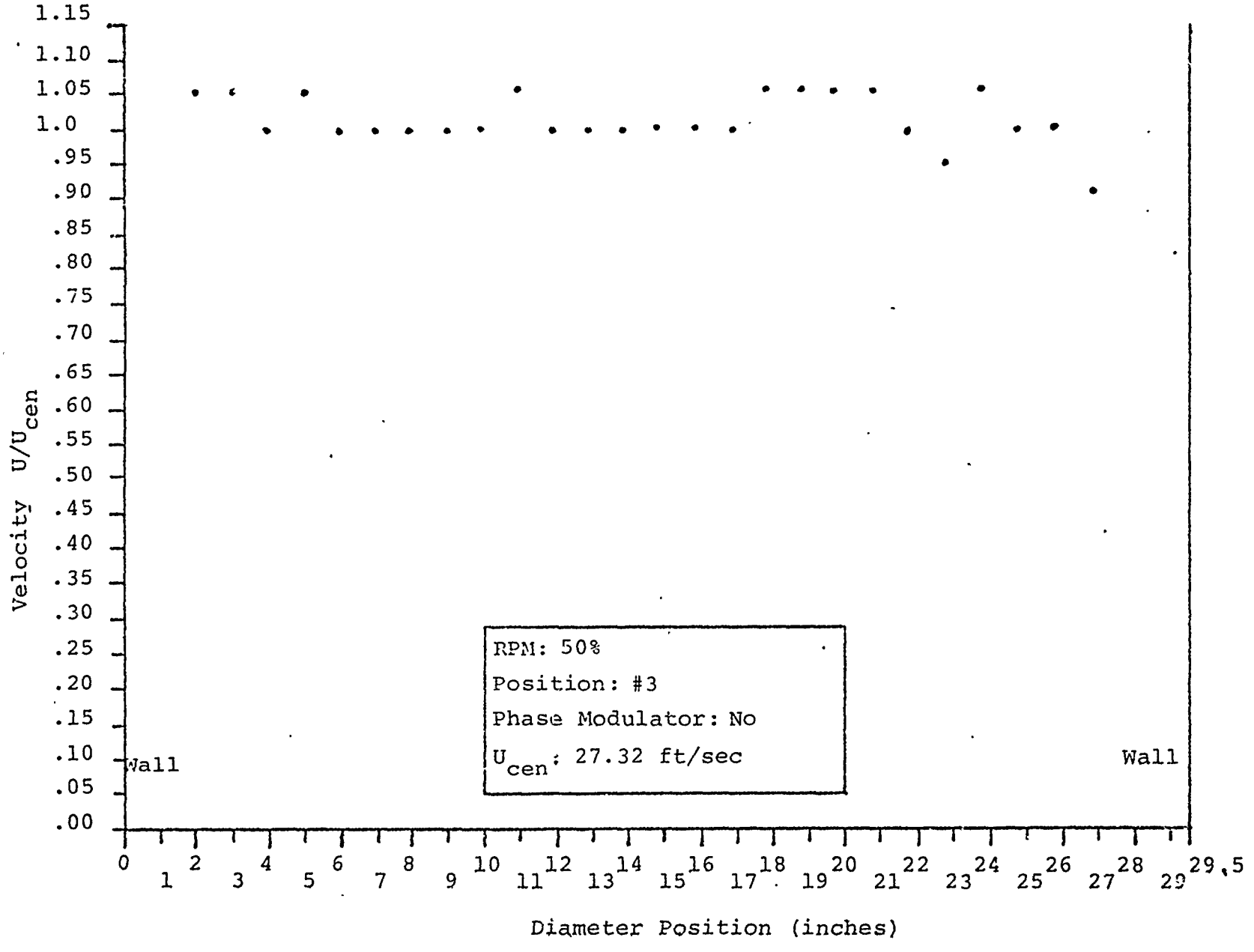

Fig 26 Velocity Profile, Laser Velocimeter

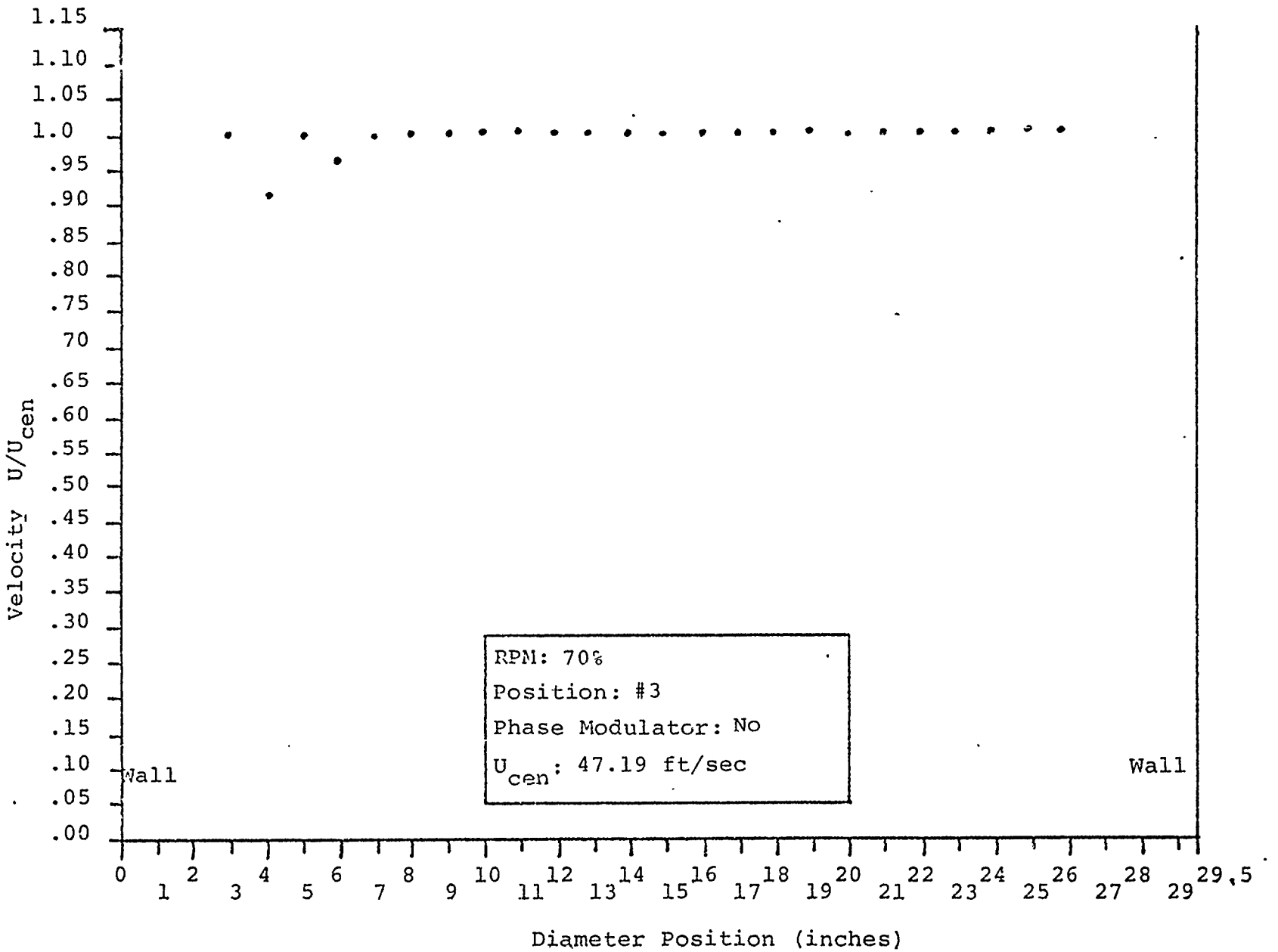

Fig 27 Velocity Profile, Laser Velocimeter

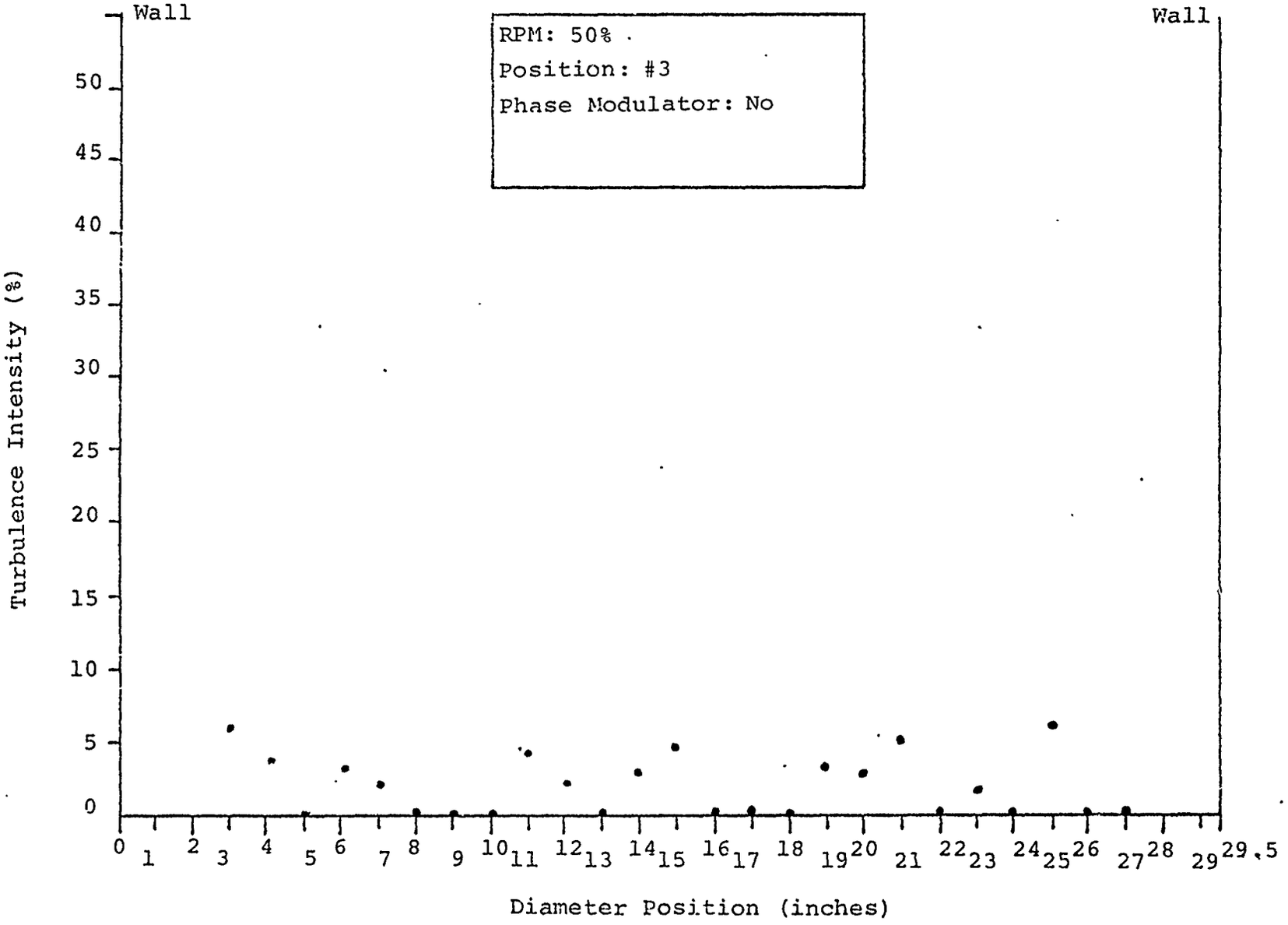

Fig 28 Turbulence Intensity Profile, Laser Velocimeter

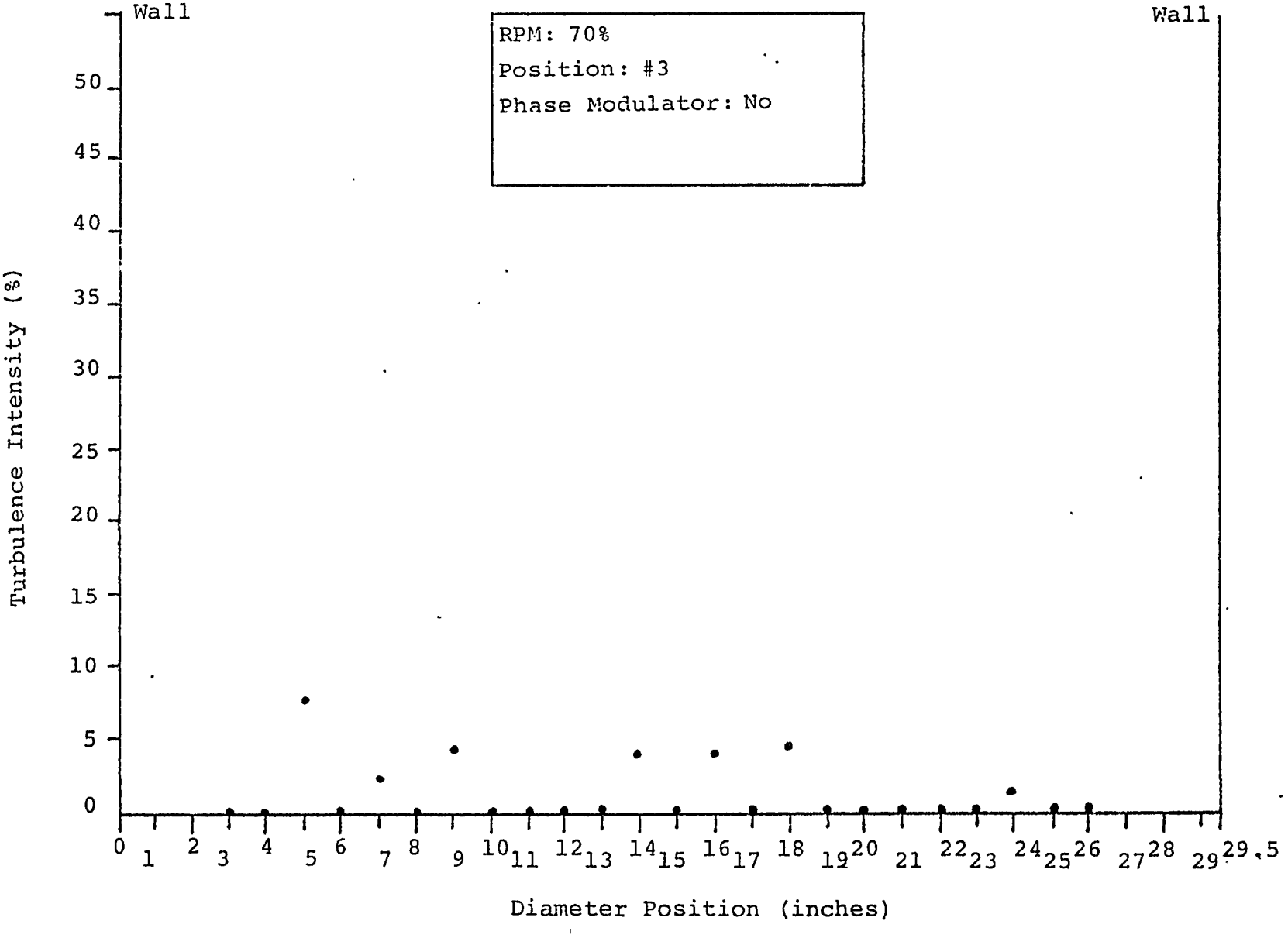

Fig 29 Turbulence Intensity Profile, Laser Velocimeter

B. Hot Wire Anemometer Results

The following are the velocity and turbulence intensity profiles as obtained by the Hot Wire Anemometer system and as produced from the data in Appendices E and F. The profiles are presented as follows:

1. Position #3; 50% RPM; Mean velocity profile
2. Position #3; 70% RPM; Mean velocity profile
3. Position #3; 50% RPM; Turbulence intensity profile
4. Position #3; 70% RPM; Turbulence intensity profile
5. Position #2; 50% RPM; Mean velocity profile
6. Position #2; 70% RPM; Mean velocity profile
7. Position #2; 50% RPM; Turbulence intensity profile
8. Position #2; 70% RPM; Turbulence intensity profile
9. Position #1; 50% RPM; Mean velocity profile
10. Position #1; 50% RPM; Turbulence intensity profile

the positions correspond to the LV positions.

1. 12 Inches Inside the Inlet Bell Mouth. As in in the LV results, an almost completely constant velocity was achieved in the velocity profiles at 50 and 70% engine RPM (Figures 30-31). Due to a restriction in the movement of the traversing mechanism, data could not be obtained in the close proximity of both walls and thus the complete velocity decay was not observed. In the case of the turbulence intensity profiles (Figures 32-33), high turbulence levels across

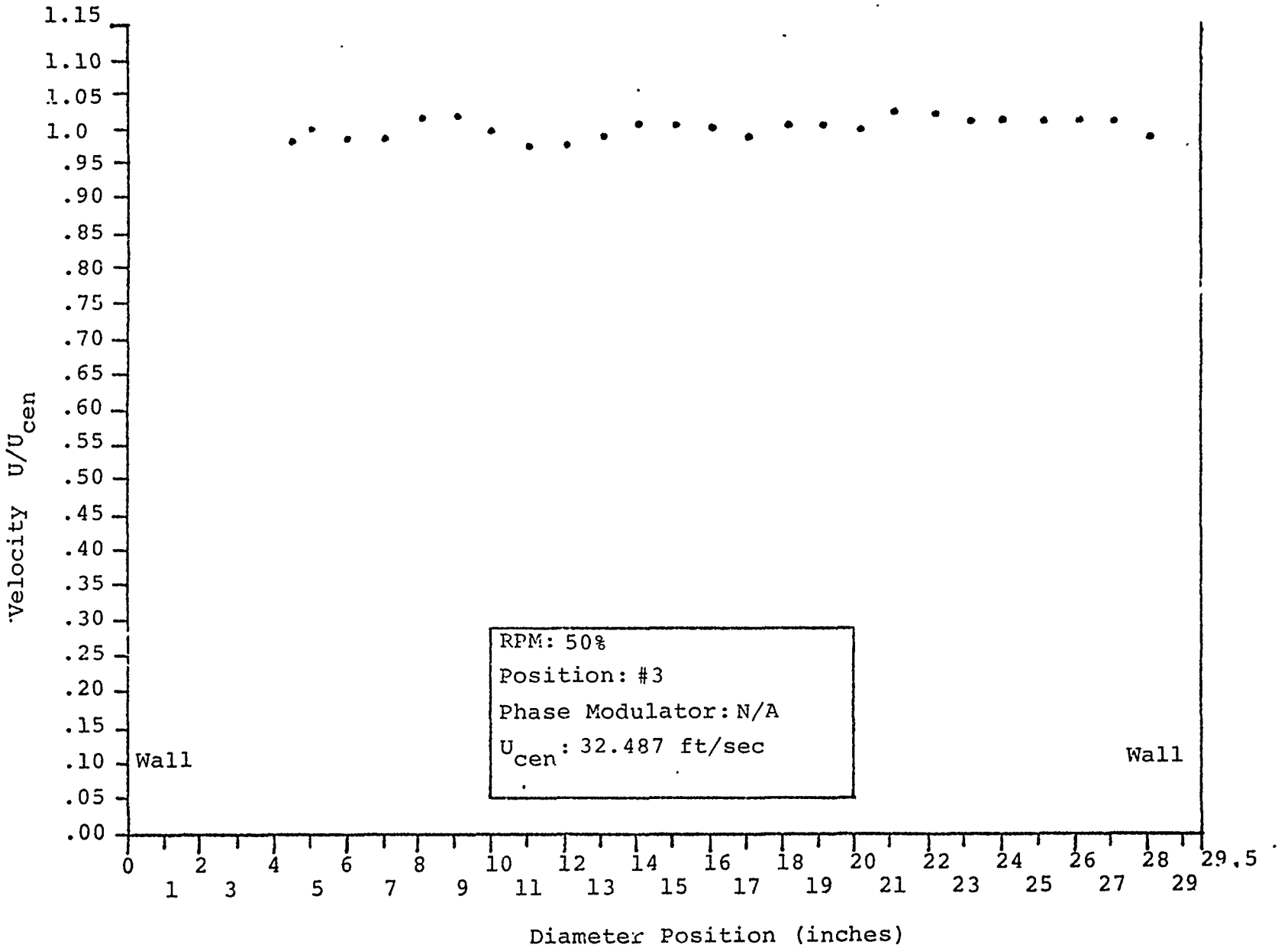

Fig 30 Velocity Profile, Hot Wire Anemometer

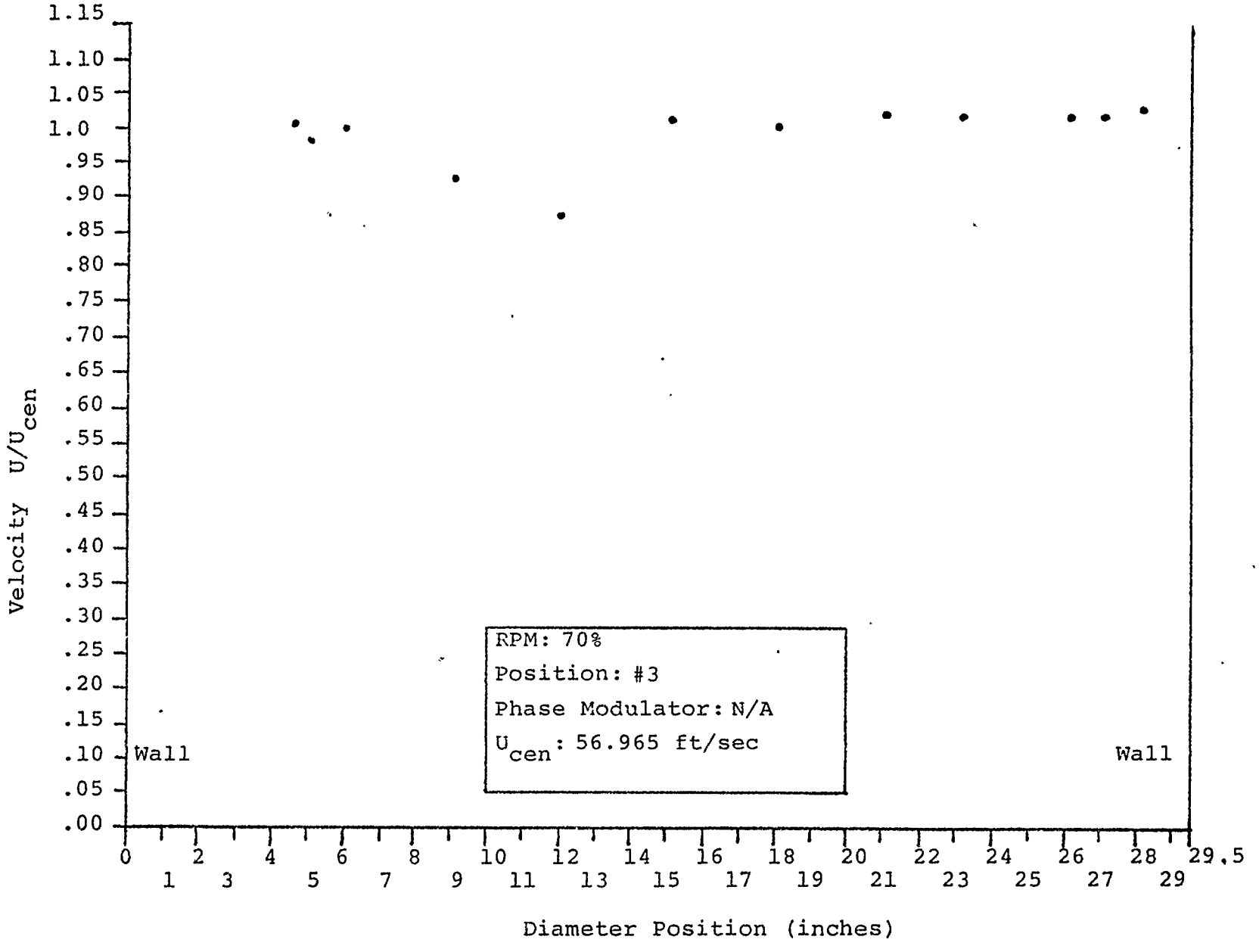

Fig 31 Velocity Profile, Hot Wire Anemometer

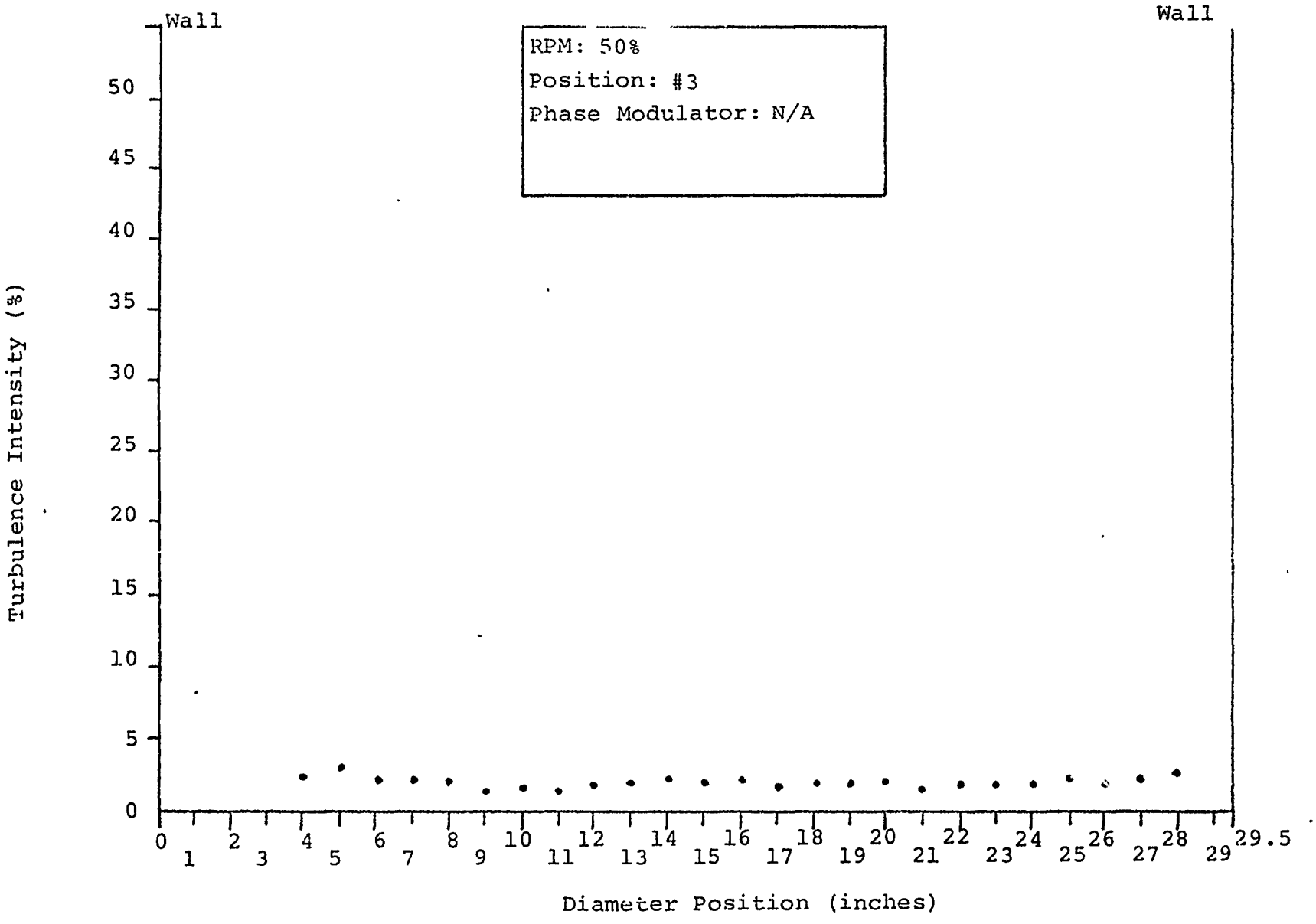

Fig 32 Turbulence Intensity Profile, Hot Wire Anemometer

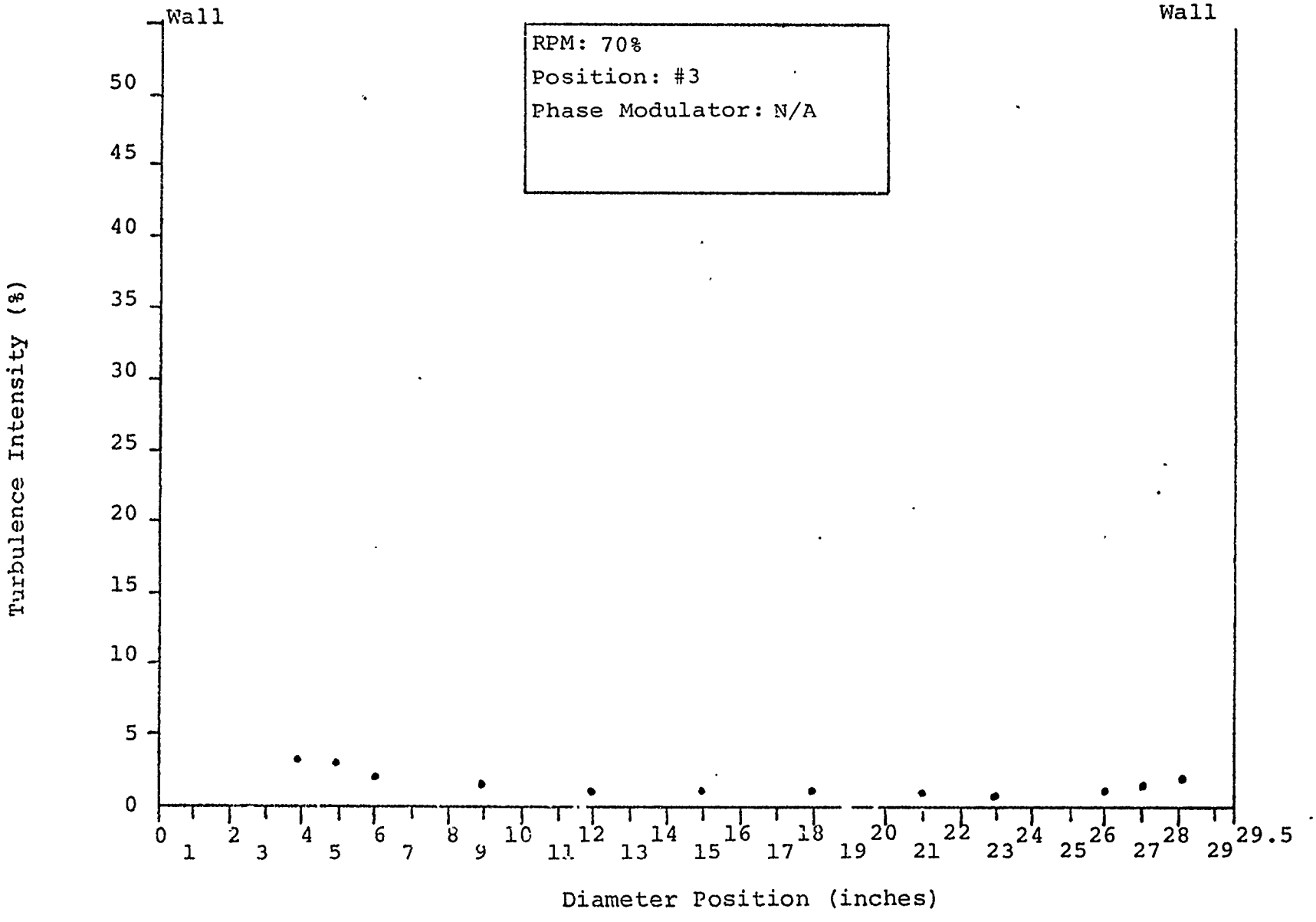

Fig 33 Turbulence Intensity Profile, Hot Wire Anemometer

the entire flow were experienced, with the lowest level being about 1.2% at the centerline when the engine was operating at 70%.

2. Ten Feet Downstream of the Flow Conditioners. Upon comparison of the Hot Wire mean velocity [illegible] (Figures 34-35) at the White Pipe [illegible]section with those obtained by the LV system, almost identically shaped profiles are the result. There exists however, a difference in the centerline velocities which in the case of the Hot Wire are 12 and 21 ft/sec lower [illegible]n at the same point as determined by the LV (for 50% and 70% RPM respectively). In addition to differing centerline velocities, the regions of constant velocity are somewhat [illegible]er in the Hot Wire profiles than they are in the LV profiles, while the velocity drop-off is at almost exactly the same rate. The turbulence intensity profiles (Figures 36-37) are very well defined and are shaped as expected with the turbulence levels approaching 12% on either side (or close to the wall) and 3% along the centerline of the pipe. These profiles are quite similar to the LV turbulence intensity profiles, especially in the area of maximum turbulence, but differ around the centerline where the LV profiles go to zero levels of turbulence.

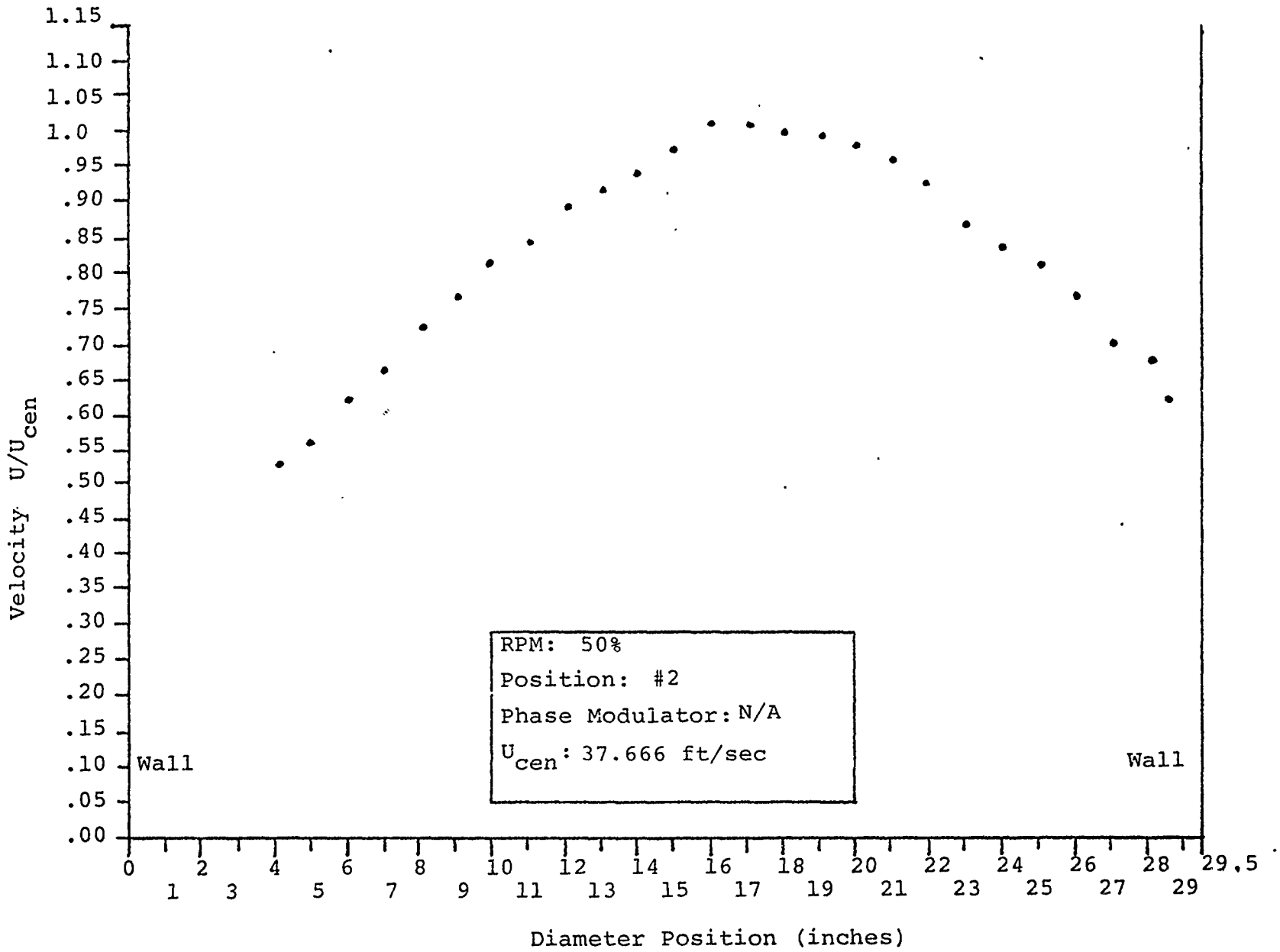

Fig 34 Velocity Profile, Hot Wire Anemometer

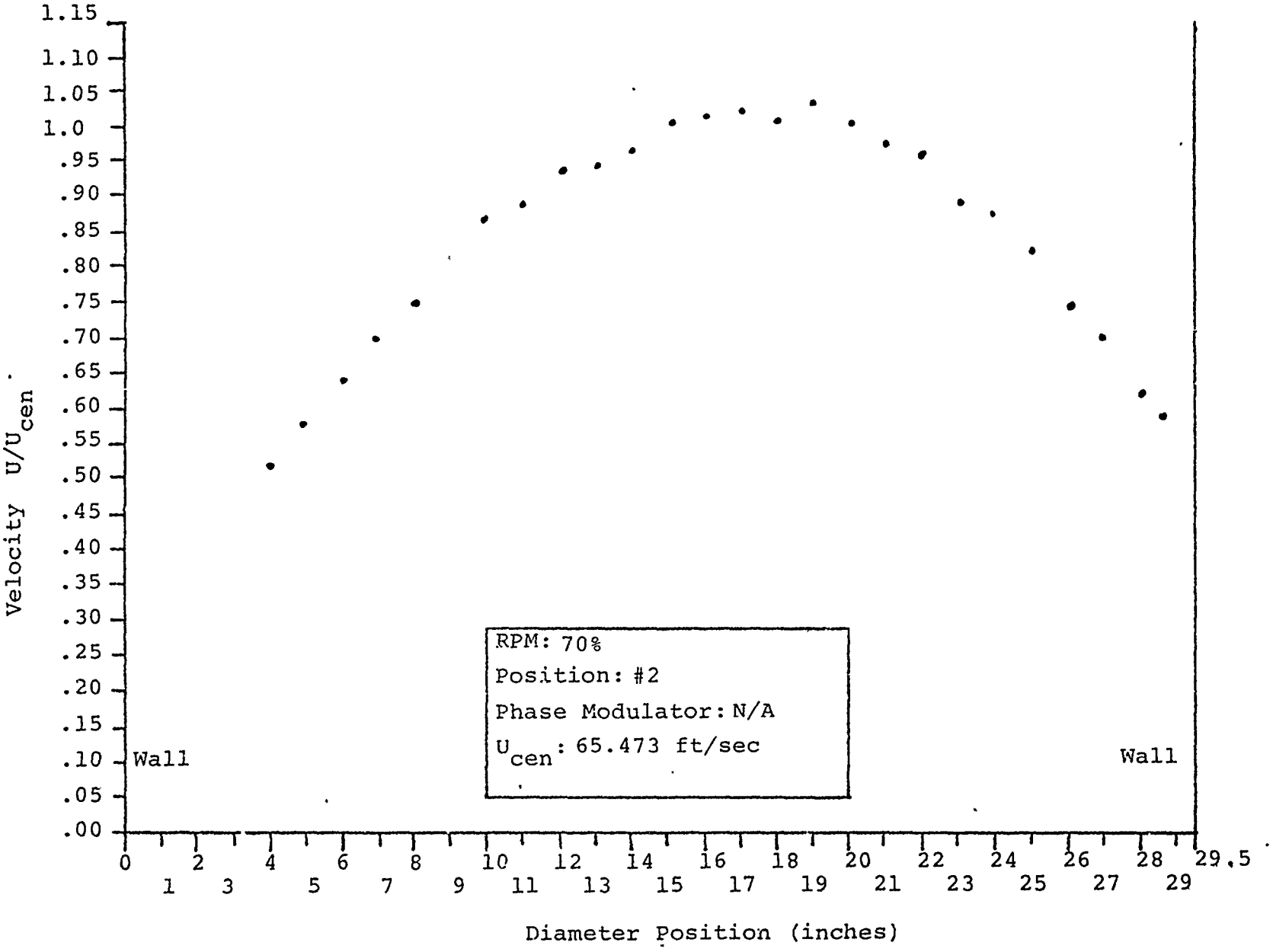

Fig 35 Velocity Profile, Hot Wire Anemometer

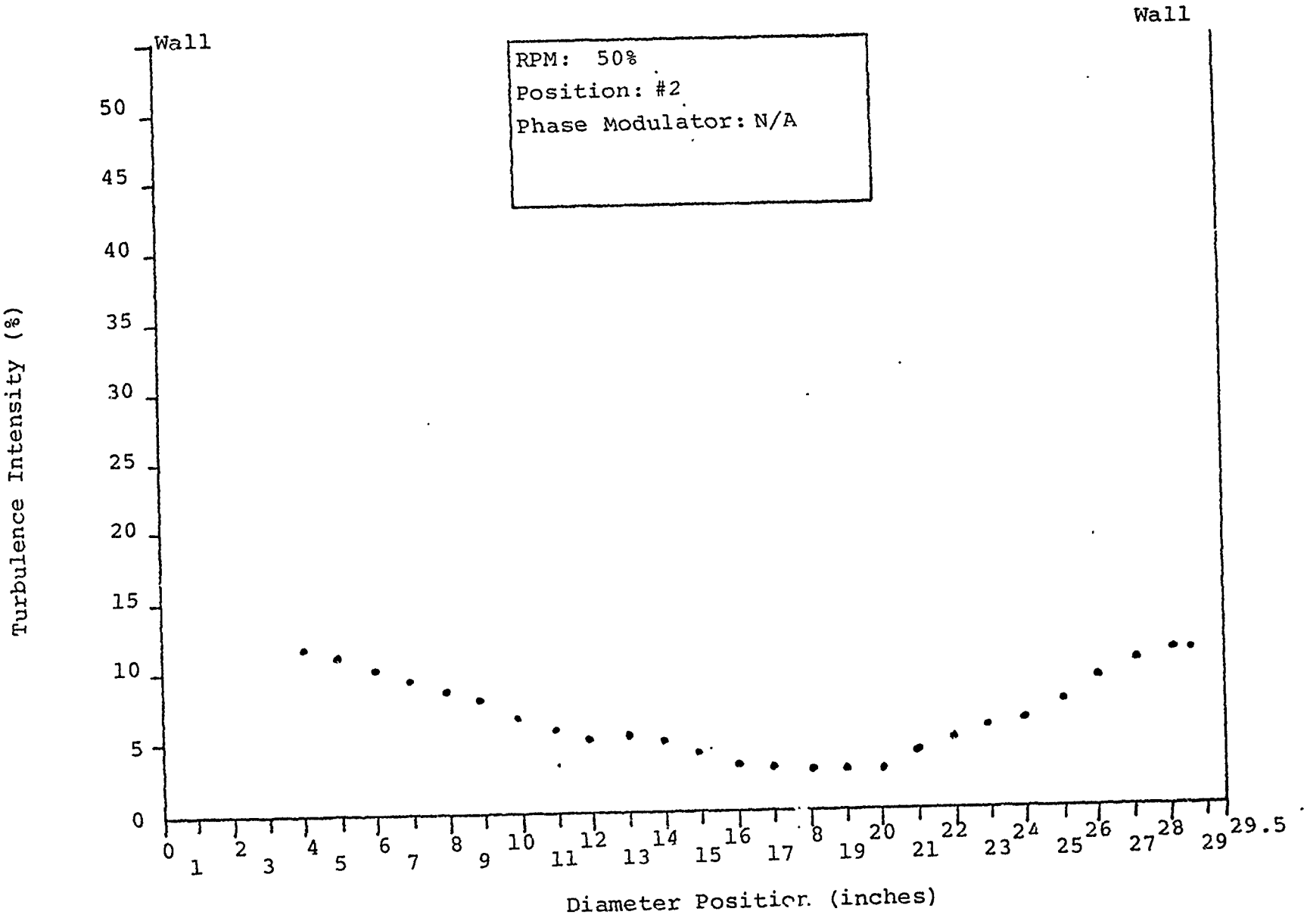

Fig 36 Turbulence Intensity Profile, Hot Wire Anemometer

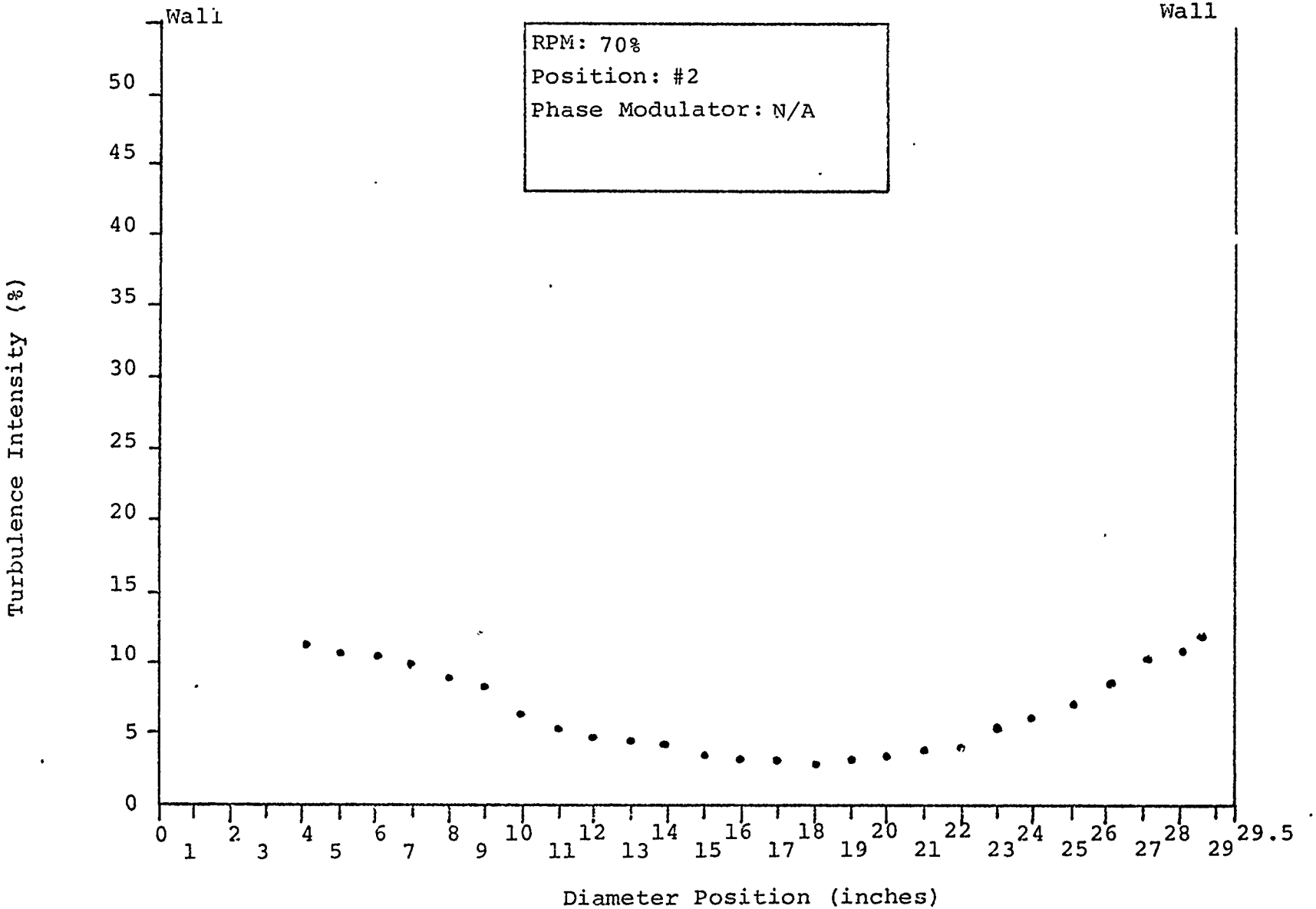

Fig 37 Turbulence Intensity Profile, Hot Wire Anemometer

3. White Pipe Midsection As expected, by the relatively close proximity of this position to the venturi, the velocity profile (Figure 38) displays an almost perfect fully developed turbulent flow velocity profile with a centerline velocity of 126 feet per second which decays to 10 feet per second at points about 4 inches from either wall. The width of the constant velocity section is about 11 inches which, when compared to the venturi throat diameter of 13.066 inches, appears very consistent. The turbulence intensity profile (Figure 39) indicates very low levels of turbulence in the center portion of the flow but soars to extreme levels on either side of this center portion. While the Hot Wire system works well up to turbulence levels of 30-35%, values above this point must be viewed with some skepticism. However, as the turbulence levels reach orders of 60% and greater on either side of the flow, it would appear that the airflow "sees" a wall or region of very slow moving air which would explain the greatly increased centerline velocity required to accommodate the same mass flow. As a point of comparison, the centerline velocity at the same point, as determined by the LV system, was found to be 114 ft/sec which agrees

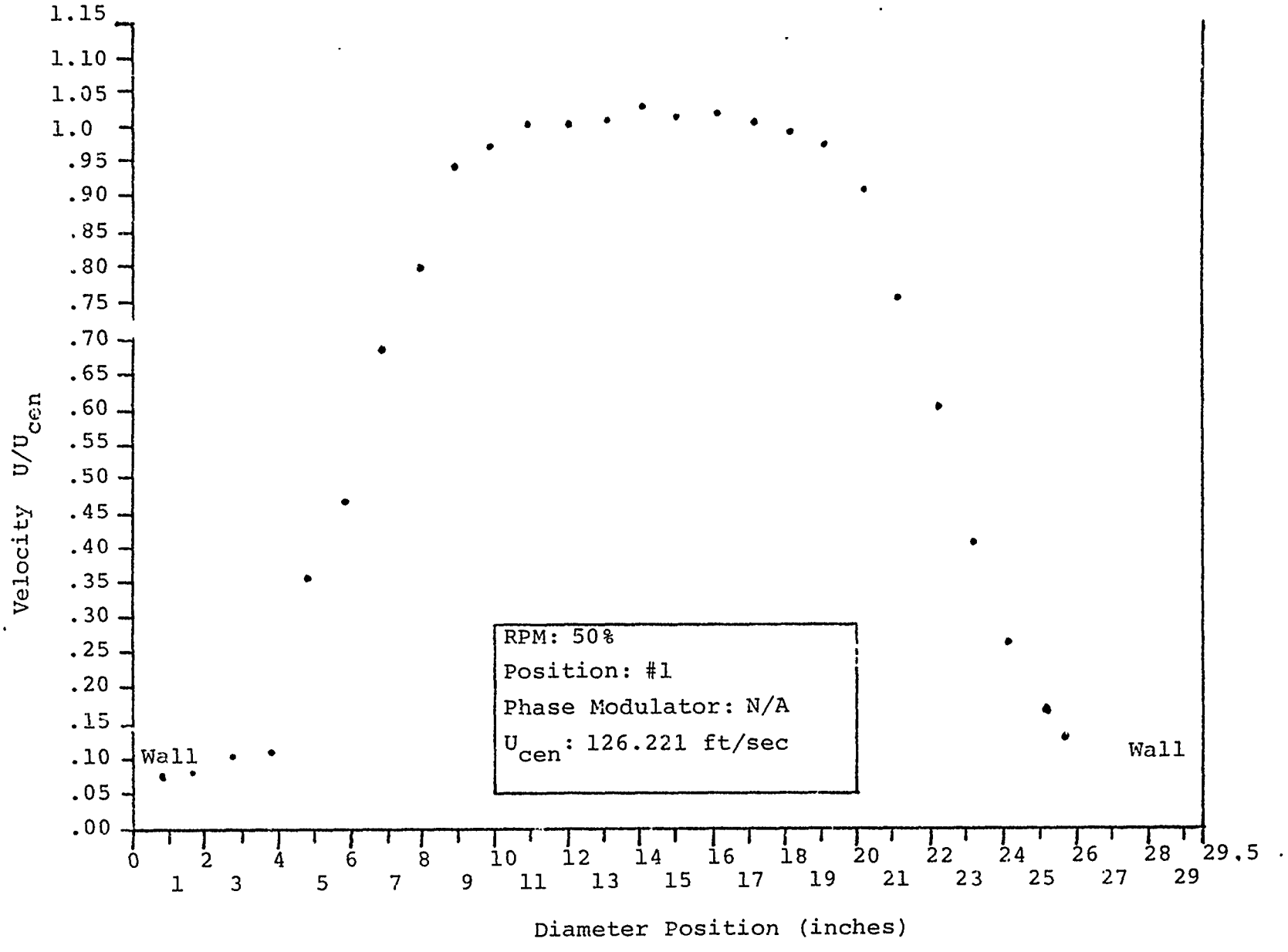

Fig 38 Velocity Profile, Hot Wire Anemometer

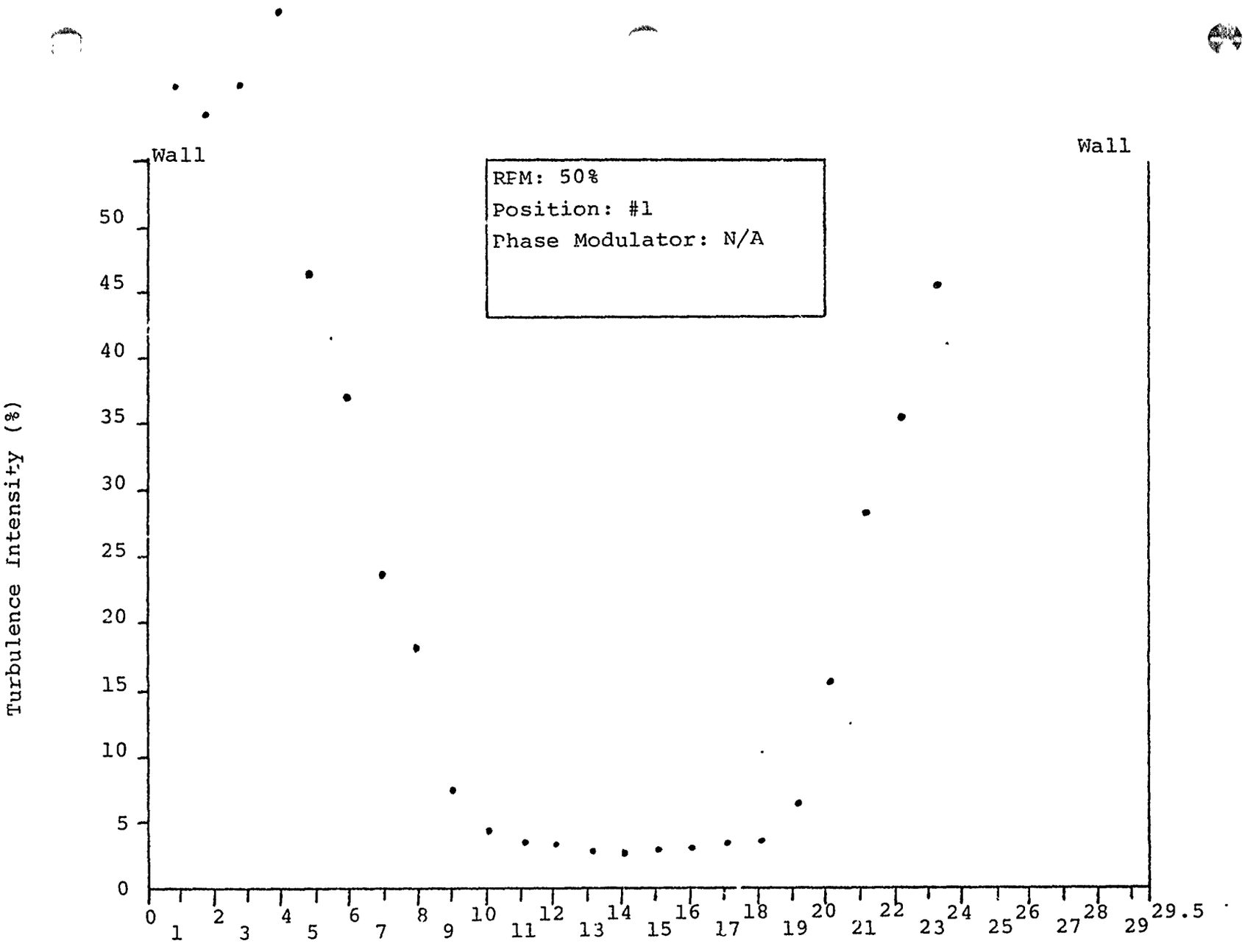

Fig 39 Turbulence Intensity Profile, Hot Wire Anemometer

well with the Hot Wire results. Also, the width of the constant velocity region is almost identical and the drop-off of velocity on either side is at the same rate. Unfortunately, with the LV system, velocities and turbulence intensity levels could not be determined as closely to the walls as could be done with the Hot Wire system. A traverse at 70% RPM could not be completed at this time due to engine control problems.

C. Pitot-Static Tube Results. As previously stated, all of the Pitot-static data was taken at a single position as indicated in Figure 14 and at the two RPM's of 50% and 70%. The data points extended from 2.82 inches from one wall to 18 inches from the same wall. On the following Figures 40-41, the mean velocities for the poitns 2.82 inches through 15 inches are displayed and then the same data is used to plot from 15 inches to 27.18 inches, creating a "mirror image" as symmetrical flow conditions were assumed. The data that was recorded is presented in Appendix G with the numerical results presented in Appendix H. As can be seen on the graphs, the centerline velocities have increased somewhat from these same values at the bell mouth inlet. This is due to the fact that the boundary layer has begun to build up and the effective area through which the air flow can pass has been reduced, causing the increase in velocity. Unfortunately, due to the

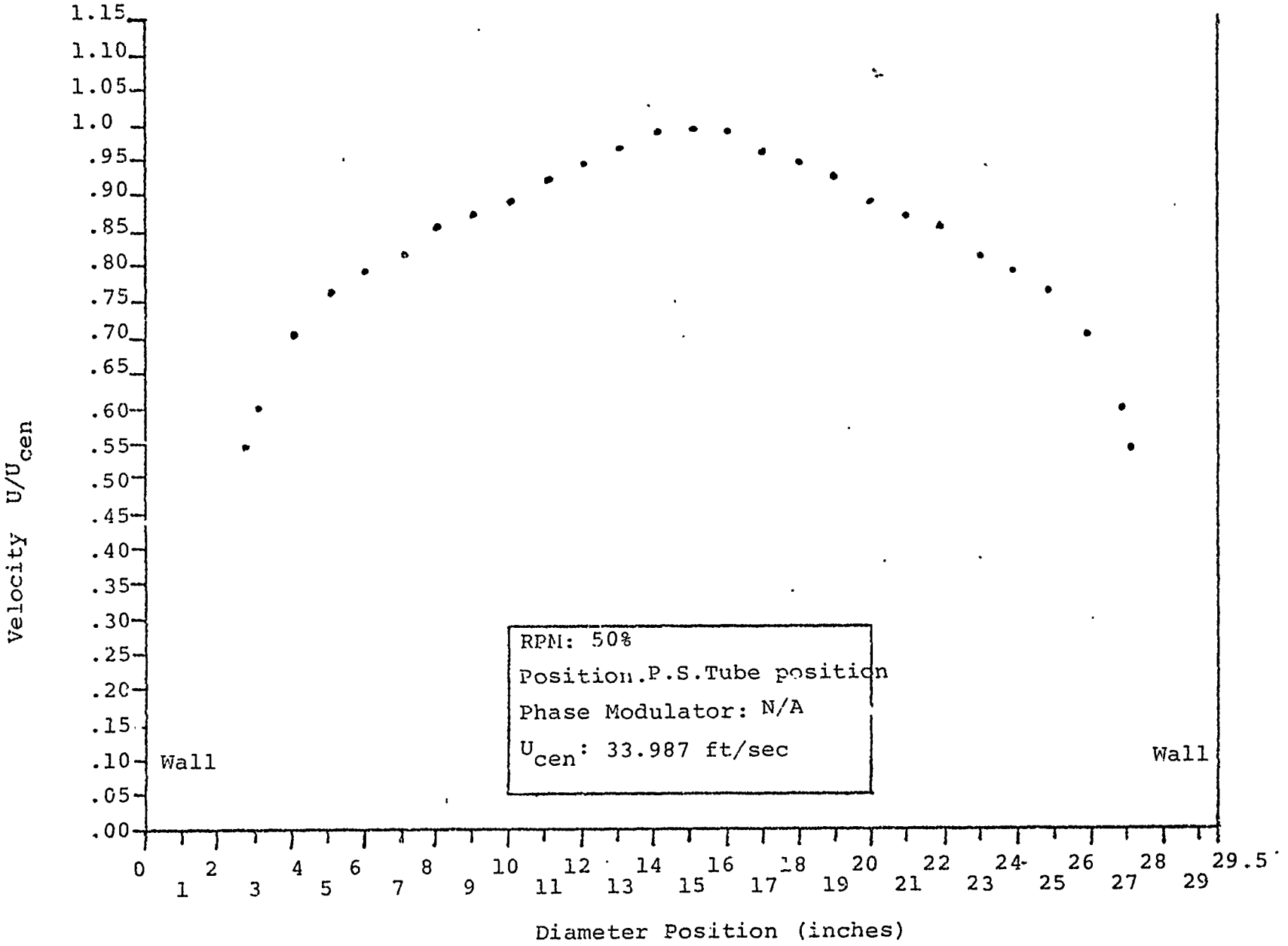

Fig 40 Velocity Profile, Pitot-Static Tube

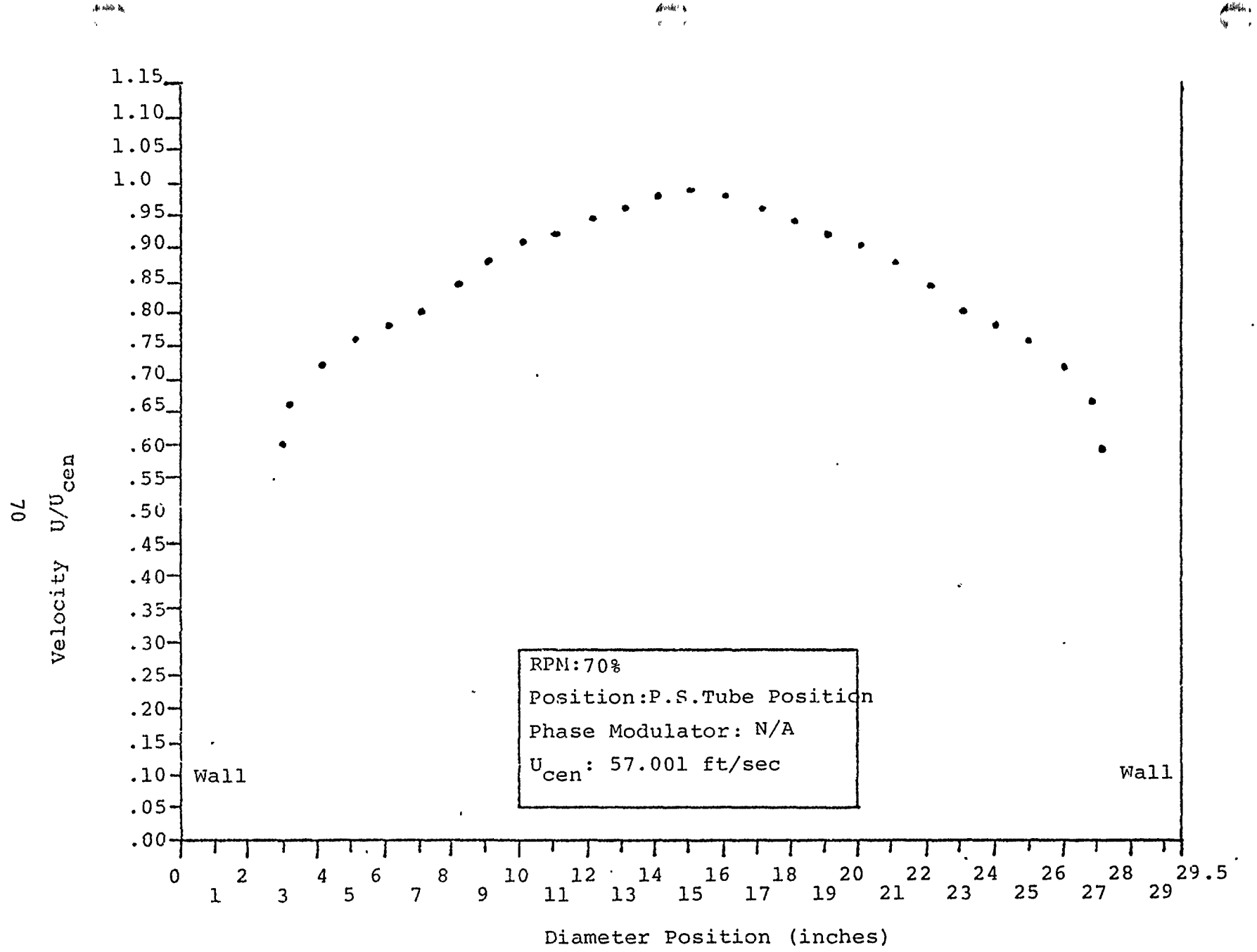

Fig 41 Velocity Profile, Pitot-Static Tube

limitations imposed by the traversing mechanism, the complete velocity drop off, and thus the width of the boundary layer, could not be determined.

VII. CONCLUSIONS

After looking back over the results as obtained, a number of conclusions have come to the fore-front. The goals that were originally set as the guides for the evaluation of this study have all been met with what the author feels is a high degree of success. The conclusions are as follows:

A. Good agreement is in evidence with respect to the mean velocity profiles obtained at the various White Pipe locations and engine RPMs, using the Laser Velocimeter System (LV) and the Hot Wire Anemometer System. By the fact that good correlation was achieved between this relatively new system and the much used and "time honored" Hot Wire System, the results obtained by the LV System can be viewed as credible.

B. With respect to the Turbulence Intensity profiles, the LV, even with the Phase Modulator in use, appears incapable of measuring turbulence levels of the order of 1.5% to 2.0% and lower. Also, by the information given in the instruction manual, values of turbulence intensity above 20% should not be trusted. In the area between 2% and 30%, the LV results have agreed quite well with the Hot Wire results and thus can be viewed as a good indication of the conditions present in these areas of the pipe.

C. At all three locations where the LV traverses were performed, centerline velocities were encountered which were different than these respective velocities as measured by teh Hot Wire Anemometer System. First of all, the LV System measures the mean velocity of the particles whereas the Hot Wire measures the mean velocity of the medium flowing in the pipe. These differences in velocity can be explained by the possible fact that due to the size of the particles in the air (which for Dayton, Ohio, a mildly industrialized area, can approach 80 μm) and the forces imparted onto these particles by upstream contractions and expansions in the flow path, velocity differences between the particles and the flow can occur. Further evaluation of this theory is contained in Appendix J.

D. Recordings of the weather conditions in existence on each day of testing were kept. Viewing these conditions, which ranged from hot and muggy to very dry days, it appears that the weather conditions had little or no effect on the results. As the LV System is so dependent on particulate matter in the air, it had been feared that periods of rain before or during a traverse could adversely affect the results. However, at no time, was any "seeding" or artificial introduction of particles into the air necessary.

E. The LV System was not hampered by the main problem inherent to the t Wire and Pitot-static Systems which concerns the placement of a traversing mechanism and probe or Pitot-tube into the flow field.

F. As the speed or RPM of the engine was set at the two distinct RPM settings by the use of a tachometer, the possibility of slight variations in actual engine RPM is a definite possibility. This, when coupled with different temperatures of the air in the White Pipe, would definitely lead to different mass flow rates in successive tests. With different mass flow rates, different velocities for the same point as determined by different flow velocity measurement methods would undoubtedly become evident which can, in part, explain the difference in these velocities, as observed.

VIII. RECOMMENDATIONS

Based on the work that has now been completed employing the Laser Velocimeter System as the principle experimental device for measurements, the following recommendations for further projects are put forth:

1. Repeat this study of flow conditions at various other locations along the length of the "White Pipe" to completely investigate and map out any velocity and turbulence intensity fluctuations. These alterations in the flow condition should be especially evident around the flow conditioners and venturis as well as any other projection in the flow such as probes and measuring devices.
2. Using the LV System, input conditions into the White Pipe flow such as different types of flow conditioners or alternate venturi designs to observe the effect on the velocity profile and subsequent turbulence intensity values.
3. If a greater resolution time correlator (of say 10×10^{-9} second as opposed to the present 50×10^{-9} second) and a Phase Modulator which can accept greater crystal voltages are available, these tests should be repeated. The improved equipment should facilitate data attainment in the close proximity of both walls of the White Pipe.

4. The case of the Phase Modulator should be re-designed to incorporate a lense holder which will allow greater ease in focusing the laser beam onto an intersection point in the same plane.

5. In the event that a similar study can be conducted in the future, close observance of the mass flow rates through the White Pipe should be made. In this way, velocity differences can be explained as possibly due to slight variations in engine RPM settings and/or temperature fluctuations of the medium being measured.

BIBLIOGRAPHY

1. Birch, A.D., D. R. Brown and J. R. Thomas. "Photon Correlation Spectroscopy and its Application to the Measurement of Turbulence Parameters in Fluid Flows," Journal of Physics D: Applied Physics, Vol. 8, pages 438-447 (1975).

2. Cerullo, N.G. An Experimental Evaluation of a Laser Velocimeter by the Study of Turbulence in a Plane Free Jet at High Subsonic Velocities, M.S. Thesis. Wright-Patterson Air Force Base, Ohio: Air Force Institute of Technology (June 1979).

3. Charschan, S.S. "Helium-Neon Lasers," Lasers in Industry. Van Nostrand Reinhold Company, Cincinnati, Ohio (1972).

4. Ditmer, E.E. and C.N. Eastlake. Flow Calibration of the Laser Test Shelter Airflow Duct. Technical Report. Wright-Patterson Air Force Base, Ohio: Air Force Aero Propulsion Laboratory (April 1976)

5. Keenan, J.H. and J. Kaye. Gas Tables. Wiley and Sons, Inc., New York (1945).

6. Malvern Instruments, Ltd. Operating and Installation Manual. Spring Lane Trading Estate, Malvern Link, Worcestershire WR14 1AL, England

7. Smart, A.E. Application of Digital Correlation to the Measurement of Velocity by Light Scattering. Technical Report. Spectron Development Laboratories, Inc., 3303 Harbor Boulevard, Suite G-3, Costa Mesa, California 92606 (February 1978).

8. Weast, R.C. CRC Handbook of Applied Engineering Science. The Chemical Rubber Company, Cleveland, Ohio (1970).

9. Wright, H.E. and G. D. Catalano. Photon Correlation Laser Velocimeter Measurements in Highly Turbulent Flow Fields. Technical Paper, AIAA-80-0344.

APPENDIX A

LASER VELOCIMETER OPERATIONAL AND SET-UP PROCEDURES

To supplement the Malvern Laser Velocimeter User's Manual (Ref 6), this Appendix has been included to assist in some of the finer points of the set-up of the equipment as well as its operation. It is assumed that some form of bench or traversing mechanism has already been procured onto which the equipment can be installed. An example of such a table is provided in the previous work for reference. The steps to be followed in the set-up, alignment and operation of the equipment are as follows:

1. Laser - Attach the laser tube to the table mounting points using the 4 allen bolts with rubber pads which are located on the base of the laser tube case. (5/32 inches allen wrench is required). Next, ensure that the beamsplitter on the front of the Laser Tube is directly in line with the tube case and parallel to the case which will align the prism in the beamsplitter with the laser tube. Connect the co-axial cable from the laser tube to the laser supply unit and then connect the power supply

unit to a 110 volt source. The laser can now be turned on by the switch on the power supply unit. Figure 42 illustrates the laser tube assembly.

2. Photomultiplier Tube - Attach the PM tube optical mounting rail (a triangular rail) to your optical bench or table at a position such that it is not directly in line with the path of the beams emitted by the laser tube. (Unless forward scatter is being employed and necessary precautions are taken to block direct radiation from entering the PM tube). It is recommended that the axis of the rail should be at about a 7-10 degree angle to the desired laser beam intersection point. Once this triangular rail has been mounted and is secured, place the PM tube on the rail and secure it by tightening the two knobs on the one side of each of its two feet. The center axis of the PM tube should be on the same plane as the laser tube. At this time, do not hook up any of the wires or co-axial cables to the rear of the PM tube. Figure 43 illustrates the PM tube.

3. Digital Correlator, Storage Unit and Oscilloscope - For best operation, this equipment should be set up according to Figure 44 with the storage unit on the bottom, the digital correlator on top of this unit and the oscilloscope on top of the correlator. This equipment should be physically located near the PM tube although a remote point is not out of the question.

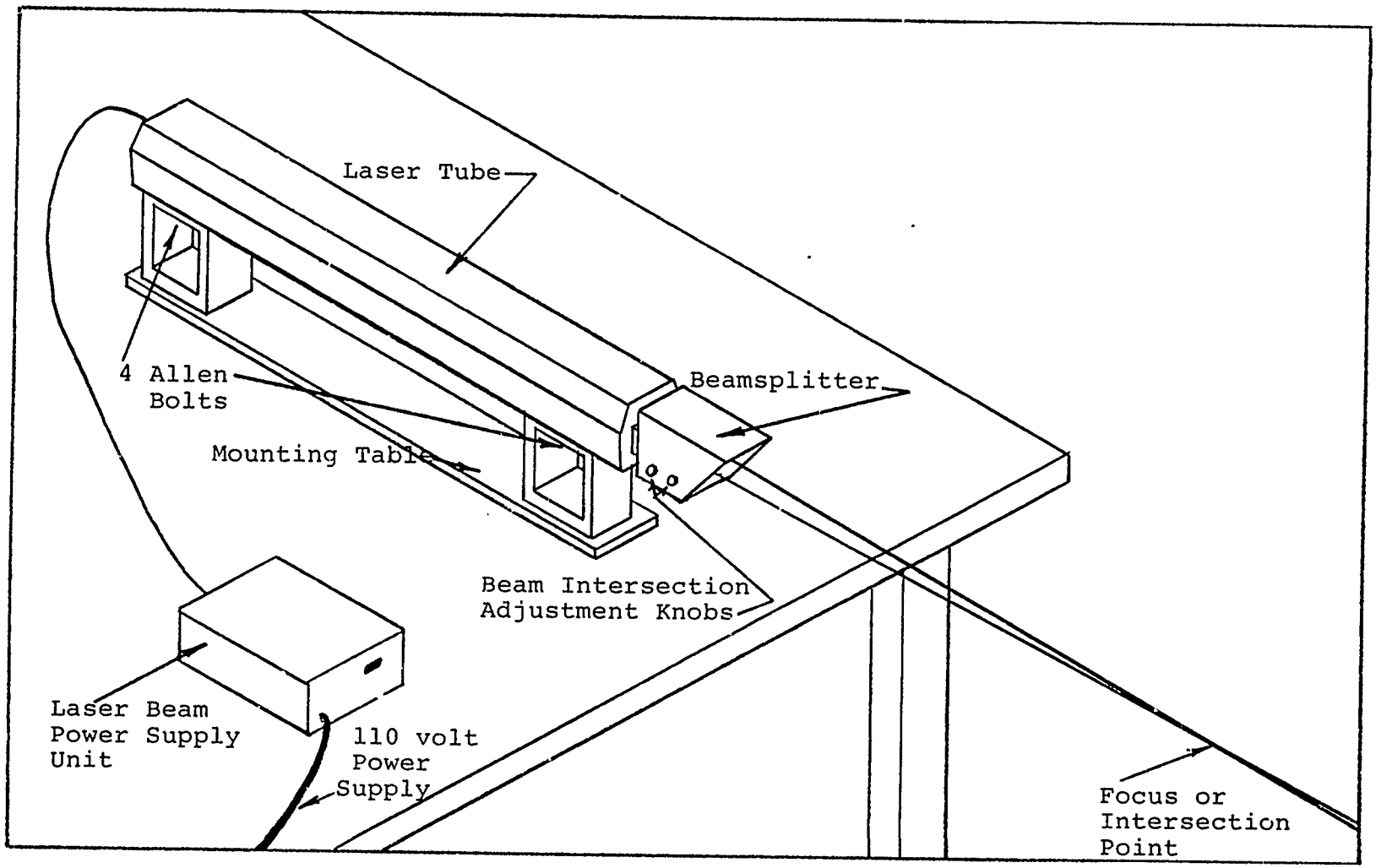

Figure 42 Laser, Laser Power Supply Unit and Beamsplitter

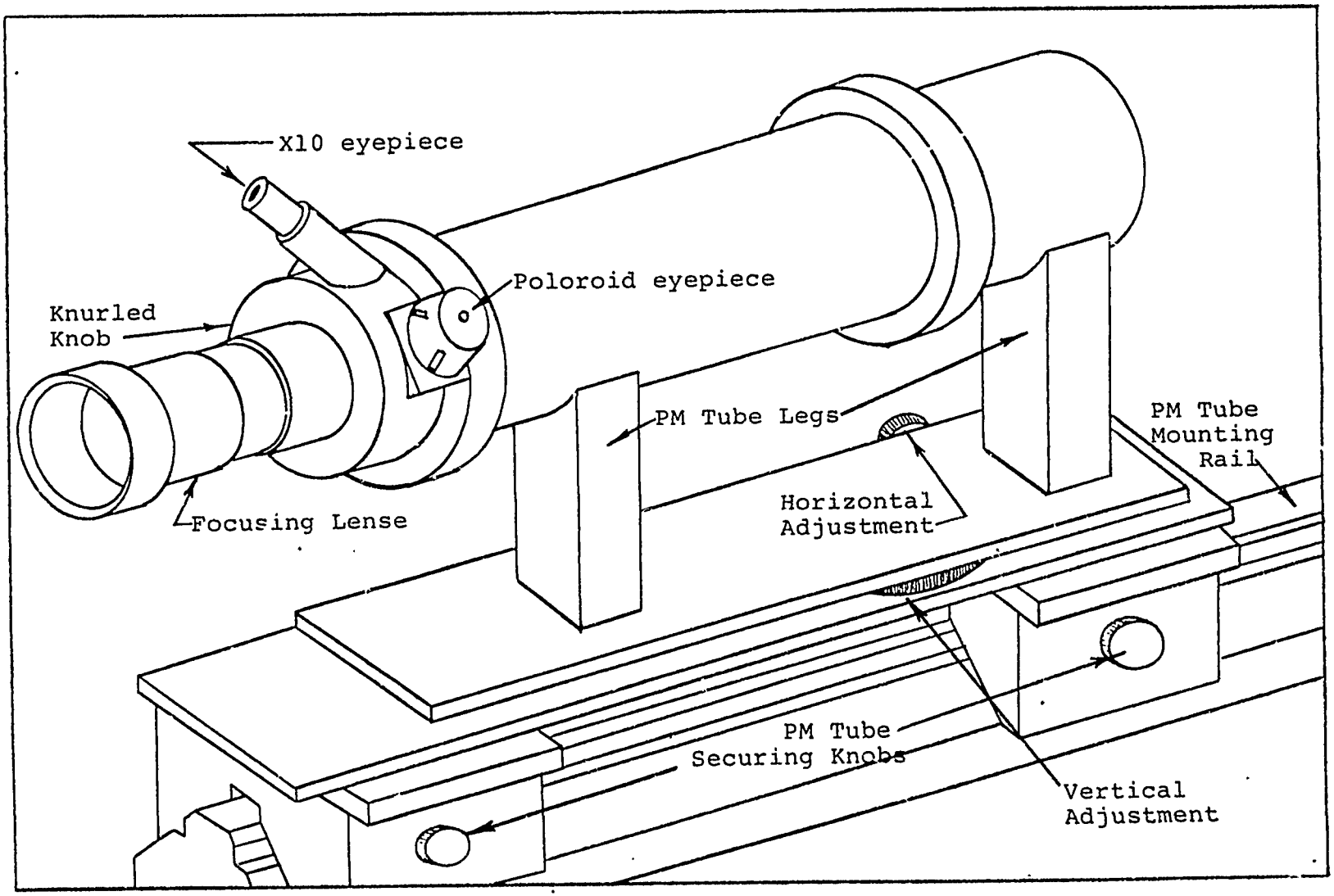

Figure 43 Photo Multiplier Tube

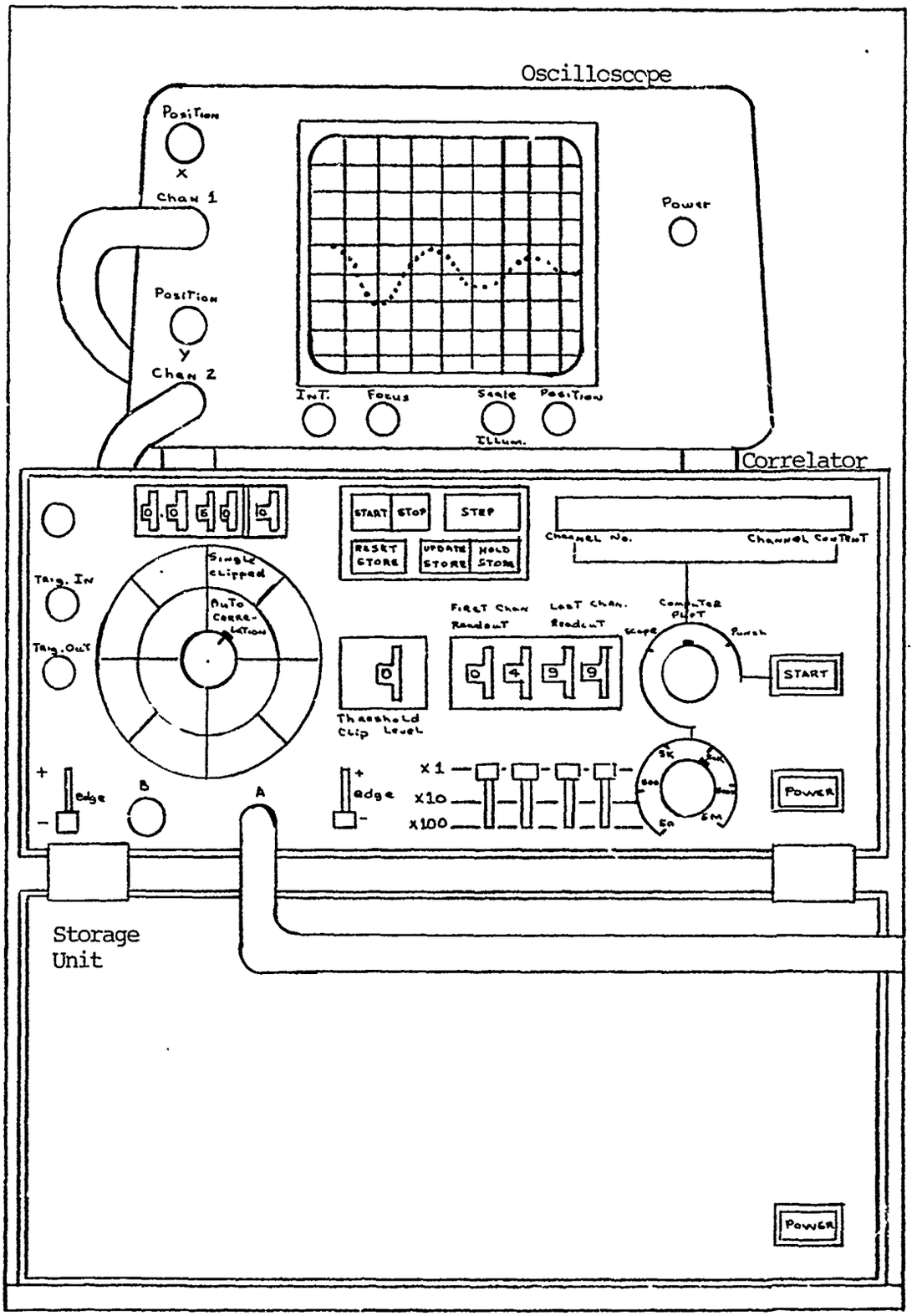

Figure 44 Digital Correlator and Oscilloscope Set up

4. Wiring - For the best explanation of the wiring procedures, Figures 45 and 46 should be examined.

5. Safety Precautions - A number of safety precautions should be implemented at this time so as to prevent any accidental injuries or damage to the equipment. The first precaution, and most important is to make all personnel who have access to the area aware that a laser is being used and that eye damage can occur if they look directly into the beam of the laser. This is best accomplished by verbal warnings and by displaying signs informing personnel of a laser in use. The second safety precaution concerns the Photo Multiplier tube which is a very expensive piece of equipment and is easily damaged. This damage can occur if, when the PM tube is connected to its power source, the PM tube is subjected to high intensity lighting (normal room lighting) or the laser beam is allowed to shine into the PM tube. So as to prevent any damage to PM tube, try to eliminate as much outside light as possible either by shielding or by turning off the lights. Also, before turning on the power supply to the PM tube, ensure that the laser is not shining into the PM tube and that its two beams definitely clear the optics on the front of the PM tube. This problem is most effectively eliminated by always operating the PM tube in side scatter or rear scatter modes as illustrated in Figure 47.

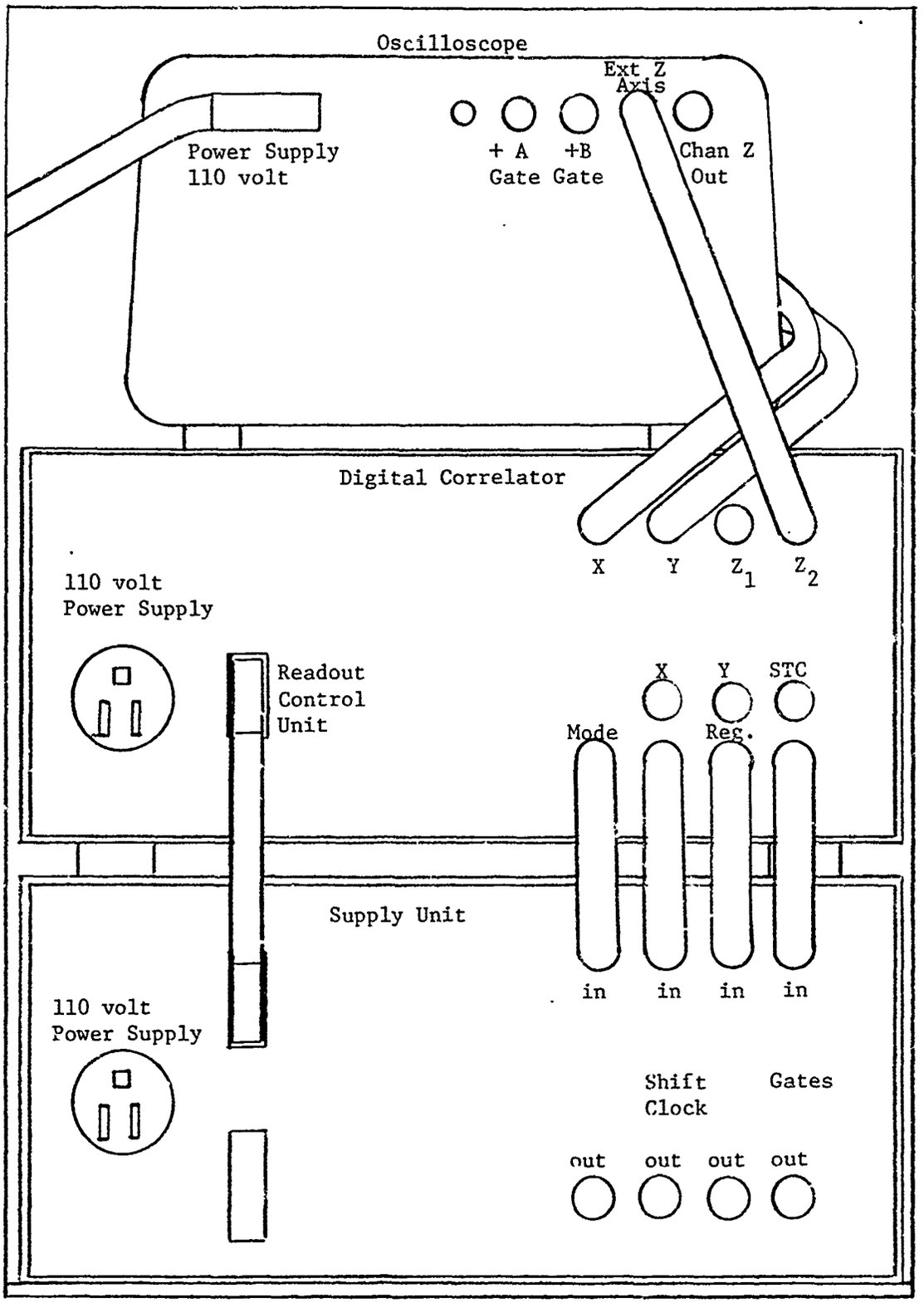

Figure 45 Digital Correlator and Oscilloscope Wiring

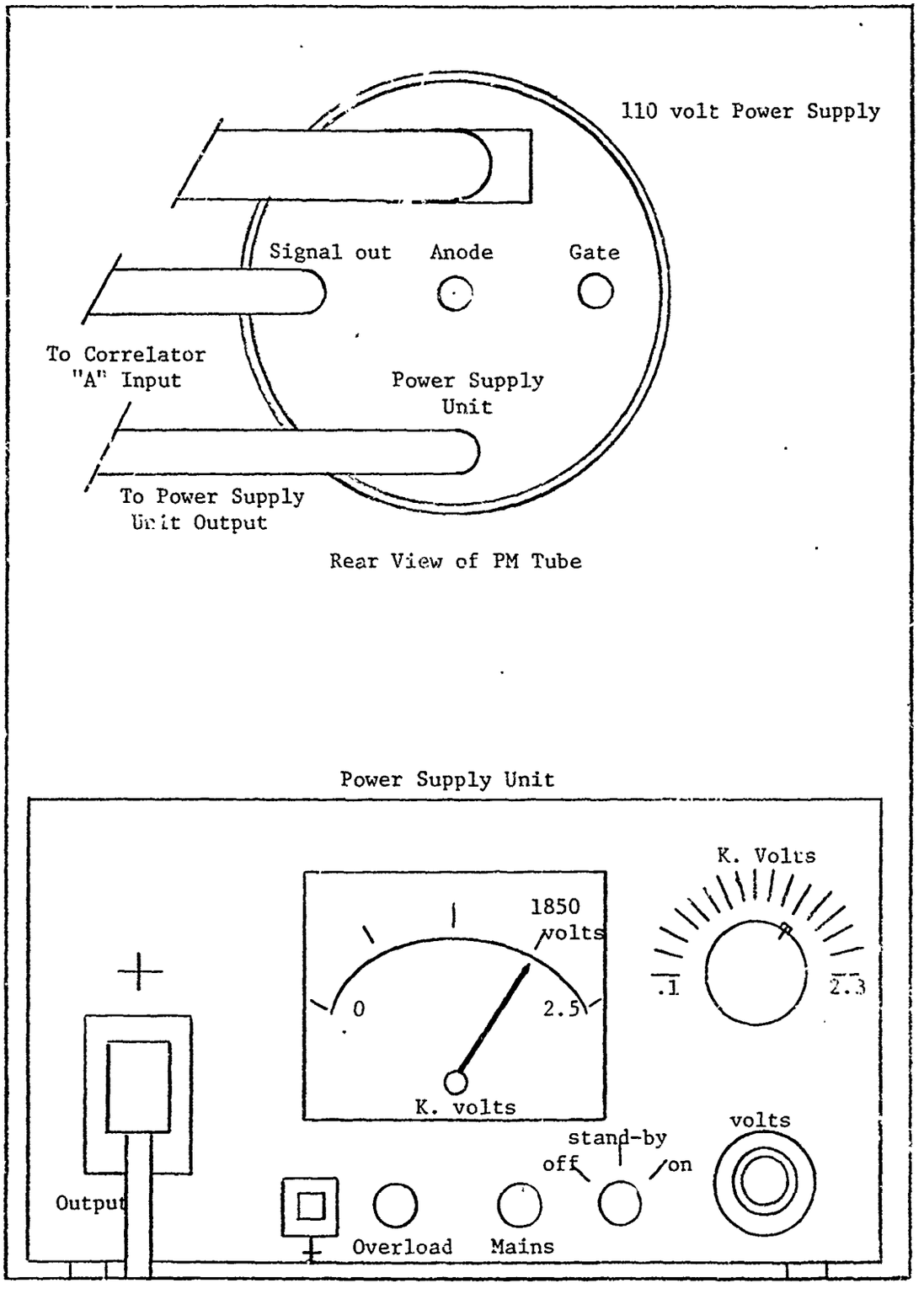

Figure 46 PM Tube and PM Tube Power Supply Unit Wiring

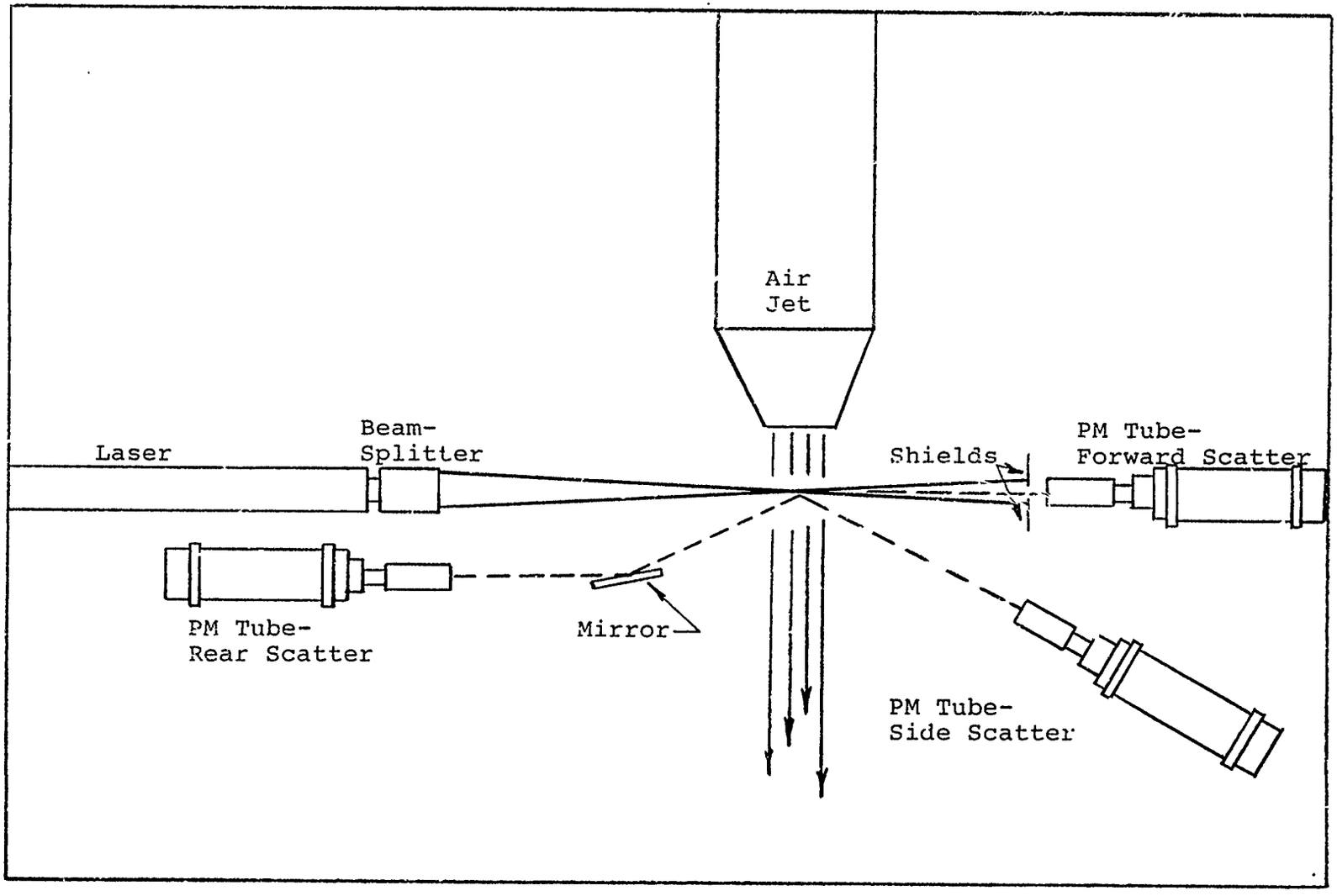

Figure 47 Various Operating Positions for the PM Tube

6. Alignment Procedures - This is, without question, the most difficult aspect of the set-up of this apparatus in addition to being the most important. The first point of consideration is that a rough estimate of how fast the medium is travelling should be known. By knowing this information, Table 1 can be used. From this Table, which relates flow velocity to fringe spacing requirements, the appropriate fringe spacing can be determined. The numerical value for the fringe spacing is calculated according to the following equation:

$$S \text{ (fringe spacing)} = \frac{L\,\lambda}{D\,\eta}$$

where:

L = distance from the intersection point of the two beams to an available perpendicular surface such as a wall. See Figure 48.

D = distance between the beams at this wall as illustrated in Figure 48.

λ = frequency of helium-neon gas = $.6328 \times 10^{-6}$m.

η = refractive index of air = 1.0.

Now, knowing the values for S, λ and η, a value can be calculated for $\frac{L}{D}$. To determine these two values, measure the distance, in inches from the available perpendicular surface, such as a well, to the point in the flow where the intersection or focal point

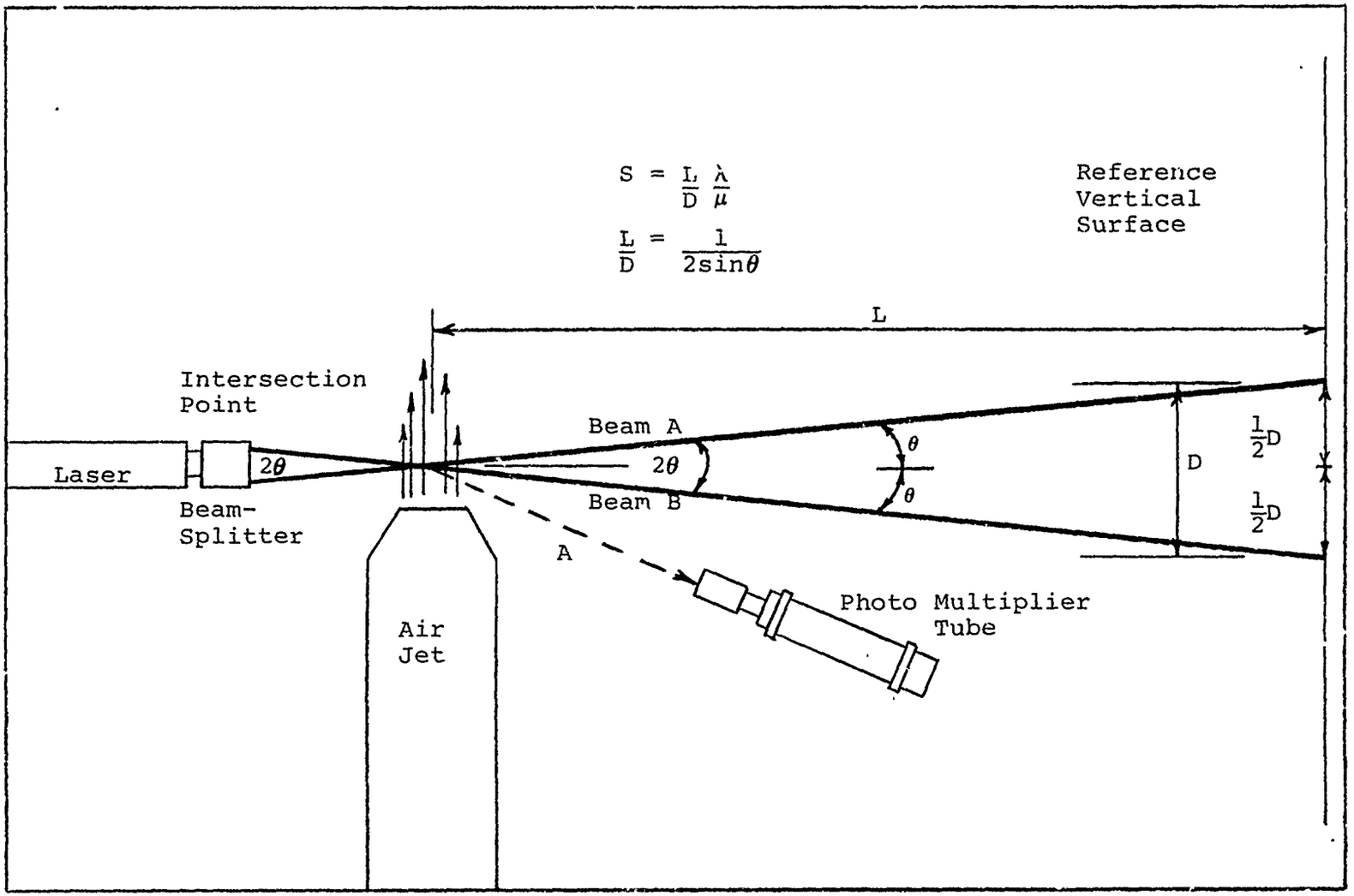

Figure 48 Fringe Spacing Calculations

TABLE I

Flow Velocity and Fringe Spacing		
Flow Velocity Lower Limit	Fringe Spacing	Flow Velocity Upper Limit
10 m/Sec	10 μm	40 m/Sec
50 m/Sec	50 μm	200 m/Sec
100 m/Sec	100 μm	400 m/Sec
500 m/Sec	500 μm	2000 m/Sec

TABLE II

Focal Combinations as Related to the Distance From the Beam Intersection to the PM Tube (A)			
Distance from Lense to Focal Point of Beams (A)	Lense - Focal Length	K	Spacer
17 cm - 20 cm	105 mm	1.0	9.0 cm (2 spacers)
20 cm - 35 cm	105 mm	1.3	6.5 cm
35 cm - 54 cm	105 mm	3.0	2.5 cm
54 cm - 70 cm	200 mm	1.8	9.0 cm (2 spacers)
70 cm - 110 cm	200 mm	2.3	6.5 cm
110 cm - 150 cm	200 mm	4.0	2.5 cm

of the two beams is desired. Knowing this, L will then permit calculation of D. Knowledge of both L and D will permit the laser to be set in the appropriate place so as to give these dimensions as indicated in Figure 48. At this point, the adjustment knobs on the beamsplitter should be taped, so as to prevent accidental adjustment, and the laser itself, checked for security on its mounts. Now, determine how far, in centimeters, it will be from the intersection or focal point of the two beams to the front of the lense of the PM tube or distance A as illustrated in Figure 48. This distance will determine which optics combination should be used in order to properly focus the PM tube. The decision on which optics combination to use should be made according to Table II. An illustration of how the correct and incorrect matching of the lense and spacer will affect the focusing of the focal point onto the pinhole of the PM tube is given in Figure 49. Once the correct combination of lense and spacer has been installed on the PM tube, roughly align the PM tube to "look" at the focal point of the two laser beams but at an axis of about 10° off from the axis of the center of the two laser beams. So as to make the ensuing aligning easier, place a piece of light grade paper at the intersection

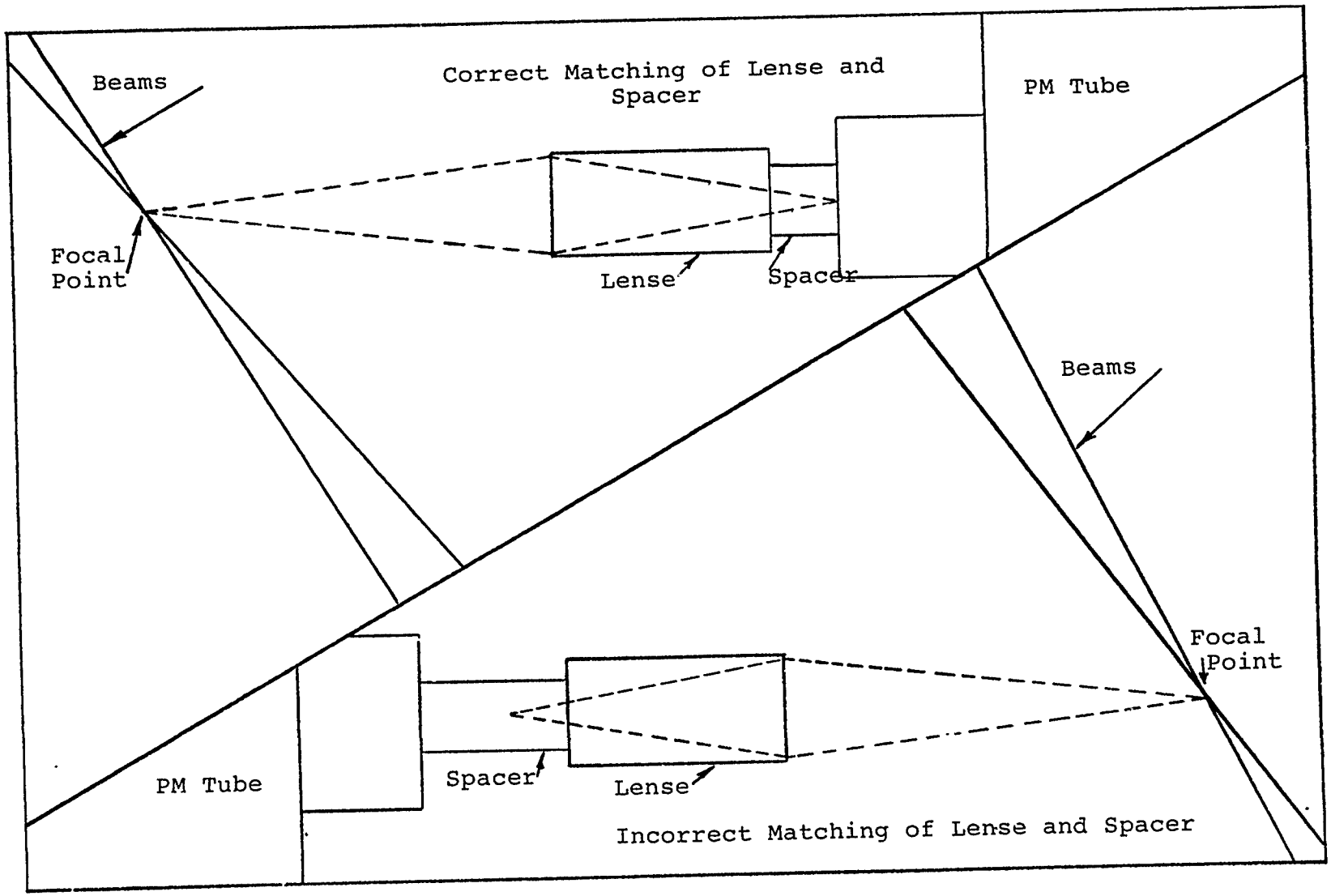

Figure 49 Correct and Incorrect Matching of Lense and Spacer

of the two beams which will enhance this point and allow easier focusing of the PM tube optics. Once this rough alignment is complete, the following instructions are to be followed: (See Figure 50 for assistance).

a. Turn the knurled knob fully counter clockwise

b. Open the aperture on the lense to the full open position

c. Looking through the polaroid eyepiece, locate the intersection of the two laser beams and by adjusting the X-control and Y-control knobs, center this intersection point onto the center of the cross-hairs of the polaroid eyepiece

d. Turn the knurled knob to the fully clockwise position

e. Looking through the X10 eyepiece, focus the light entering the lense and center this light onto the pinhole of the PM tube. When centered and in focus, what will be seen through the X10 eyepiece will be as shown in Figure 51. Centering of the light onto this pinhole is again accomplished by the X and Y control knobs, and by adjusting the lense. In the case of the 110 mm lense, which is a fixed lense, focusing can be accomplished by moving the PM tube back and forth on its rail.

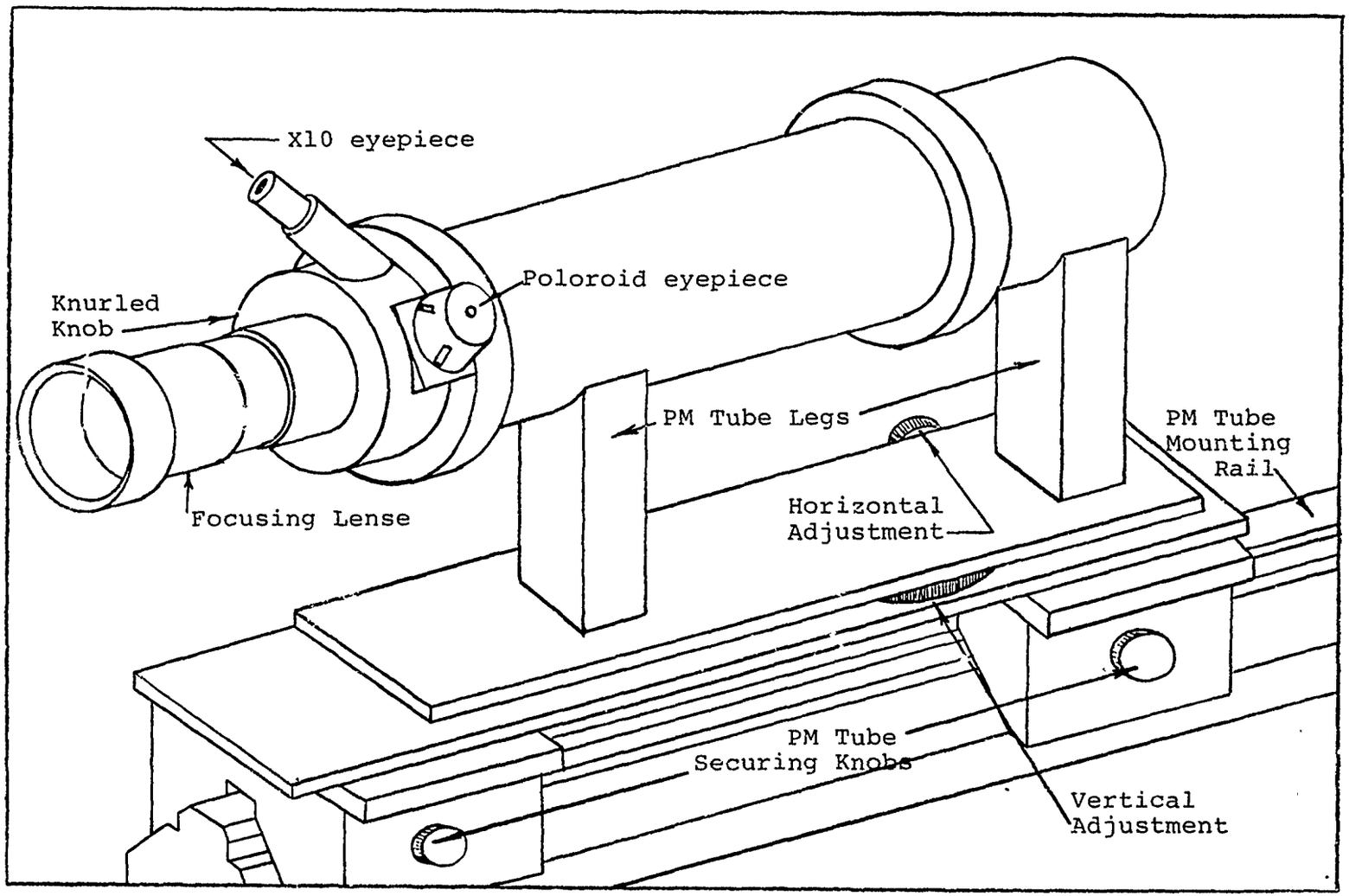

Figure 50 Photo Multiplier Tube

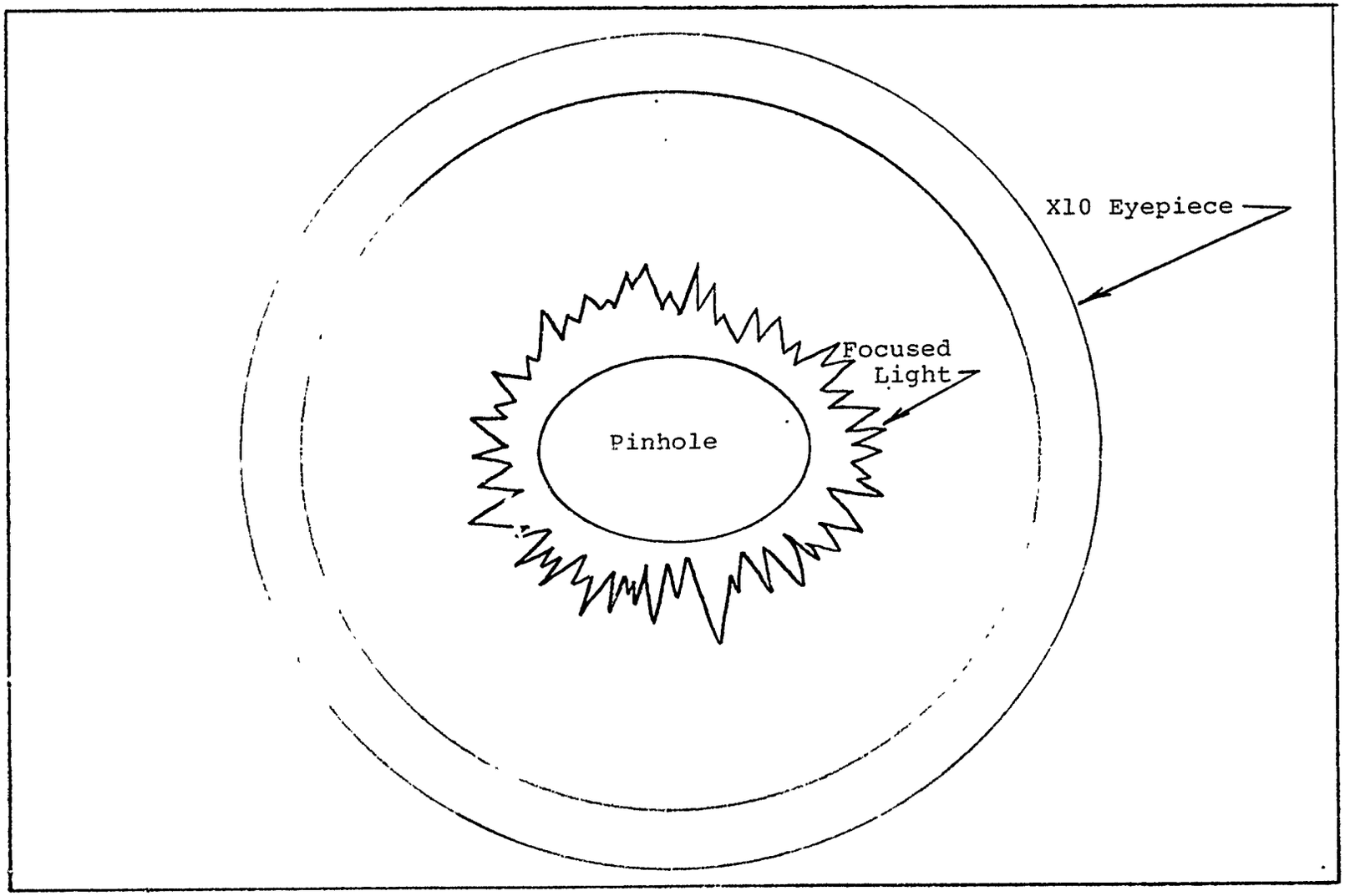

Figure 51 View as seen through the X10 Eyepiece during Focusing and Alignment of the PM Tube Optics

f. Once the PM tube is focused as required, ensure it is secure on its rail and ensure all wires are attached as indicated in Figure 46.

7. Measurements Requiring the Use of a Phase Modulator - On occasion, flow conditions will be encountered where the PM tube and Digital Correlator are incapable of producing an output from which mean velocity or turbulence intensity information can be obtained. This may be caused by the fact that the flow is moving at a rate which is either too fast, too slow or too turbulent for the limitations on the PM Tube and Correlator. If these conditions are encountered (which will produce an almost straight line, devoid of any peaks and valleys, on the oscilloscope) then it will be necessary to mount a Phase Modulator ahead of the Beamsplitter. The first step to be followed when installing the Phase Modulator is to ensure that the two beams from the Beamsplitter are parallel to one another. To do this, move the two beams until they are roughly parallel to one another and then measure from the center of one beam to the center of the other at a point immediately in front of the beamsplitter. Now, at a point some distance away, measure this same distance again, and if the beams are parallel, these measurements will be the same. Once the beams have been made parallel, set the Phase Modulator on the rail ahead of the beamsplitter as shown in Figure 52, and

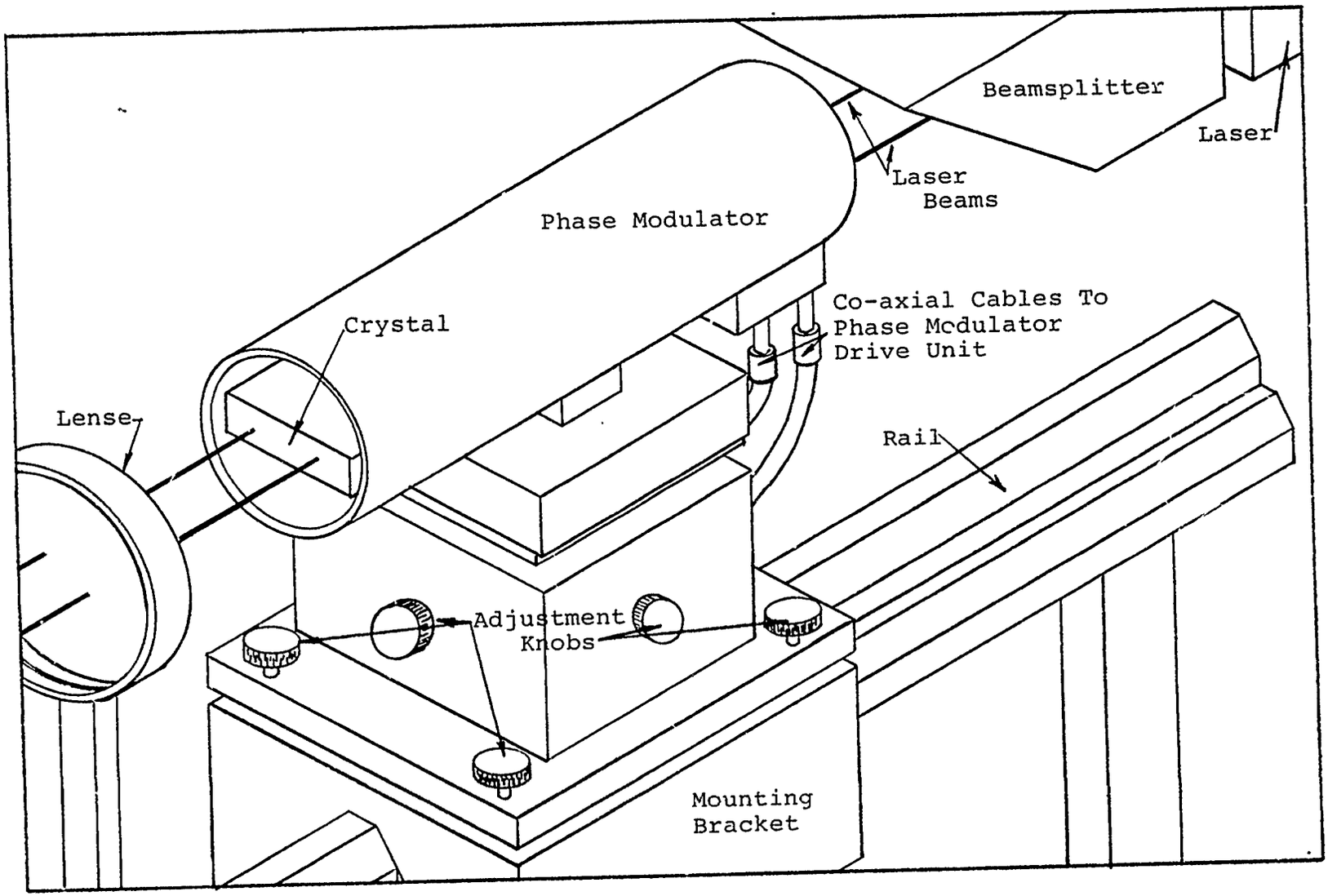

Figure 52 Phase Modulator Assembly

secure it on the rail. As illustrated, the Phase Modulator should be immediatley in front of the beamsplitter and at the same level so as the beams enter the crystal as indicated in Figure 53. In order to allow alignment of the Phase Modulator, it is necessary that the center axis of the Phase Modulator be 2.5 mm off to the left of the axis formed by the Laser and Beamsplitter. With the adjustment knobs, adjust the position of the body of the Phase Modulator until there are two beams coming out at equal intensity and parallel to one another. After completing this alignment, hook the Phase Modulator up to the Laser Anemometer Phase Modulator Drive Unit with two co-axial cables (50 ohms) as illustrated in Figures 52 and 54. To the Phase Modulator Drive Unit connect a counter so as to measure the exact frequency shift being delivered to the crystal. Once this equipment has been set up, obtain a lense of the desired focal length to focus the two beams back onto a focal point onto which the PM tube can be aligned. It might be necessary to measure the L and D values again as the combination of Phase Modulator and lense might have changed these respective values.

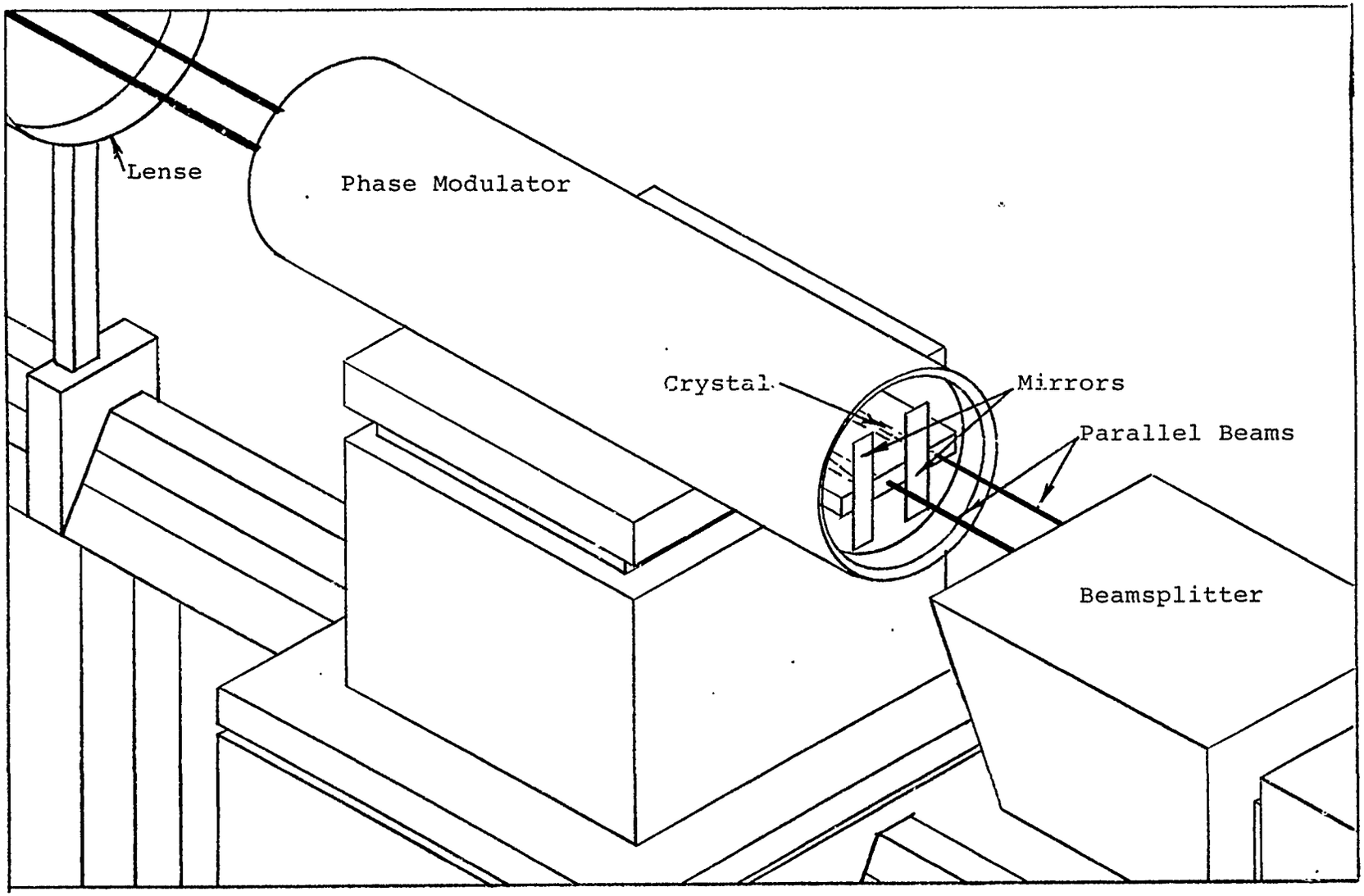

Figure 53 Phase Modulator Crystal

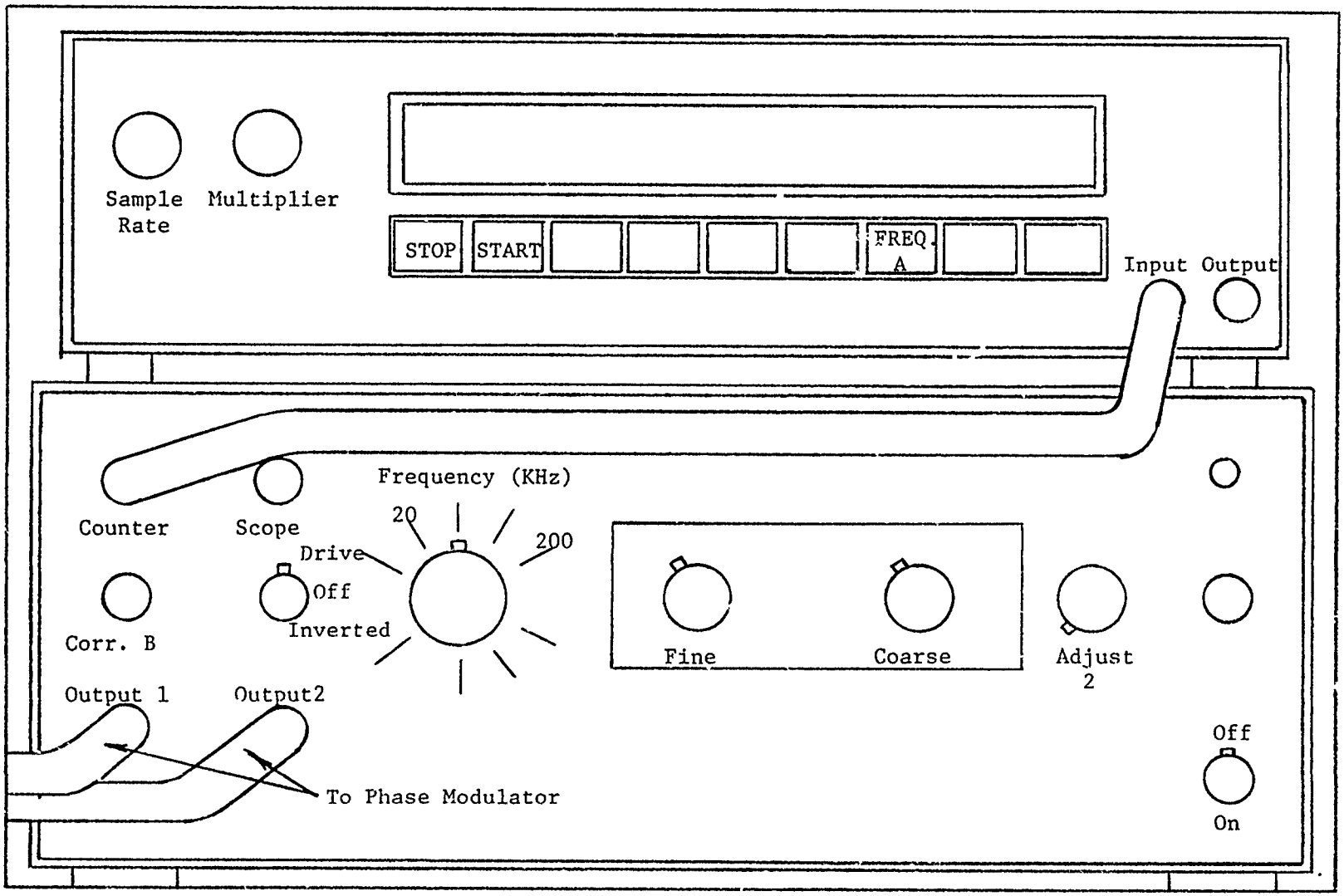

Figure 54 Phase Modulator Drive Unit and Frequency Counter

8. The First Measurement - The warm-up period for all the equipment associated with the laser anemometer system is approximately 15 minutes. Equipment which requires this warm-up are the PM Power Supply Unit (turn control to stand-by), Digital Correlator Storage Unit (Power button ON), Digital Correlator (Power button ON, Readout mode START button illuminated and red STOP button illuminated), Oscilloscope (Power button out) and the Laser Unit. In addition, if the Phase Modulator is in the circuit, the Phase Modulator Drive Unit should be turned on as well as the counter. Once all the equipment is warmed up, ensure all unnecessary lighting is turned off (the test area should be as dark as possible), turn the PM tube power supply unit control knob to ON and then push the green START button on the Digital Correlator. With reference to the Digital Correlator, this piece of equipment should be set up as follows for a standard velocity and turbulence intensity determination:

a) Sample time: $.050 \times 10^{-6}$ seconds
   Number of samples x $10^{n} = 0$
b) Control knob: Single clipped
c) Output level: A
d) Threshold clip lever: 0

e) First channel readout: 04

f) Last channel readout: 99

g) Readout mode: SCOPE

h) Number of counts displayed per volt: 50K

i) Monitor channels: x1

Once the desired output has been achieved on the Oscilloscope, push the red STOP button on the Digital Correlator which will then freeze the display on the Oscilloscope and allow the data for mean velocity and turbulence intensity calculations to be taken. If there is a requirement for the Phase Modulator to be in the circuit, as explained previously, then a number of adjustments will have to be made to the Phase Modulator Drive Unit to facilitate the velocity and turbulence intensity measurements. If the flow is low speed or highly turbulent put the drive unit in the INVERTED mode and vary the frequency to get the desired output on the Oscilloscope. Similarly, with the high speed flow, put the drive unit in the DRIVE mode to get the desired output. Once the Oscilloscope has given a desired output, again push the STOP button and proceed as before only ensuring that the value on the counter is taken down. The procedure to be followed in the reduction of the data to obtain the mean velocity and turbulence intensity values is included in Appendix C of this thesis.

APPENDIX B

LASER VELOCIMETER DATA

A total of eight traverses were made with the Laser Velocimeter and on each of these runs, a large amount of data was obtained. This data has been broken down as follows:

1. Location: White Pipe midsection
   Engine RPM: 50%
   Date: 26 July 79
   Weather Conditions: Hot and muggy
   87°F
   Clear skies
   Comments: Experimental run for equipment checkout

2. Location: White Pipe midsection
   Engine RPM: 50%
   Date: 31 July 79
   Weather Conditions: Hot and muggy
   84°F
   Clear skies
   Comments: Phase Modulator not in use

3. Location: White Pipe midsection
   Engine RPM: 50%
   Date: 7 August 79
   Weather Conditions: Cloudy
   76°F
   Comments: Phase Modulator in use

4. Location: White Pipe midsection

   Engine RPM: 70%

   Date: 7 August 79

   Weather Conditions: Cloudy
   76°F

   Comments: Phase Modulator in use

5. Location: 10 Ft. Downstream of
   Flow Conditioners

   Engine RPM: 50%

   Date: 9 August 79

   Weather Conditions: Hot and Cloudy
   80°F
   Humid

   Comments: Phase Modulator not in use

6. Location: 10 Ft. Downstream of
   Flow Conditioners

   Engine RPM: 70%

   Date: 9 August 79

   Weather Conditions: Hot and Cloudy
   80°F
   Humid

   Comments: Phase Modulator not in use

7. Location: 12 inches Inside Inlet
   Bell Mouth

   Engine RPM: 50%

   Date: 14 August 79

   Weather Conditions: Cool, cloudy
   76°F

   Comments: Phase Modulator not in use

8.	Location:	12 inches Inside Inlet Bell Mouth
	Engine RPM:	70%
	Date:	14 August 79
	Weather Conditions:	Cool, cloudy 76°F

Comments: Phase Modulator not in use

Table III follows and includes all of the data as taken on each of the traverses with the exception of the first traverse which was a trial run to check out the operation of the equipment and to refine the operating techniques.

TABLE III

LASER VELOCIMETER DATA

Date: 31 July 79

Weather Conditions: No rain for two days; Hot and muggy

TATM: 84°F

PATM: 29.20 in Hg

% Engine RPM: 50%

Traverse Location: White Pipe Midsection - downstream of venturi

Position (in)	Sample Time ($\times 10^{-9}$ sec)	Peak	Freq. KHz	g_1	g_2	g_3
Wall						
1/8						
1/4						
1/2						
1.0						
1.5						
2			Flow	too turbulent		
3						
4			to	obtain data		
5	100	32		(24)21566794	(32)21594321	(62)21549684
6	100	30		(18)9544906	(30)9731173	(51)9636875
7	100	25		(15)5062397	(25)5275805	(36)5202579
8	100	23		(15)2065265	(23)2222948	(32)2152042
9	100	21		(12)6847298	(21)7496020	(29)7047685
10	100	19		(11)1476562	(19)1687189	(27)1500647
11	100	18		(11)1496536	(18)1707496	(26)1496316
12	100	18		(11)2087491	(18)2357730	(26)2080223
13	100	18		(11)6190220	(18)6944124	(26)6167245
14	100	18		(11)4394590	(18)4938586	(26)4377327
15	100	18		(11)1462778	(18)1636425	(26)1455117
16	100	18		(11)1446932	(18)1622612	(26)1441649
17	100	18		(11)6156426	(18)7043879	(26)6119244
18	100	18		(11)3129577	(18)3724825	(26)3108495
19	100	18		(11)1048426	(18)1251455	(26)1045243
20	100	18		(11)1425452	(18)1687269	(26)1426486
21	100	19		(12)826645	(19)948534	(27)847137
22	100	21		(13)1415532	(21)1560040	(30)1478246
23	100	24		(14)1438367	(24)1528025	(32)1500492
24	100	26		(17)2168541	(26)2191092	(41)2184549
25						
26						
27			Flow	too turbulent		
28						
28.5			to	obtain data		
29.0						
Wall						

TABLE III (cont'd)

Date: 7 August 1979

Weather Conditions: Cloudy; Hot and Muggy

TATM: 76°F

PATM: 29.3 in Hg

% Engine RPM: 50%

Traverse Location: White Pipe Midsection - downstream of venturi

Position (in)	Sample Time -9 (x10 sec)	Peak	Freq. KHz	g_1	g_2	g_3
Wall						
1/8						
1/4						
1/2						
1.0						
1.5			Flow too turbulent to			
2				obtain data		
3						
4	200	12	435.4	(7)28120616	(12)28155057	(18)28141918
5	200	11	406.5	(7)3570705	(11)3620148	(13)3603075
6	200	9	429.9	(6)2167834	(9)2256313	(12)2226423
7	100	14	425.8	(9)6554466	(14)6611841	(19)6584163
8	100	14	443.5	(8)16909250	(14)16995827	(17)16950803
9	50	22	424.5	(12)4515813	(22)4585277	(30)4553083
10	50	20	431.6	(12)655115	(20)733854	(28)691272
11	50	20	428.3	(12)1047158	(20)1188134	(28)1105225
12	50	23	201.7	(13)2111759	(23)2243086	(33)2140869
13	50	23	201.9	(13)6119823	(23)6267218	(33)6156589
14	50	27	OFF	(15)10222955	(27)10714216	(39)10210296
15	50	26	OFF	(15)825487	(26)950506	(38)822943
16	50	26	OFF	(15)492206	(26)595234	(38)488608
17	50	26	OFF	(15)475148	(26)587439	(38)471885
18	50	27	OFF	(15)452579	(27)558458	(38)451168
19	50	27	OFF	(15)465768	(27)576543	(38)463985
20	50	27	OFF	(15)451831	(27)552867	(39)453649
21	50	28	OFF	(15)505907	(28)610181	(40)521444
22	50	30	OFF	(17)663802	(30)762109	(43)698886
23	50	30	201.4	(18)1511884	(30)1622475	(43)1586784
24	100	14.5	428.7	(8.5)2063763	(14.5)2147049	(17)2112897
25	100	15	449.7	(9)2579699	(15)2658597	(20)2627501
26	200	11	466.1	(7)11114477	(11)11262845	(15)11187261
27	200	12	461.3	(8)26113302	(12)26206576	(19)26151738
28						
28.5			Flow too turbulent			
29.0			to obtain data			
Wall						

TABLE III (cont'd)

Date: 7 August 1979

Weather Conditions: Cloudy; Hot and Muggy

TATM: 76°F

PATM: 29.3 in Hg

% Engine RPM: 70%

Traverse Location: White Pipe Midsection - downstream of venturi

Position (in)	Sample Time ($\times 10^{-9}$ sec)	Peak	Freq. KHz	g_1	g_2	g_3
Wall						
1/8						
1/4						
1/2						
1.0						
1.5						
2			Flow too turbulent to obtain data			
3						
4						
5	50	25	450			
6	50	19	450			
7	50	16	450	(11)2910572	(16)2935814	(22)2924349
8	50	16	450	(10)5524261	16)5569545	(22)5542501
9	50	18	OFF	(11)283100	18)298691	(25)285677
10	50	17	OFF	(10)170702	17)221082	(24)172542
11	50	17	OFF	(10)228537	17)284601	(24)227429
12	50	17	OFF	(10)917536	17)972003	(24)912725
13	50	17	OFF	(10)1488620	17)1545255	(24)1488042
14	50	17	OFF	(10)2026183	16)2138165	(24)2059325
15	50	17	OFF	(10)613665	17)684482	(24)611508
16	50	17	OFF	(10)428275	17)519230	(24)427478
17	50	17	OFF	(10)517022	17)620985	(24)514414
18	50	16	201.7	(10)442777	16)519808	(22)453310
19	50	16	202.3	(10)432739	16)515539	(22)442737
20	50	16	202.3	(10)431842	16)511524	(23)446011
21	50	16	202	(10)1421940	16)1651761	(23)1472504
22	50	17	202.3	(10)849031	17)961261	(24)889312
23	100	10	464.6	(7)4412423	10)4710944	(12)4574755
24	100	10	458.1	(7)3176170	10)3359851	(14)3306032
25	100	12	462.9	(8)4619898	12)4734000	(18)4714457
26	200	9	462.2	(6)9206946	9)9274611	(13)9249040
27	200	12	465.2	(8.5)1626573	12)1667111	(18)1644383
28						
28.5			Flow too turbulent to obtain data			
29.0						
Wall						

TABLE III (cont'd)

Date: 9 August 1979

Weather Conditions: Hot and Muggy; Cloudy

TATM: 80°

PATM: 29.9 in Hg

% Engine RPM: 50%

Traverse Location: 10 Feet downstream from flow conditions

Position (in)	Sample Time ($\times 10^{-9}$ sec)	Peak	Freq. KHz	g_1	g_2	g_3
Wall						
1/8						
1/4			Flow too turbulent			
1/2			to obtain data			
1.0						
1.5						
2						
3	100	35		(18)15560555	(35)15752448	(51)15578521
4	100	32		(17)424792	(32)520829	(47)435619
5	100	29		(16)256801	(29)323414	(44)262745
6	100	29		(16)284668	(29)357915	(41)287569
7	100	27		(15)261557	(27)331407	(39)263005
8	100	27		(15)314701	(27)396065	(38)314751
9	100	26		(15)438844	(26)552396	(38)437123
10	100	25		(14)280910	(25)352519	(37)280990
11	100	24		(14)478196	(24)575624	(35)476802
12	100	24		(14)847178	(24)987599	(35)842220
13	100	24		(13)543486	(24)620550	(35)541862
14	100	24		(13)548784	(24)612410	(35)545961
15	100	25		(13)604889	(25)659831	(34)603295
16	100	24		(13)660930	(24)721293	(34)659732
17	100	24		(13)655692	(24)713300	(34)654759
18	100	24		(14)1043554	(24)1147614	(35)1039499
19	100	25		(15)1063584	(25)1174962	(36)1060374
20	100	26		(15)642866	(26)725200	(38)643145
21	100	27		(15)868899	(27)985960	(39)870453
22	100	28		(16)891130	(28)992034	(40)893590
23	100	29		(16)1075380	(29)1181281	(42)1080484
24	100	31		(17)1467532	(31)1593107	(45)1481935
25	100	34		(18)1485796	(34)1591301	(49)1498302
26	200	19		(11)4581320	(19)4673377	(27)4594534
26.5	200	20		(12)9509324	(20)9568392	(28)9515021
28						
28.5			Flow too turbulent			
29.0			to obtain data			
Wall						

TABLE III (cont'd)

Date: 9 August 1979

Weather Conditions: Hot and Muggy; Cloudy

TATM: 80°F

PATM: 29.9 in Hg

% Engine RPM: 70%

Traverse Location: 10 Feet downstream of the flow conditions

Position (in)	Sample Time ($\times 10^{-9}$ sec)	Peak	Freq. KHz	g_1	g_2	g_3
Wall						
1/8						
1/4						
1/2				Flow too turbulent to obtain data		
1.0						
1.5						
2	200	13				
3	200	12		(7)24105821	(12)24173578	(16)24135666
4	200	11.5		(8)6030855	(11.5)6085943	(16)6033957
5	100	19		(12)653475	(19)683387	(28)656437
6	100	18		(11)834292	(18)922187	(26)840525
7	100	17		(11)213420	(17)258603	(25)214722
8	100	17		(10)217725	(17)269563	(24)217300
9	100	16		(10)204563	(16)251134	(24)204955
10	100	16		(10)234257	(16)284757	(23)234179
11	100	15		(10)236478	(15)280573	(22)234540
12	100	15		(10)339072	(15)343746	(28)338160
13	100	15		(10)492253	(15)544224	(22)488237
14	100	15		(10)902919	(15)973729	(22)898881
15	100	15		(10)1071694	(15)1142019	(22)1067223
16	100	15		(10)583821	(15)624640	(22)580567
17	100	15		(10)1056135	(15)1121813	(22)1050343
18	100	16		(9)522677	(16)567442	(22)522024
19	100	16		(10)514979	(16)568982	(23)513812
20	100	16		(10)513822	(16)581191	(24)514600
21	100	17		(10)461152	(17)521469	(24)462363
22	100	17		(10)484825	(17)531354	(25)485843
23	100	18		(11)350325	(18)380276	(26)350935
24	100	19		(11)494122	(19)530063	(27)498444
25	200	12		(8)2095773	(12)2158717	(17)2101316
26	200	13		(8)3528064	(13)3579746	(17)2528785
27	200	13		(8)1231293	(13)1269461	(18)1233399
28	200	14		(8)6585646	(14)6643596	(19)6598593
28.5						
29.0				Flow too turbulent to obtain data		
Wall						

TABLE III (cont'd)

Date: 14 August 1979

Weather Conditions: Cool; Cloudy

TATM: 76°F

PATM: 29.74 in Hg

% Engine RPM: 50%

Traverse Location: 12 inches inside Inlet Bell Mouth

Position (in)	Sample Time ($\times 10^{-9}$ sec)	Peak	Freq. KHz	g_1	g_2	g_3
Wall						
1/8			Flow	too turbulent		
1/4			to	obtain data		
1/2						
1.0	400	9				
1.5						
2	400	12				
3	300	15		(8)14695670	(15)14713189	(18)14696885
4	200	22		(12)21629326	(22)21677593	(31)21630616
5	200	21		(12)16513922	(21)16558774	(32)16511220
6	200	22		(12)2517181	(22)2611933	(32)2519044
7	200	22		(12)2002023	(22)2103693	(32)2002767
8	200	22		(12)875975	(22)935869	(32)874304
9	200	22		(12)1625910	(22)1678255	(32)1624484
10	200	22		(12)2491226	(22)2522280	(30)2490536
11	200	21		(12)2874723	(21)2899781	(32)2875601
12	200	22		(12)4735449	(22)4768427	(31)4735656
13	200	22		(12)2885029	(22)2908513	(31)2884216
14	200	22		(12)3587837	(22)3615577	(32)3588500
15	200	22		(12)3011622	(22)3035870	(32)3012613
16	200	22		(12)1849608	(22)1873099	(30)1848131
17	200	21		(13)930947	(21)955172	(31)930890
18	200	21		(12)506048	(21)532066	(31)505524
19	200	21		(12)481574	(21)507459	(32)482180
20	200	21		(12)469053	(21)495111	(31)469508
21	200	21		(12)683058	(21)714456	(32)684698
22	200	22		(12)956819	(22)980122	(31)956728
23	200	23		(14)4580805	(23)4605263	(31)4580902
24	200	21		(11)4122770	(21)4152630	(30)4119637
25	200	22		(13)31763264	(22)31794766	(32)31765819
26	200	22		(12)4986239	(22)4997042	(31)4984290
27	200	24				
28						
28.5			Flow	too turbulent		
29.0			to	obtain data		
Wall						

TABLE III (cont'd)

Date: 14 August 1979

Weather Conditions: Cool; Cloudy

TATM: 76°F

PATM: 29.74 in Hg

% Engine RPM: 70%

Traverse Location: 12 inches inside the Inlet Bell Mouth

Position (in)	Sample Time ($x10^{-9}$ sec)	Peak	Freq. KHz	g_1	g_2	g_3
Wall						
1/8			Flow	too turbulent		
1/4			to	obtain data		
1/2						
1.0						
1.5						
2						
3	200	14		(9)12634916	(14)12682856	(21)12632156
4	200	15		(9)12822860	(15)12858346	(21)12817671
5	200	14		(8)10419959	(14)10454637	(20)10423683
6	200	14.5		(9)1547597	(14.5)1580663	(20)1544669
7	200	14		(9)887005	(14)921072	(20)887320
8	200	14		(8)892228	(14)926464	(20)891385
9	200	14		(9)1933236	(14)1975473	(20)1934665
10	200	14		(9)3104333	(14)3135995	(20)3101416
11	200	14		(8)5872926	(14)5906459	(20)5869768
12	200	14		(9)6572190	(14)6606513	(20)6567694
13	200	14		(9)3948264	(14)3970150	(20)3946309
14	200	14		(8)3648992	(14)3676448	(20)3649722
15	200	14		(8)2940503	(14)2961741	(20)2939379
16	200	14		(9)1738402	(14)1757662	(20)1738934
17	200	14		(9)974527	(14)998525	(20)972445
18	200	14		(9)506000	(14)529381	(20)506797
19	200	14		(8)496758	(14)524118	(20)496656
20	200	14		(9)501683	(14)528086	(20)500855
21	200	14		(9)549775	(14)571728	(20)548812
22	200	14		(8)1210951	(14)1236828	(20)1210166
23	200	14		(9)8080714	(14)8116125	(20)8080115
24	200	14		(10)28440603	(14)28464170	(20)28441120
25	200	14		(9)12882528	(14)12899257	(20)12880598
26	200	15		(10)3656545	(15)3665448	(21)3655973
27						
28			Flow	too turbulent		
28.5			to	obtain data		
29.0						
Wall						

APPENDIX C

LASER VELOCIMETER DATA REDUCTION METHOD

The first step in the Reduction of the Laser Velocimeter data is to calculate the fringe spacing:

$$S = \frac{L}{D}\frac{\lambda}{\mu}$$

where: S = fringe spacing

L = distance from Laser Beam intersection point to a reference perpendicular surface onto which the beams shine (See Figure 48)

D = the distance the two beams are apart at the reference surface (See Figure 48)

λ = frequency of helium-neon = $.6328 \times 10^{-6}$m,

μ = refractive index of air = 1.0

The next step is to calculate the included angle that the two Laser Beams make at the focal point (See Figure 48):

$$\tan\theta = \frac{\frac{1}{2}D}{L}$$

included angle = $2(\theta)$

The third step is to calculate the number of fringes present in the intersection of the two beams:

$$\#\text{ of fringes} = \frac{\text{beam width}}{S}$$

where: beam width = 1.1 mm (in this application)

The fourth step involves the calculation of the mean velocity at the point in the flow. The formula to be used here is:

$$U = \frac{S}{(\text{Peak} - 3)\ (\text{Sample Time})}$$

At this point, the Peak can be found from the Oscilloscope display as indicated in Figure 55. The sample time is as set on the Digital Correlator and has the units of micro seconds ($\times 10^{-6}$ second).

The fifth step, or the turbulence intensity calculation, involves first, the calculation of R:

$$R = \frac{g_2 - g_1}{g_2 - g_3}$$

where:

g_1 = the first minimum point

g_2 = the first peak

g_3 = the second minimum point

g_1, g_2 and g_3 are illustrated on Figure 55.

then

$$\eta = \frac{1}{\pi} \left(\frac{1}{2} (R-1) + \frac{1}{2N^2} \right)^{1/2}$$

where: η = turbulence intensity

$$N = \frac{r_o}{S}$$

r_o = laser beam radius = .55 mm

S = fringe spacing

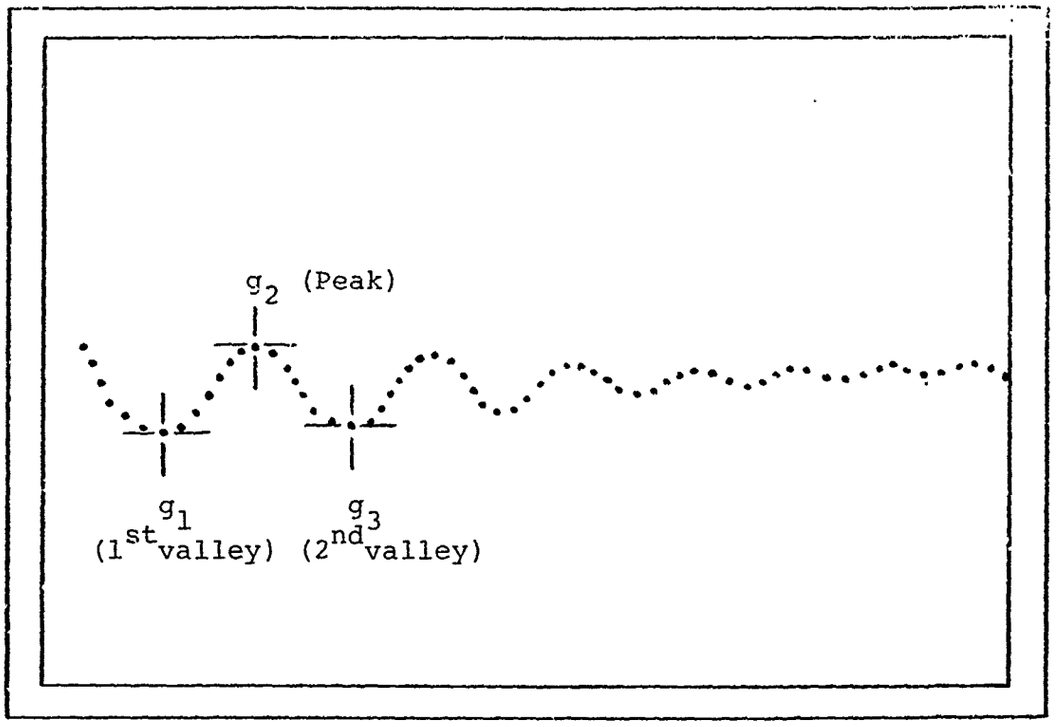

Oscilloscope Readout

Pictorial View

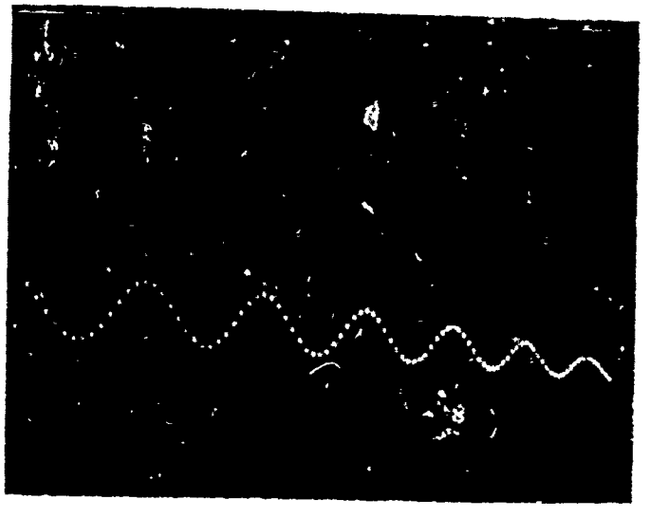

Figure 55 Oscilloscope Readout for Mean Velocity and Turbulence Intensity Calculations.

If, during the calculation of η, a negative value is arrived at, then the value of the turbulence intensity at that point is taken to be zero.

If the Phase Modulator is in the circuit while the data is being taken, then the calculation of mean velocity and turbulence intensity is slightly different.

First, calculate mean velocity by the standard method:

$$U^* = \frac{S}{(\text{Peak} - 3)\ (\text{Sample time})}$$

Next, calculate the doppler shift frequency with the Phase Modulator Input:

$$F_d^* = \frac{2U^* \cdot \sin\ (2\theta)}{\lambda}$$

where:

F_d^* = doppler shift frequency with Phase Modulator

U^* = mean velocity with Phase Modulator

(2θ) = included angle

λ = frequency of helium-neon - $.6328 \times 10^{-6}$m

Next, calculate the doppler shift frequency without the Phase Modulator:

$$F_d = F_d^* \pm \Delta F$$

where

F_d = doppler shift frequency without Phase Modulator

ΔF = the frequency shift imposed on the Phase Modulator by the drive unit. This will be plus or minus depending on whether the drive unit is in the drive (+) or inverted (-) mode.

Now, calculate the true velocity:

$$U = \frac{F_d \quad \lambda}{2 \sin (2\theta)}$$

where:

U = mean velocity without the Phase Modulator.

To caucluate the Turbulence Intensity involves a slightly different formula than before

$$\eta = \frac{1}{\P} \left[\frac{1}{2} (R-1) \quad \frac{U}{U^*} + \frac{1}{2N^2} \right]^{1/2.}$$

APPENDIX D

LASER VELOCIMETER NUMERICAL RESULTS

Employing the data reduction method as described in Appendix C and the data from Appendix B, mean velocities and turbulence intensities have been calculated for the data points of each traverse. Each set of calculations for each of the respective traverses contains only those data points where readings were made and excludes those points where the flow was too turbulent or slow moving to obtain the required information.

TABLE IV

Date: 31 July 1979

Position: White Pipe Midsection

Engine RPM: 50%

Comments: No Bragg Cell (Phase Modulator)

$S = 51.66 \times 10^{-6} M$

Position (in)	Sample Time ($\times 10^{-9}$ sec)	Peak	U* ft/sec	f_d* Hz	Δf Hz	f_d Hz	U ft/sec	$\frac{U}{U^*}$	R	η(%)	U/U_{cen}
5	100	32					58.44		.616686	0	.5172
6	100	30					62.77		1.975302	22.329	.555
7	100	25					77.04		2.914375	31.214	.681
8	100	23					84.74		2.223832	24.989	.750
9	100	21					94.16		1.446958	15.196	.8333
10	100	19					105.93		1.129113	8.359	.9375
11	100	18					112.99		.998972	1.990	1.0
12	100	18					112.99		.973810	0	1.0
13	100	18					112.99		.970427	0	1.0
14	100	18					112.99		.969242	0	1.0
15	100	18					112.99		.957746	0	1.0
16	100	18					112.99		.970806	0	1.0
17	100	18					112.99		.959787	0	1.0
18	100	18					112.99		.965794	0	1.0
19	100	18					112.99		.984564	0	1.0
20	100	18					112.99		1.003965	2.545	1.0
21	100	19					105.93		1.202097	10.337	.9375
22	100	21					94.16		1.766731	19.822	.8333
23	100	24					80.71		3.256383	33.876	.7143
24	100	26					73.69		3.446584	35.269	.6522

TABLE IV (Cont'd)

Date: 7 August 1979

Position: White Pipe Midsection

Engine RPM: 50%

Comments: Bragg Cell (Phase Modulator)

$S = 39.61 \times 10^{-6} M$

Position (in)	Sample Time ($\times 10^{-9}$ sec)	Peak	U* ft/sec	f_d* Hz x 10^6	Δf Hz x 10^6	f_d Hz x 10^6	U ft/sec	$\frac{U}{U^*}$	R	η (%)	U/U_{cen}
4	200	12	72.2	1.36886	.4354	.93346	49.24	.6820	2.62128	23.723	.4358
5	200	11	81.22	1.53987	.4065	1.13337	59.78	.7360	2.89898	26.638	.5290
6	200	9	108.30	2.05329	.4299	1.62339	85.63	.7909	2.96015	28.068	.7578
7	100	14	118.04	2.23795	.4258	1.81215	95.58	.8097	2.07295	21.042	.8458
8	100	14	118.04	2.23795	.4435	1.79445	94.65	.8019	1.92291	19.431	.8376
9	50	22	136.79	2.59344	.4245	2.16894	114.40	.8363	2.15767	22.206	1.012
10	50	20	152.89	2.89868	.4316	2.46708	130.12	.8511	1.84911	19.203	1.152
11	50	20	152.89	2.89868	.4383	2.47038	130.30	.8511	1.70037	17.453	1.152
12	50	23	129.95	2.46376	.2017	2.26206	119.31	.9181	1.28479	11.623	1.056
13	50	23	129.95	2.46376	.2019	2.26186	119.30	.9181	1.33234	12.534	1.056
14	50	27					108.3		.97488	0	.9584
15	50	26					113.0		.980057	0	1.0
16	50	26					113.0		.966257	0	1.0
17	50	26					113.0		.971762	0	1.0
18	50	27					108.3		.986849	0	.9584
19	50	27					108.3		.984159	0	.9584
20	50	27					108.3		1.018323	3.451	.9584
21	50	28					103.96		1.175090	9.557	.920
22	50	30					96.26		1.554925	16.845	.8519
23	50	30	96.26	1.82502	.2014	1.62362	85.64	.8897	3.098568	30.798	.7579
24	100	14.5	113.01	2.14259	.4287	1.71389	90.40	.7999	2.438686	24.200	.80
25	100	15	108.3	2.05329	.4497	1.60359	84.58	.7810	2.53724	24.715	.7485
26	200	11	81.22	1.53987	.4661	1.07377	56.64	.6974	1.969551	18.579	.5013
27	200	12	72.2	1.36888	.4613	.907558	47.86	.6629	1.700901	15.428	.4235

TABLE IV (Cont'd)

Date: 7 August 1979

Position: White Pipe Midsection

Engine RPM: 70%

Comments: Bragg Cell (Phase Modulator)
$S = 39.61 \times 10^{-6}$ m

Position (in)	Sample Time ($\times 10^{-9}$ sec)	Peak	U* ft/sec	f_d* Hz x 10^6	Δf Hz x 10^6	f_d Hz x 10^6	U ft/sec	$\frac{U}{U^*}$	R	η (%)	$\frac{U}{U_{cen}}$
5	50	25	118.14	2.23985	.450	1.78985	94.4	.7991		0	.4722
6	50	19	162.44	3.07974	.450	2.62974	138.70	.8539		0	.6937
7	50	16	199.93	3.79052	.450	3.34052	176.19	.8813	2.201657	23.219	.8813
8	50	16	199.93	3.79052	.450	3.34052	176.19	.8813	1.674456	17.429	.8813
9	50	18					173.27		1.198018	10.146	.8667
10	50	17					185.65		1.037907	4.672	.9286
11	50	17					185.65		.980620	0	.9286
12	50	17					185.65		.918840	0	.9286
13	50	17					185.65		.989897	0	.9286
14	50	16					199.93		.963749	0	1.0
15	50	17					185.65		.970442	0	.9286
16	50	17					185.65		.991314	0	.9286
17	50	17					185.65		.975528	0	.9286
18	50	16	199.93	3.79052	.2017	3.58822	189.29	.9468	1.158396	8.866	.9468
19	50	16	199.93	3.79052	.2023	3.58822	189.29	.9468	1.137332	8.276	.9468
20	50	16	199.93	3.79052	.2023	3.58822	189.29	.9468	1.216278	10.313	.9468
21	50	16	199.93	3.79052	.2020	3.58852	189.29	.9468	1.282075	11.744	.9468
22	50	17	185.65	3.51979	.2023	3.31749	174.98	.9425	1.559855	16.430	.8752
23	100	10	185.65	3.51979	.4646	3.05519	161.14	.8680	2.191961	22.952	.8060
24	100	10	185.65	3.51979	.4581	3.06169	161.15	.8680	3.412940	32.614	.8060
25	100	12	144.39	2.73753	.4629	2.27463	119.97	.8309	5.838510	45.159	.60
26	200	9	108.30	2.05329	.4622	1.59109	89.92	.7749	2.646162	25.473	.4197
27	200	12	72.20	1.36886	.4652	.90366	47.66	.6601	1.783615	16.269	.2384

TABLE IV (Cont'd)

Date: 9 August 1979

Position: 10 feet Downstream of Flow Conditioners

Engine RPM: 50%

Comments: No Bragg Cell (Phase Modulator)

$S = 32.102 \times 10^{-6} M$

Position (in)	Sample Time ($\times 10^{-9}$ sec)	Peak	U ft/sec	f_d* Hz	Δf Hz $\times 10^6$	f_d Hz	U ft/sec	$\frac{U}{U_{cen}}$	R	η (%)	$\frac{U}{U_{cen}}$
3	100	35	32.91		.5415				1.10327	7.233	.6562
4	100	32	36.32		.5393				1.12706	8.023	.7242
5	100	29	40.51		.5403				1.09797	7.045	.8078
6	100	27	43.88		.5403				1.04124	4.571	.8750
7	100	27	43.88		.5406				1.02117	3.275	.8750
8	100	26	45.79		.5406				1.0006149	0.558	.9131
9	100	25	47.87		.5410				.98507	0	.9545
10	100	24	50.15		.5414				1.00112	0.753	1.0
11	100	24	50.15		.5408				.985894	0	1.0
12	100	24	50.15		.5408				.96590	0	1.0
13	100	24	50.15						.97936	0	1.0
14	100	24	50.15						.95752	0	1.0
15	100	25	47.87						.97181	0	.9545
16	100	24	50.15						.98054	0	1.0
17	100	24	50.15						.98406	0	1.0
18	100	24	50.15						.96249	0	1.0
19	100	25	47.87						.97199	0	.9545
20	100	26	45.79						1.00340	1.857	.9131
21	100	27	43.88						1.01345	2.922	.8750
22	100	28	42.13						1.02499	3.793	.8401
23	100	29	40.51						1.04072	4.728	.8078
24	100	31	37.62						1.12956	8.207	.7502
25	100	34	33.98						1.13448	8.358	.6776
26	200	19	32.91		.5412				1.16760	9.215	.6562
26.5	200	20	30.98		.5418				1.10674	7.354	.6177

TABLE IV (Cont'd)

Date: 9 August 1979

Position: 10 Feet Downstream of Flow Conditioners

Engine RPM: 70%

Comments: No Bragg Cell (Phase Modulator)

$S = 32.102 \times 10^{-6} M$

Position (in)	Sample Time ($\times 10^{-9}$ sec)	Peak	U* ft/sec	f_d* Hz	Δf Hz $\times 10^6$	f_d Hz	U ft/sec	$\frac{U}{\bar{U}_{cen}}$	R	η (%)	$\frac{U}{\bar{U}_{cen}}$
2	200	13	52.66		.540					0	.60
3	200	12	58.51		.540				.600258	0	.6667
4	200	11.5	61.95		.5418				1.05967	5.498	.7058
5	100	19	65.83		.5428				1.10997	7.464	.750
6	100	18	70.21						1.02734	3.947	.80
7	100	17	75.23						1.02967	4.094	.8571
8	100	17	75.23						.99187	0	.8571
9	100	16	81.02						1.00849	2.455	.9231
10	100	16	81.02						.99846	0.972	.9231
11	100	15	87.77						.95790	0	1.0
12	100	15	87.77						.83673	0	1.0
13	100	15	87.77						.92827	0	1.0
14	100	15	87.77						.94605	0	1.0
15	100	15	87.77						.94022	0	1.0
16	100	15	87.77						.92617	0	1.0
17	100	15	87.77						.91903	0	1.0
18	100	16	81.02						.98562	0	.9231
19	100	16	81.02						.97885	0	.9231
20	100	16	81.02						1.01168	2.765	.9231
21	100	17	75.23						1.02049	3.479	.8571
22	100	17	75.23						1.02237	3.616	.8571
23	100	18	70.21						1.02079	3.501	.80
24	100	19	65.83						1.13669	8.425	.75
25	200	12	58.66						1.09657	7.116	.6683
26	200	13	52.66						1.09264	6.976	.60
27	200	13	52.66						1.05840	5.596	.60
28	200	14	47.87		.5414				1.28796	12.078	.5454

TABLE IV (Cont'd)

Date: 14 August 1979

Position: 12 inches Inside Inlet Bell Mouth

Engine RPM: 50%

Comments: No Bragg Cell (Phase Modulator)

$S = 31.64 \times 10^{-3}$ mm

Position (in)	Sample Time ($\times 10^{-9}$ sec)	Peak	U* ft/sec	f_d* Hz	Δf Hz	f_d Hz	U ft/sec	$\frac{U}{U^*}$	R	η (%)	$\frac{U}{U_{cen}}$
2	400	12					28.84			0	1.056
3	300	15					28.83		1.07452	6.279	1.056
4	200	22					27.32		1.02746	3.948	1.0
5	200	21					28.84		.94318	0	1.056
6	200	22					27.32		1.02006	3.441	1.0
7	200	22					27.32		1.00737	2.326	1.0
8	200	22					27.32		.97286	0	1.0
9	200	22					27.32		.97348	0	1.0
10	200	22					27.32		.97826	0	1.0
11	200	21					28.84		1.03631	4.480	1.056
12	200	22					27.32		1.00632	2.209	1.0
13	200	22					27.32		.96654	0	1.0
14	200	22					27.32		1.02449	3.753	1.0
15	200	22					27.32		1.04261	4.823	1.0
16	200	22					27.32		.940844	0	1.0
17	200	22					27.32		.99765	0.697	1.0
18	200	21					28.84		.98026	0	1.056
19	200	21					28.84		1.02397	3.718	1.056
20	200	21					28.84		1.01777	3.268	1.056
21	200	21					28.84		1.05511	5.440	1.056
22	200	22					27.32		.99611	0	1.0
23	200	23					25.95		1.00398	1.922	.9499
24	200	21					28.84		.90504	0	1.056
25	200	22					27.32		1.08826	6.811	1.0
26	200	22					27.32		.84716	0	1.0
27	200	24					24.72			0	.9048

TABLE IV (Cont'd)

Date: 14 August 1979

Position: 12 inches Inside Inlet Bell Mouth

Engine RPM: 70%

Comments: No Bragg Cell (Phase Modulator)

$S = 31.64 \times 10^{-3}$ mm

Position (in)	Sample Time ($\times 10^{-9}$ sec)	Peak	U* ft/sec	f_d* Hz	Δf Hz	f_d Hz	U ft/sec	$\frac{U}{U^*}$	R	η (%)	$\frac{U}{U_{cen}}$
3	200	14					47.19		.94556	0	1.0
4	200	15					43.25		.87243	0	.9165
5	200	14					47.19		1.12031	7.914	1.0
6	200	14.5					45.13		.91865	0	.9563
7	200	14					47.19		1.00933	2.530	1.0
8	200	14					47.19		.97597	0	1.0
9	200	14					47.19		1.03502	4.407	1.0
10	200	14					47.19		.91562	0	1.0
11	200	14					47.19		.91393	0	1.0
12	200	14					47.19		.88418	0	1.0
13	200	14					47.19		.91796	0	1.0
14	200	14					47.19		1.02731	3.932	1.0
15	200	14					47.19		.94974	0	1.0
16	200	14					47.19		1.02841	4.009	1.0
17	200	14					47.19		.92017	0	1.0
18	200	14					47.19		1.03529	4.422	1.0
19	200	14					47.19		.99629	0	1.0
20	200	14					47.19		.96959	0	1.0
21	200	14					47.19		.95798	0	1.0
22	200	14					47.19		.97056	0	1.0
23	200	14					47.19		.98337	0	1.0
24	200	14					47.19		1.00243	1.705	1.0
25	200	14					47.19		.89557	0	1.0
26	200	14					47.19		.93963	0	1.0

APPENDIX E

HOT WIRE ANEMOMETER DATA

A total of five traverses were made with the Hot Wire Anemometer equipment and the following Table V is a listing of the data as obtained.

TABLE V

HOT WIRE ANEMOMETER DATA

Date: 23 August 1979

Position: 12 inches inside Inlet Bell Mouth

Probe: 8477

R_{set} 8.69

P_o = 29.21 in Hg
= 14.3466 lb_f/in^2
= 397.1100 in H_2O

T_o = 75°F

RPM: 50%

Position (in)	Volts	RMS	P (in. H_2O)	P (PSI)	Temp. (°F)
18	2.495	.0075	.3645	14.33343	75
16.9	2.493	.0072	.3705	14.33322	75
16	2.496	.008	.365	14.33341	75
15	2.497	.0079	.3695	14.33325	75
14	2.497	.009	.3635	14.33347	75
13	2.492	.009	.3595	14.33361	75
12	2.487	.008	.3640	14.33345	75
11	2.487	.006	.3790	14.332910	75
10	2.495	.0065	.3805	14.33285	75
9	2.499	.006	.3820	14.33280	75
8	2.501	.008	.3810	14.33284	75
7	2.492	.008	.3820	14.33280	75
6	2.490	.0095	.3820	14.33280	75
5	2.495	.011	.3820	14.33280	75
4.5	2.488	.01	.3830	14.33276	75
18.3	2.503	.007	.3830	14.33276	75
19	2.498	.0075	.3856	14.33267	75
20	2.496	.0075	.3820	14.33280	75
21	2.503	.007	.3830	14.33276	75
22	2.505	.0075	.3840	14.33273	75
23	2.502	.0065	.3835	14.33275	75
24	2.501	.0065	.3860	14.33265	75
25	2.502	.009	.3778	14.33295	75
26	2.499	.008	.3750	14.33305	75
27.1	2.492	.009	.3765	14.33300	75
28	2.490	.01	.3755	14.33303	75
17.5	2.493	.007	.3785	14.33293	75

TABLE V (cont'd)

HOT WIRE ANEMOMETER DATA

Date: 23 August 1979

Position: 12 inches inside Inlet Bell Mouth

Probe: 8477

R_{set}: 8.69

P_o = 29.16 in Hg
= 14.3220 lb_f/in^2
= 396.3220 in H_2O

T_o = 76.5 °F

RPM: 70%

Position (in)	Volts	RMS	P (in. H_2O)	P (PSI)	Temp. (°F)
18	2.695	.0068	1.0045	14.28571	76.5
15	2.698	.0058	1.0030	14.28576	76.5
12	2.640	.0065	1.0065	14.28563	76.5
9	2.665	.0084	1.005	14.28569	76.5
6	2.691	.0093	1.0046	14.28571	76.5
5	2.6875	.0130	1.006	14.28566	76.5
4.5	2.693	.0135	1.006	14.28566	76.5
18	2.6925	.00975	1.006	14.28566	76.5
21	2.701	.006	1.0075	14.28560	76.5
23	2.7025	.0058	1.0068	14.28563	76.5
26	2.702	.0072	1.011	14.28546	76.5
27	2.704	.0074	1.011	14.28546	76.5
28	2.7045	.0086	1.0085	14.28557	76.5
18	2.695	.0065	1.0085	14.28557	76.5

TABLE V (cont'd)

HOT WIRE ANEMOMETER DATA

Date: 31 August 1979 P_o = 29.74 in Hg

Position: 10 feet downstream from Flow Conditioners = 14.60687 lb_f/in^2

= 404.32 in H_2O

Probe: 8477 T_o = 76°F

R_{set} : 8.69 RPM: 50%

Position (in)	Volts	RMS	P (in. H_2O)	P (PSI)	Temp. (°F)
18	2.553	.011	3.341	14.48617	76
17	2.553	.012	3.315	14.48711	76
16	2.554	.013	3.3115	14.48723	76
15	2.540	.017	3.3110	14.48725	76
14	2.530	.020	3.3110	14.48725	76
13	2.520	.020	3.3040	14.48751	76
12	2.510	.019	3.3040	14.48751	76
11	2.490	.021	3.3090	14.48732	76
10	2.480	.024	3.3060	14.48743	76
9	2.460	.027	3.2935	14.48788	76
8	2.440	.029	3.2935	14.48788	76
7	2.410	.031	3.2935	14.48788	76
6	2.390	.033	3.2935	14.48788	76
5	2.360	.035	3.2900	14.48801	76
4.1	2.340	.035	3.2900	14.48801	76
18	2.5480	.011	3.2900	14.48801	76
19	2.5480	.011	3.280	14.48837	76
20	2.547	.012	3.266	14.48888	76
21	2.536	.016	3.266	14.48888	76
22	2.524	.019	3.266	14.48888	76
23	2.500	.021	3.266	14.48888	76
24	2.490	.022	3.266	14.48888	76
25	2.480	.027	3.270	14.48873	76
26	2.460	.032	3.270	14.48873	76
27	2.430	.035	3.270	14.48873	76
28	2.420	.036	3.297	14.48776	76
28.55	2.390	.035	3.293	14.48790	76
18	2.549	.0105	3.285	14.48819	76

TABLE V (cont'd)

HOT WIRE ANEMOMETER DATA

DATE: 31 August 1979 P_o = 29.74 in Hg

Position: 10 feet downstream from Flow Conditioners = 14.60687 lb_f/in^2 = 404.32 in H_2O

Probe: 8477 T_o = 77°F

R_{set}: 8.69 RPM: 70%

Position (in)	Volts	RMS	P (in. H_2O)	P (PSI)	Temp. (°F)
18	2.754	.0125	8.768	14.29014	77
17	2.757	.0135	8.7845	14.28951	77
16	2.753	.014	8.789	14.28935	77
15	2.750	.015	8.80	14.28895	77
14	2.730	.0195	8.80	14.28895	77
13	2.723	.020	8.8008	14.28885	77
12	2.720	.0205	8.746	14.29090	77
11	2.697	.023	8.7605	14.29038	77
10	2.690	.027	8.8215	14.28817	77
9	2.665	.033	8.7966	14.28907	77
8	2.630	.035	8.7880	14.28938	77
7	2.600	.038	8.6750	14.29347	77
6	2.570	.039	8.6750	14.29347	77
5	2.530	.039	8.733	14.29137	77
4.1	2.49	.0410	8.733	14.29137	77
18	2.753	.0125	8.826	14.28801	77
19	2.76	.0155	8.826	14.28801	77
20	2.750	.016	8.789	14.28935	77
21	2.736	.017	8.749	14.29079	77
22	2.73	.0185	8.770	14.29003	77
23	2.70	.023	8.770	14.29003	77
24	2.692	.025	8.770	14.29003	77
25	2.67	.0285	8.648	14.29444	77
26	2.63	.033	8.658	14.29408	77
27	2.60	.039	8.733	14.29137	77
28	2.56	.041	8.707	14.29231	77
28.55	2.54	.043	8.707	14.29231	77
18	2.740	.013	8.720	14.29184	77

TABLE V (cont'd)

HOT WIRE ANEMOMETER DATA

Date: 18 October 1979 P_o = 29.41 in Hg

Position: White Pipe Midsection = 14.44479 lb_f/in^2

Probe: 8477 T_o = 70°F

P_{set}: 8.58 RPM: 50%

Position (in)	Volts	RMS	P (in. H_2O)	P (PSI)	Temp. (°F)
18	2.930	.014	2.4190	14.35764	70
17	2.935	.012	2.4085	14.35802	70
16	2.930	.014	2.4085	14.35802	70
15	2.925	.016	2.3965	14.35845	70
14	2.925	.019	2.4178	14.35768	70
13	2.910	.0225	2.4178	14.35768	70
12	2.90	.0350	2.4178	14.35768	70
11	2.820	.080	2.4178	14.35768	70
10	2.750	.100	2.4178	14.35768	70
9	2.60	.140	2.4250	14.35742	70
8	2.50	.165	2.4387	14.35693	70
7	2.50	.160	2.4140	14.35782	70
6	2.150	.145	2.4190	14.35764	70
5	2.100	.130	2.4305	14.35723	70
4.2	2.100	.135	2.4155	14.35777	70
18	2.930	.0130	2.4130	14.35786	70
19	2.930	.0150	2.4258	14.35740	70
20	2.925	.01650	2.4258	14.35740	70
21	2.920	.01650	2.4258	14.35740	70
22	2.910	.030	2.4258	14.35740	70
23	2.880	.070	2.4258	14.35740	70
24	2.80	.120	2.4258	14.35740	70
25	2.70	.145	2.4258	14.35740	70
26	2.55	.165	2.4283	14.35731	70
27	2.40	.180	2.4178	14.35768	70
28	2.30	.170	2.4325	14.35715	70
28.55	2.20	.160	2.4325	14.35715	70
18	2.930	.012	2.4325	14.35715	70

APPENDIX F

HOT WIRE ANEMOMETER NUMERICAL RESULTS

Employing the data from the five traverses, as presented in Appendix E, the following Table VI is a list of the numerical results with each traverse being on a separate page of the Table. The data, from which the numerical results were obtained, was reduced employing a computer program developed by Dr. Richard Rivir of the Propuls ion Laboratory.

TABLE VI

HOT WIRE ANEMOMETER RESULTS

Date: 23 August 1979 RPM: 50%

Position: 12 inches inside Inlet Bell Mouth

Average Velocity: 32.374 ft/sec

Mass Flow Rate: 11.122 lb_m/sec

U_{cen} = 32.487 ft/sec

Position (in)	Mean Velocity (ft/sec)	Turbulence Intensity	$\frac{U}{U_{cen}}$
18.0	32.284	.02339	1.000
16.9	32.084	.02250	.988
16.0	32.385	.02492	.997
15.0	32.486	.02459	.999
14.0	32.486	.02801	.999
13.0	31.982	.02815	.984
12.0	31.485	.02515	.969
11.0	31.487	.01886	.969
10.0	32.286	.02027	.994
9.0	32.690	.01864	1.006
8.0	32.894	.02480	1.012
7.0	31.984	.02502	.984
6.0	31.786	.02977	.978
5.0	32.286	.03430	.994
4.5	31.586	.03140	.972
18.3	33.098	.02165	1.000
19.0	32.589	.02332	1.003
20.0	32.387	.02336	.997
21.0	33.098	.02165	1.019
22.0	33.304	.02316	1.025
23.0	32.996	.02013	1.016
24.0	32.894	.02015	1.012
25.0	32.996	.02787	1.016
26.0	32.689	.02485	1.006
27.1	31.984	.02815	.985
28.0	31.784	.03134	.978
17.5	32.084	.02187	1.000

TABLE VI (cont'd)

HOT WIRE ANEMOMETER RESULTS

Date: 23 August 1979 RPM: 70%

Position: 12 inches inside Inlet Bell Mouth

Average Velocity: 56.502 ft/sec

Mass Flow Rate: 19.299 lb_m/sec

U_{cen} = 56.965 ft/sec

Position (in)	Mean Velocity (ft/sec)	Turbulence Intensity	$\frac{U}{\bar{U}_{cen}}$
18.0	57.089	.01775	1.000
15.0	57.538	.01510	1.010
12.0	49.286	.01775	.865
9.0	52.735	.02247	.926
6.0	56.495	.02435	.992
5.0	55.979	.03413	.983
4.5	56.792	.03529	.997
18.0	56.717	.02550	1.000
21.0	57.989	.01558	1.018
23.0	58.216	.01505	1.023
26.0	58.141	.01869	1.021
27.0	58.444	.01917	1.026
28.0	58.519	.02227	1.027
18.0	57.090	.01696	1.000

TABLE VI (cont'd)

HOT WIRE ANEMOMETER RESULTS

Date: 31 August 1979 RPM: 50%

Position: 10 feet downstream of flow conditioners

Average Velocity: 31.193 ft/sec

Mass Flow Rate: 10.812 lb_m/sec

U_{cen} = 37.666 ft/sec

Position (in)	Mean Velocity (ft/sec)	Turbulence Intensity	$\frac{U}{U_{cen}}$
18	38.005	.03246	1.000
17	38.002	.03541	1.009
16	38.114	.03832	1.012
15	36.562	.05078	.971
14	35.486	.06031	.942
13	34.421	.06090	.914
12	33.383	.05843	.886
11	31.372	.06588	.833
10	30.397	.07606	.807
9	28.511	.08736	.757
8	26.705	.09585	.709
7	24.144	.10589	.641
6	22.532	.11532	.598
5	20.251	.12672	.538
4.1	18.819	.12986	.500
18	37.442	.03261	1.000
19	37.441	.03261	.994
20	37.328	.03561	.991
21	36.123	.04797	.959
22	34.839	.05763	.925
23	32.364	.06522	.859
24	31.369	.06901	.833
25	30.395	.08557	.807
26	28.509	.10354	.757
27	25.830	.11694	.686
28	24.979	.12161	.663
28.55	22.514	.12231	.600
18	37.552	.03110	1.000

TABLE VI (cont'd)

HOT WIRE ANEMOMETER RESULTS

Date: 31 August 1979 RPM: 70%

Position: 10 feet downstream of flow conditioners

Average Velocity: 55.009 ft/sec

Mass Flow Rate: 18.778 lb_m/sec

U_{cen} = 65.473

Position (in)	Mean Velocity (ft/sec)	Turbulence Intensity	$\frac{U}{U_{cen}}$
18	66.291	.03116	1.000
17	66.791	.03358	1.020
16	66.129	.03493	1.010
15	65.636	.03751	1.002
14	62.407	.04952	.953
13	61.303	.05107	.936
12	60.826	.05247	.929
11	57.316	.05995	.875
10	56.285	.07077	.860
9	52.673	.08829	.804
8	47.893	.09645	.732
7	44.029	.10751	.672
6	40.398	.11337	.617
5	35.887	.11772	.548
4.1	31.728	.12874	.485
18	66.135	.03119	1.000
19	67.299	.03847	1.028
20	65.635	.04001	1.002
21	63.356	.04297	.968
22	62.402	.04698	.953
??	57.767	.05981	.882
24	56.573	.06543	.864
25	53.361	.07594	.815
26	47.877	.09094	.731
27	44.036	.11033	.673
28	39.278	.12029	.600
28.55	36.986	.12856	.565
18	63.994	.03276	1.000

TABLE VI (cont'd)

HOT WIRE ANEMOMETER RESULTS

Date: 18 October 1979 RPM: 50%

Position: White Pipe Midsection

Average Velocity: 84.393 ft/sec

Mass Flow Rate: 29.354 lb_m/sec

U_{cen} = 126.221 ft/sec

Position (in)	Mean Velocity (ft/sec)	Turbulence Intensity	$\frac{\bar{U}}{\bar{U}_{cen}}$
18	126.220	.02912	1.000
17	127.539	.02489	1.010
16	126.216	.02912	.999
15	124.901	.03338	.989
14	124.907	.03964	.990
13	121.029	.04737	.959
12	118.492	.07414	.939
11	99.547	.17823	.789
10	84.833	.23346	.672
9	58.581	.36503	.464
8	44.636	.46751	.354
7	13.552	.66660	.107
6	13.552	.60411	.107
5	10.919	.58304	.087
4.2	10.918	.60547	.087
18	126.218	.02704	1.000
19	126.222	.03120	1.000
20	124.910	.03443	.990
21	123.607	.03453	.979
22	121.031	.06316	.959
23	113.535	.15012	.900
24	95.173	.27086	.754
25	75.318	.35064	.597
26	51.279	.44800	.406
27	33.172	.55956	.263
28	23.910	.58686	.189
28.55	16.575	.62302	.131
18	126.224	.02496	1.000

APPENDIX G

PITOT-STATIC TUBE DATA

Two traverses were made with the pitot-static tube, one at 50% engine RPM and the other at 70%. The position of the pitot-static tube was 25.5 feet in front of the J-85 engine compressor or about 12 inches in front of the venturi. The following is the data which is presented in the following order:

A. 50% Engine RPM

B. 70% Engine RPM

TABLE IV

PITOT-STATIC TUBE DATA

Date: 14 June 1979, Run 1

Engine RPM: 50%

P_o = 29.42 in Hg = 399.965 in H_2O

T_o = 77°F = 536.69°R

Position (In)	$\triangle P$ (In. H_2O)
2.82	.0168
3	.0228
4	.1304
5	.1564
6	.1676
7	.1792
8	.1948
9	.2032
10	.2104
11	.2252
12	.2328
13	.2404
14	.2500
15	.2508
16	.2528
17	.2596
18.0	.2596

TABLE IV (Cont'd)

PITOT-STATIC TUBE DATA

Date: 14 June 1979, Run 2

Engine RPM: 70%

P_o = 29.42 in Hg = 399.965 in H_2O

T_o = 77°F = 536.69°R

Position (In)	$\triangle$ P (In. H_2O)
2.82	.2536
3	.3196
4	.3824
5	.4216
6	.4408
7	.4676
8	.5216
9	.5708
10	.6032
11	.6271
12	.6519
13	.6695
14	.6896
15	.7056
16	.7222
17	.7331
18.0	.7440

APPENDIX H

PITOT-STATIC TUBE RESULTS

Using the results as presented in Appendix G, the P was converted to inches of water and then divided by the room pressure which was assumed to be total pressure, giving P/P_o. This was then used to determine the flow Mach number from the Gas Tables. The room total temperature was used to determine the speed of sound which when combined with the Mach number, gives the flow velocity. The results are presented as follows:

A. 50% Engine RPM

B. 70% Engine RPM

TABLE VIII

PITOT-STATIC TUBE RESULTS

Date: 14 June 1979, Run 1

Engine RPM: 50%

U_{cen} = 33.987 ft/sec

P_o = 29.42 in Hg

= 399.965 in H_2O

T_o = 77°F

= 536.69°R

Pos. (in)	P in. H_2O	$\frac{P}{P_o}$	M	ft/sec	U ft/sec	$\frac{U}{U_{cen}}$
2.82	399.948	.999958	.016022	1135.86	18.199	.535
3	399.942	.999943	.018155	1135.86	20.621	.607
4	399.835	.999674	.021322	1135.86	24.219	.713
5	399.809	.999609	.023167	1135.86	26.314	.774
6	399.798	.999581	.023959	1135.86	27.214	.801
7	399.786	.999552	.024793	1135.86	28.161	.829
8	399.770	.999513	.025902	1135.86	29.421	.866
9	399.762	.999492	.026524	1135.86	30.127	.886
10.	399.755	.999474	.0270166	1135.86	30.687	.903
11	399.740	.999437	.028095	1135.86	31.912	.939
12	399.732	.999418	.028627	1135.86	32.516	.957
13	399.725	.999399	.029163	1135.86	33.125	.975
14	399.715	.999375	.029845	1135.86	33.900	.997
15	399.714	.999373	.0299219	1135.86	33.987	1.000
16	399.712	.999368	.030040	1135.86	34.121	1.004
17	399.706	.999351	.030384	1135.86	34.512	1.015
18	399.706	.999351	.030384	1135.86	34.512	1.015

TABLE V III (cont'd)

PITOT-STATIC TUBE RESULTS

Date: 14 June 1979, Run 2

Engine RPM: 70%

U_{cen}: 57.001 ft/sec

P_o = 29.42 in Hg

= 399.965 in H_2O

T_o = 77°F

= 536.69°R

Pos. in.	P in. H_2O	$\frac{P}{P_o}$	M	ft/sec	U ft/sec	$\frac{U}{U_{cen}}$
2.82	399.711	.999366	.030075	1135.86	34.161	.599
3	399.645	.999201	.033447	1135.86	37.991	.667
4	399.583	.999044	.036646	1135.86	41.625	.730
5	399.543	.998946	.038648	1135.86	43.899	.770
6	399.524	.998898	.039629	1135.86	45.013	.790
7	399.497	.998831	.040775	1135.86	46.315	.813
8	399.443	.998696	.042896	1135.86	48.724	.855
9	399.394	.998573	.044873	1135.86	50.969	.894
10	399.362	.998492	.046159	1135.86	52.430	.920
11	399.338	.998432	.047114	1135.86	53.515	.939
12	399.313	.998370	.048095	1135.86	54.629	.958
13	399.295	.998326	.048789	1135.86	55.417	.972
14	399.276	.998276	.049592	1135.86	56.329	.988
15	399.259	.998236	.050183	1135.86	57.001	1.00
16	399.243	.998194	.050722	1135.86	57.613	1.01
17	399.232	.998167	.051075	1135.86	58.014	1.02
18.0	399.221	.998140	.051425	1135.86	58.412	1.03

APPENDIX J

PARTICLE DIAMETER AND VELOCITY DIFFERENCE DETERMINATION

In order to determine the reason why differences in centerline velocities occurred (under similar engine RPM conditions, but with different measuring devices) a decision was made to attempt to develop a mathematical method to help explain these differences. The following method, developed with the assistance of Capt. (Dr.) George Catalano of the Air Force Flight Dynamics Laboratory, will be used to determine how the size of the particles in the airstream might affect the extent of velocity differences, as well as how the velocity differences might be a function of the upstream expansions and contractions in the flow.

U_p = particle velocity

U_a = air velocity

α = slope of the divergent or convergent section

x = the distance, in inches, from the beginning of a divergent or convergent section to the point of testing

μ = viscosity of air

ρ_p = density of the particles or dust in the air

D = the diameter of the particles

$U = U_g - U_p$

$$K = \frac{18\mu}{\rho_p D^2}$$

Force = Mass x Acceleration

$$\frac{dU_p}{dt} = K(U_g - U_p)$$

$$U_g = \alpha X$$

$$U = U_g - U_p$$

$$U_p = U_g - U$$

$$\frac{d}{dt}(U_g - U) = KU$$

or $$\frac{d}{dt}(U_g) - \frac{d}{dt}(U) = KU$$

becomes

$$U_g \frac{d}{dx}(U_g) - U \frac{d}{dx}(U) = KU$$

or $$U \frac{dU}{dx} + KU - U_g \frac{dU_g}{dx} = 0$$

or $$U \frac{dU}{dx} + KU - \alpha^2 x = 0$$

as $$\frac{dU_g}{dx} = \alpha \qquad \text{and } U_g = \alpha x$$

let $U = Y$, $K = A$, and $\alpha^2 = A_2$

$$Y \frac{dy}{dx} + A_1 Y - A_2 x = 0$$

now, let $Y = vx$

$$\frac{dy}{dx} = \frac{d}{dx}(vx) = v + x \frac{dv}{dx}$$

$$(vx)\ \left(v + x\frac{dv}{dx}\right) + A_1vx - A_2x = 0$$

$$vx^2\frac{dv}{dx} = A_2x - A_1vx - v^2x$$

$$\frac{dv}{dx} = \frac{A_2x - A_1xv - xv^2}{vx^2}$$

$$x\frac{dv}{dx} = \frac{A_2x - A_1xv - xv^2}{xv}$$

or $$x\frac{dv}{dx} = \frac{A_2 - A_1v - v^2}{v}$$

or $$x\frac{dv}{dx} = \frac{A_2 - A_1v - v^2}{v}$$

or $$\frac{1}{x}\frac{dx}{dv} = \frac{v}{A_2 - A_1v - v^2}$$

$$\frac{1}{x}dx = \frac{v}{A_2 - A_1v - v^2}dv$$

$$\log kx = \int \frac{v}{A_2 - A_1v - v^2}dv$$

$$= -\int \frac{v}{(v^2 + A_1v - A_2)}dv$$

$$\log kx = -\int \frac{v}{(v^2 + A_1v - A_2)}dv$$

now, $$v^2 + A_1v - A_2 = \left(v + \frac{A_1}{2}\right)^2 - \frac{A_1^2}{4} - \frac{A_1}{2}$$

let $$w = v + \frac{A_1}{2} \quad \& \quad v = w - \frac{A_1}{2}$$

$$v^2 + A_1 v - A_2 = w^2 - \frac{A_1^2}{4} A_2$$

let $A_3^2 = \frac{A_1^2}{4} + A_2$

$$v^2 + A_1 v - A_2 = w^2 - A_3^2 = (w + A_3)(w - A_3)$$

now, $\frac{v}{(v^2 + A_1 v - A_2)} = \frac{w - (A_1/2)}{(w + A_3)(w - A_3)}$

let $A_1' = \frac{A_1}{2}$

now $\frac{w - A_1'}{(w - A_3)(w + A_3)} = \frac{C_1}{(w - A_3)} + \frac{C_2}{(w - A_3)}$

$$w - A_1' = C_1 (w - A_3) + C_2 (w + A_3)$$

$$= C_1 w - C_1 A_3 + C_2 w + C_2 A_3$$

or $w - A_1' = (C_1 w + C_2 w) - (C_1 A_3 - C_2 A_3)$

$$w = C_1 w + C_2 w$$

$$C_1 + C_2 = 1$$

$$-A_1' = -C_1 A_3 + C_2 A_3$$

$$-\frac{A_1'}{A_3} = -C_1 + C_2$$

$$\frac{A_1'}{A_3} = C_1 - C_2$$

thus:

$$C_1 + C_2 = 1$$

$$C_1 - C_2 = \frac{A_1'}{A_3}$$

$$2C_1 = 1 + \frac{A_1'}{A_3}$$

or

$$C_1 = \frac{A_3 + A_1'}{2A_3}$$

similarly, $C_2 = 1 - \frac{A_3 + A_1'}{2A_3} = \frac{2A_3 - A_3 + A_1'}{2A_3}$

$$= \frac{A_3 - A_1'}{2A_3}$$

$$\therefore \int \frac{w - A_1'}{(w + A_3)(w - A_3)}\, dw = \int \frac{A_3 + A_1'}{2A_3} \frac{1}{(w + A_3)}\, dw + \int \frac{A_3 - A_1'}{2A_3} \frac{1}{(w - A_3)} dw$$

$$= \frac{A_3 + A_1'}{2A_3} \int \frac{dw}{(w + A_3)} + \frac{A_3 A_1'}{2A_3} \int \frac{dw}{(w - A_3)}$$

$$= \frac{A_3 + A_1'}{2A_3} \log (w + A_3) + \frac{A_3 - A_1'}{2A_3} \log (w - A$$

thus, $\log kx = \frac{A_3 + A_1'}{2A_3} \log (w + A_3) + \frac{A_3 - A_1'}{2A_3} \log (w - A_3)$

$$\text{or} \quad kx = \left[(w + A_3) \frac{A_3 + A_1'}{2A_3} \right] \left[(w - A_3) \frac{A_3 - A_1'}{2A_3} \right]$$

now again, $w = v + \frac{A_1}{2}$

$$A_1' = \frac{A_1}{2}$$

$$A_3^2 = \frac{A_1^2}{4} + A_2$$

$$w + A_3 = v + \frac{A_1}{2} + A_3$$

$$= v + \frac{A_1}{2} + \left(\frac{A_1^2}{4} + A_2\right)^{1/2}$$

and

$$w - A_3 = v + \frac{A_1}{2} - \left(\frac{A_1^2}{4} + A_2\right)^{1/2}$$

$$kx = \left[v + \frac{A_1}{2} + \left(\frac{A_1^2}{4} + A_2\right)^{1/2} \right]^{\frac{A_3 + A_1'}{2A_3}} \left[v + \frac{A_1}{2} - \left(\frac{A_1^2}{4} + A_2\right)^{1/2} \right]^{\frac{A_3 - A_1'}{2A_3}}$$

$$\frac{A_3 + A_1'}{2A_3} = \frac{\left(\frac{A_1^2}{4} + A_2\right)^{1/2} + \frac{A_1}{2}}{2\left(\frac{A_1^2}{4} + A_2\right)^{1/2}}$$

$$= \frac{1}{2}\left(1 + \frac{\frac{A_1}{2}}{\left(\frac{A_1^2}{4} + A_2\right)^{1/2}} \right)$$

similarly

$$\frac{A_3 - A_1'}{2A_3} = \frac{1}{2}\left[1 - \frac{\frac{A_1}{2}}{\left(A_1^2 + A_2\right)^{1/2}}\right]$$

$$\frac{1}{2}\left[1 + \frac{\frac{A_1}{2}}{\left(\frac{A_1^2}{4} + A_2\right)^{1/2}}\right] = \frac{1}{2}\left[1 + \frac{\frac{A_1}{2}}{\frac{1}{2}\left(A_1^2 + 4A_2\right)^{1/2}}\right]$$

$$= \frac{1}{2}\left[1 + \frac{A_1}{\left(A_1^2 + 4A_2\right)^{1/2}}\right]$$

similarly

$$\frac{A_3 - A_1'}{2A_3} = \frac{1}{2}\left[1 - \frac{A_1}{\left(A_1^2 + 4A_2\right)^{1/2}}\right]$$

now, $kx = \left[v + \frac{A_1}{2} + \left(\frac{A_1^2}{4} + A_2\right)^{1/2}\right] \frac{1}{2}\left(1 + \frac{A_1}{\left(A_1^2 + 4A_2\right)^{1/2}}\right)^{1/2}$

$$\left[v + \frac{A_1}{2} - \left(\frac{A_1^2}{4} + A_2\right)^{1/2}\right] \left(1 - \frac{A_1}{\left(A_1^2 + 4A_2\right)^{1}}\right)^{1/2}$$

now, $v = \frac{y}{x}$

$$\left\{y + \left[\frac{A_1}{2} + \left(\frac{A_1^2}{4} + A_2\right)^{1/2}\right]x\right\} \left(1 + \frac{A_1}{\left(A_1^2 + 4A_2\right)^{1/2}}\right)^{1/2}$$

$$= k\left\{y + \left[\frac{A_1}{2} - \left(\frac{A_1^2}{4} + A_2\right)^{\frac{1}{2}}x\right\}\right. \left(1 - \frac{A_1}{\left(A_1^2 + 4A_2\right)^{1/2}}\right)^{1/2} \quad (1)$$

now

$$A_1 = K$$

$$A_2 = \alpha^2$$

thus, equation (1) becomes:

$$\left\{y + \frac{1}{2}\left[K + (K^2 + 4\alpha^2)^{1/2}\right]x\right\}^{-1/2\left(1 + \frac{K}{(K^2 + 4\alpha^2)^{1/2}}\right)} =$$

$$k\left\{y + \frac{1}{2}\left[K - (K^2 + 4\alpha^2)^{1/2}\right]x\right\}^{1/2\left(1 - \frac{K}{(K^2 + 4^2)^{1/2}}\right)}$$

now, let $\beta^2 = K^2 + 4\alpha^2$

$$\left\{y + \frac{1}{2}\left[K + \beta\right]x\right\}^{-1/2\,(1+\frac{K}{\beta})} = k\left\{y + \frac{1}{2}(K - \beta)\right\}x^{1/2\,(1-\frac{K}{\beta})}$$

$$\text{or } k = \frac{\left\{y + \frac{1}{2}\left[K - \beta\right]x\right\}^{1/2\,(1-\frac{K}{\beta})}}{\left\{y + \frac{1}{2}\left[K + \beta\right]x\right\}^{-1/2\,(1+\frac{K}{\beta})}}$$

$$k = \frac{\left\{y + \frac{1}{2}(K - \beta)\,x\right\}^{1/2\,(1-\frac{K}{\beta})}}{\left\{y + \frac{1}{2}(K + \beta)\,x\right\}^{1/2\,(1+\frac{K}{\beta})}}$$

$$y = U$$

$$k = \frac{\left\{U + \frac{1}{2}(K - \beta)\,x\right\}^{1/2\,(1-\frac{K}{\beta})}}{\left\{U + \frac{1}{2}(K + \beta)\,x\right\}^{1/2\,(1+\frac{K}{\beta})}}$$

where

$$U = U_g - U_p$$

$$K = \frac{18\mu}{\rho_p D^2}$$

$$\beta = (K^2 + 4^2)^{1/2}$$

Now, by selecting a value for D and a centerline velocity difference, U, the value of K was determined. Then, by using this constant K and varying the value of D, the effect on the U was observed. It was noted that by varying the D, little change in U was observed except when the values of D got to be larger than D - 3 x 10^{-6}m. However, it was observed that when the D was held constant and α was changed, considerable change in U was observed. Here, the α refers to the velocity change between two points in the flow divided by the distance between the two points, where the velocity change is due to an upstream contraction or expansion of the flow area. Table IX illustrates the change in centerline velocity brought on by a change in α :

TABLE IX

VARIATION OF U WITH CHANGES IN α

Particle Diameter ($x10^{-6}$m)	α (sec^{-1})	U (ft/sec)
3.0	5	13.000
3.0	10	13.000
3.0	25	13.020
3.0	50	13.060
3.0	100	13.250
3.0	150	13.555
3.0	148	13.540
3.0	500	18.780
3.0	1000	33.560
3.0	1500	54.380
3.0	3000	140.485

Referring to the table, for an α of 148, which actually exists from the venturi to Position #1, a velocity difference of 13.54 ft/sec was calculated which corresponds well to an actual velocity difference of 13.2 ft/sec. The velocity difference of 13.2 ft/sec is the difference in velocity between the Hot Wire and LV Systems for the centerline of Position 1 at 50% Engine RPM.

VITA

Captain Harley J. V. Rogers was born in Moose Jaw, Saskatchewan, Canada in 1953. Upon graduation from high school in the spring of 1971, he applied, and was subsequently accepted, to attend the Royal Military College of Canada (Royal Roads Campus) in Victoria, British Columbia. After two years at Royal Roads, he transferred to the Royal Military College in Kingston, Ontario where, in the spring of 1975, he graduated with a Bachelor's Degree in Industrial Engineering. Following graduation and Military Specialty training, he was posted to Canadian Forces Base, North Bay, Ontario where, for the next two and one-half years, he held the positions of Aircraft Repair Officer and Aircraft Servicing Officer for the 414 Electronic Warfare Squadron. In the spring of 1978, Captain Rogers' application for Post Graduate Training was approved and in June of the same year, commenced on an eighteen month program at the United States Air Force Institute of Technology in the Graduate Aeronautical Engineering Division.

Permanent Address: 948 Normandy Drive
Moose Jaw, Saskatchewan
Canada

UNCLASSIFIED

SECURITY CLASSIFICATION OF THIS PAGE *(When Data Entered)*

REPORT DOCUMENTATION PAGE		READ INSTRUCTIONS BEFORE COMPLETING FORM
1. REPORT NUMBER AFIT/GAE/AA/79D-16	2. GOVT ACCESSION NO.	3. RECIPIENT'S CATALOG NUMBER
4. TITLE *(and Subtitle)* VELOCITY PROFILES IN A LONG INLET DUCT EMPLOYING A PHOTON CORRELATING LASER VELOCIMETER WITHOUT SEEDING		5. TYPE OF REPORT & PERIOD COVERED M.S. Thesis 6. PERFORMING ORG. REPORT NUMBER
7. AUTHOR(s) Harley J.V. Rogers Capt CAF		8. CONTRACT OR GRANT NUMBER(s)
9. PERFORMING ORGANIZATION NAME AND ADDRESS Air Force Institute of Technology (AFIT/EN) Wright-Patterson AFB, OH 45433		10. PROGRAM ELEMENT, PROJECT, TASK AREA & WORK UNIT NUMBERS
11. CONTROLLING OFFICE NAME AND ADDRESS		12. REPORT DATE December 1979 13. NUMBER OF PAGES 172
14. MONITORING AGENCY NAME & ADDRESS*(if different from Controlling Office)*		15. SECURITY CLASS. *(of this report)* Unclassified 15a. DECLASSIFICATION/DOWNGRADING SCHEDULE

16. DISTRIBUTION STATEMENT *(of this Report)*

Approved for public release; distribution unlimited

17. DISTRIBUTION STATEMENT *(of the abstract entered in Block 20, if different from Report)*

18. SUPPLEMENTARY NOTES

Approved for public release; IAW AFR 190-17

Joseph P. Hipps, Maj, U
Director of Information

19. KEY WORDS *(Continue on reverse side if necessary and identify by block number)*

Laser Velocimeter	J-85 Jet Engine Inlet Duct
Velocity Profiles	Hot Wire Anemometer
Mean Velocity	Pitot-Static Tube
Turbulence Intensity	

20. ABSTRACT *(Continue on reverse side if necessary and identify by block number)*

This thesis involves a practical application of the Malvern Laser Velocimeter System (LV). In this work, the LV was used to measure mean velocity profiles across the inside diameter of a duct which supplies air to the compressor of a jet engine. The engine, which is a General Electric J-85 turbo-jet engine is located in the Propulsion Laboratories of Wright-Patterson Air

DD FORM 1 JAN 73 1473 EDITION OF 1 NOV 65 IS OBSOLETE

UNCLASSIFIED

SECURITY CLASSIFICATION OF THIS PAGE *(When Data Ent*

Force Base in Ohio. In addition to the mean velocity profiles, the LV was used to measure turbulence intensity profiles across the inside diameter of the duct at each of the three test points. To analyse the quality of the LV data as obtained, alternate mean velocity profiles and turbulence intensity profiles were obtained with the aid of a Hot Wire Anemometer System and a Pitot-Static Tube.

During each of the traverses, or tests, with the LV System, the Hot Wire System and the Pitot-Static Tube, the engine was held at a fixed RPM, being 50% or 70% of maximum engine RPM. Good correlation was achieved between each of the three systems in respect to the mean velocity profiles obtained at each of the three test positions while the turbulence intensity profiles matched well in the regions of the flow where turbulence levels of 2% to 30% were encountered.